

# UC San Diego

## IMR Reference

### Title

Physical Oceanography Of The Region Near Point Arguello

### Permalink

<https://escholarship.org/uc/item/3s86s8vh>

### Author

Reid, Joseph L, Jr.

### Publication Date

1965-07-01

M. Tsuchiya

PHYSICAL OCEANOGRAPHY OF THE REGION NEAR POINT ARGUELLO

by  
Joseph L. Reid, Jr.

A technical report on  
Environmental Studies in the Vicinity of Point Arguello  
Under AEC Contract AT(11-1)-34, Project 111

Institute of Marine Resources  
University of California

July 1965

IMR Reference 65-19

UCSD 34P111-11

Point Arguello, 1965 IMR Ref. 65-19

## TABLE OF CONTENTS

- I. General description of the California Current
  - A. Current
    - 1. Surface current
    - 2. Subsurface current
    - 3. Flow at great depth
  - B. Upwelling
  - C. Temperature and salinity
    - 1. At the surface
    - 2. At depth
- II. Description of the area off Point Arguello
  - A. Current
    - 1. Surface current
    - 2. Subsurface current
    - 3. The deeper transport
  - B. Temperature and salinity
    - 1. Distribution of temperature and salinity at various depths,  
in January and in June
    - 2. Vertical sections across the flow
    - 3. Seasonal variations at particular positions
  - C. Oxygen and nutrients
    - 1. Oxygen
    - 2. Nutrients
- III. Results of the more closely spaced observations off Point Arguello in  
January and June of 1964
  - A. January 1964
    - 1. Current

TABLE OF CONTENTS (cont'd.)

- a. Surface current
- b. Subsurface current
- 2. Temperature and salinity
  - a. Horizontal distribution
  - b. Vertical sections
- B. June 1964
  - 1. Current
    - a. Surface current
    - b. Subsurface current
  - 2. Temperature and salinity
    - a. Horizontal distribution
    - b. Vertical sections
- C. Oxygen and nutrient distribution in January and June 1964
- IV. Comment on the nature of the eddies of upwelled water
- V. Disposition of the waters in the Point Arguello region
  - A. Flow and dilution
    - 1. The surface flow
    - 2. The California Current water
    - 3. The California Countercurrent water
    - 4. The basin water
  - B. Effect upon other water masses

## I. GENERAL DESCRIPTION OF THE CALIFORNIA CURRENT

Various investigators have described the California Current system, the most recent extensive study being that of Reid, Roden, and Wyllie (1958). Since then various small-scale studies with drogues and with close spacing of stations have been made over much of the area but the Pt. Arguello area had not received particular attention until the work in January 1964.

The Point Arguello area lies in an inshore area of the California Current system, which is briefly described below.

California Current is the name that has been given to the eastern limb of the wind-driven subtropical anticyclone of the North Pacific Ocean: it applies to the southeastward flow carrying water from the West Wind Drift to the North Equatorial Current. Its eastern boundary is the coast of North America where it flows past the states of Washington, Oregon, California and Baja California: it has no well-marked western boundary, but it has been common to define one arbitrarily at a distance 1000 km from shore.

### I.A. Current.

I.A.1. Surface current. The surface currents near the coast vary with season: those waters within about 150 km of the coast flow northwestward along most of the coast in the period from about October through February (fig. 1) and southeastward during the rest of the year (fig. 2). Within the channel islands off southern California, flow is to the northwest throughout most of the year and a nearly permanent Southern California Eddy obtains (Schwartzlose, 1963). The inshore countercurrent at the surface appears in winter all along the coast except off northern Baja California, just south of the Southern California Eddy (Reid, Schwartzlose and Brown, 1963).

The speed of surface flow is usually less than 25 cm/sec, though speeds

as high as 100 cm/sec have been observed occasionally in the shoal water of the inter-island passages. Drift bottles released near the coast off central California in winter (Schwartzlose, 1963) have sometimes been recovered more than 1000 km northward at time intervals indicating average speeds of at least 25 cm/sec (fig. 3).

Short-period variations in the strength of flow have been observed of the same order as the strength of flow (5 to 15 cm/sec). Some of these, particularly in the offshore region may be inertial rotations of period 1/2 pendulum day (Reid, 1962a and Knauss, 1962a). Others may be related to the tidal flow (Reid, 1958): in any case a great deal of short-period variation about the mean flow has been observed.

Likewise vertical oscillations (internal waves) of considerable magnitude have been encountered throughout the area (Reid, 1956 and 1958; Reid and Schwartzlose, 1962): these appear to have a substantial component with the lunar semidiurnal period (12.42 hours), especially in the region within 100 miles of the coast.

I.A.2. Subsurface current. Near the coast (within about 100 km) the waters below about 150 m depth flow northwestward throughout the year at speeds of 25 cm/sec or less (fig. 4) (Sverdrup and Fleming, 1941). Direct measurements with drogues have confirmed the existence of the flow (Reid; 1962b and 1963). As a result the inshore deep waters have more of the characteristics of lower-latitude waters than do those offshore.

I.A.3. Flow at great depth. The major inferences about deeper flow are based on the distribution of temperature, salinity, and oxygen as principal parameters and upon phosphate-phosphorus, carbon-14 and other parameters when they are available.

The general northward flow of the deep water in the Pacific was first postulated by Prestwich (1875) on the basis of temperature distribution.

Wüst (1937) refined this with more temperature data, documenting a northward increase of bottom temperature. Wooster and Volkmann (1960) further refined the results and showed that the deep oxygen values decreased from south to north, consonant with the earlier notions. Bien et al. (1960) for the first time, using carbon-14 data, estimated the rate of flow at 3500 m between 40°S and 15°N to be about  $0.06 \pm 0.02$  cm/sec. Knauss (1962b) used the more accurate salinity measurements to show that the salinity decreases from south to north as a consequence of mixing with the less saline overlying water.

Recently the temperature, salinity, and oxygen content of the deeper waters of the California Current have been measured in greater detail, and the resulting distributions of these properties have been compared (Reid and Lynn, 1964) with the general central Pacific patterns.

These distributions suggest that in the California Current the circulation between 2 and 3 km below the surface is like the shallower, wind-driven circulation above, with the principal flow from north to south and some evidence of a narrow northward flow along the coast. This northward flow, or countercurrent, appears to extend from about 150 or 200 m beneath the surface to at least 2000 m and to extend at least 150 km from the coast near Point Arguello.

There is no obvious indication at 4 km of a circulation like that of the wind-driven surface waters. Offshore in the central ocean the 4-km temperature increases to the north and the 4-km salinity decreases. Knauss (1962) has shown this for the 5-km and 4.5-km levels also. At 3.5 km a more complex situation exists, with some geostrophic effect in the central South Pacific indicated by various high temperatures in Knauss' 3.5-km map (Knauss, 1962: fig. 4). In the North Pacific, and particularly in the California

Current, there is some evidence (Reid and Lynn, 1964) of higher temperatures at 3 and 4 km depth where the bottom begins to rise toward the coasts. The temperature minimum, which is at about 3.8 km in the central North Pacific, is found at successively shallower levels approaching the coast of the Californias, reaching about 3.1-3.5 km off Baja California. This temperature increase may be a result of the coastward shoaling of the bottom, so that heat from the earth's interior enters the water at shallower levels than it does offshore. At any rate, it makes temperature-based inferences about flow at 4 km very doubtful in the California Current.

That the deep transport is slow seems fairly certain. That the abyssal flow under the California Current is in the same direction as the (northward) flow of the central ocean seems likely, but is far from certain. The geopotential anomaly of the 1000- and 2000-decibar surfaces with respect to the 3000-decibar surface varies by less than 2 dynamic centimeters over the area of the California Current and this variation is erratic, not systematic. The observed variation undoubtedly reflects the general margin of accuracy of the salinity and temperature measurements more than any systematic variation from which a geostrophic flow could be inferred.

#### I.B. Upwelling.

The prevailing winds are from the northwest throughout the year except in the northern area (north of about 40°N). The longshore component of the wind-stress combined with the effect of the earth's rotation drives some of the surface waters offshore: they are replaced by deeper waters rising near the coast. This process is known as upwelling and it is extremely important to the heat, salt and nutrient distributions in the California Current. It varies seasonally with the winds: these vary in such a way that it is most marked north of 35°N in mid-summer but occurs earlier (March-May) off Baja California. Estimates of the offshore transport indicate extreme values as



high as 10 kg/cm/sec. This may correspond to an upward speed of a few meters per month in the inshore areas. In the northern area downwelling is indicated in winter when the winds are from the southwest.

I.C. Temperature and salinity.

I.C.1. At the surface. Since the southward-flowing waters come from the higher-latitude West Wind Drift, they are relatively low in temperature and salinity compared to the water of the central North Pacific Ocean and the California Current is known as a cool current. Surface temperatures vary from less than 9°C in the north in the colder months to more than 26°C in the south in the warmer months (fig. 5). Salinity in the open ocean varies from about 32.5 parts per mille in the north to more than 34.5 ‰ in the south (fig. 6). Near the mouth of the Columbia River the surface salinity may be less than 30 ‰ but these low values are confined within the upper 10 meters and do not extend far offshore.

The seasonal variation of temperature and salinity has been discussed by Reid et al. (1958) and figure 7 is reproduced from that source. Since then more detailed mapping has been carried out (C.C.O.F.I., 1963) and a major study of the magnitude and phase of seasonal variations is underway.

Temperature and salinity vary as a result of seasonal differences in insolation, upwelling, and flow (fig. 7a). The normal period of minimum ocean temperature in the northern ocean is February-May and this overlaps the period of upwelling of colder water off southern Baja California. Therefore the range of variation there is about 6°, more than twice that of the central Pacific at that latitude. North of 35°N the period of maximum of upwelling occurs in midsummer and the range is correspondingly reduced (to about 3°C, while the central ocean values at that latitude may reach 8 or 10°C.

Since salinity increases with depth near the coast (especially in the north) upwelling brings up more saline water and a marked seasonal variation

occurs, with the highest values found in July-September. In the south the seasonal variation of salinity is dominated by the winter countercurrent that brings high salinity water northward so that the maximum value occurs in December-January. In the central area of the current these two effects nearly cancel each other and the range is small (fig. 7b). This is not to say that because the seasonal range is low, there is little seasonal difference in the region: on the contrary we have already noted the reversal of surface flow and it is clear that the two strong effects make large differences in other aspects of the system.

I.C.2. At depth. Temperature decreases monotonically with depth with a few minor exceptions. Beneath the thermocline and offshore there is a well-marked salinity minimum that is probably a consequence of the surface waters having mixed laterally with the higher-salinity waters to the west. There is another salinity minimum at about 350 m depth that indicates the presence of North Pacific Intermediate Water, whose characteristics are acquired in the extreme North Pacific and are transmitted southward by mixing and flow (Reid, in press).

## II. DESCRIPTION OF THE AREA OFF POINT ARGUELLO

### II.A. Current.

II.A.1. Surface current. The Point Arguello area is an especially interesting part of the California Current because it is characterized by a remarkable and systematic seasonal reversal in flow.

The surface flow is represented in figs. 8-10 by the topography of the sea surface relative to the 500-decibar surface: the horizontal gradient of this quantity is proportional to the speed of the geostrophic flow and the direction of this flow is given by the arrows.

The figures represent the averages of data taken in the period from 1950 through the summer of 1964. The coverage was not complete in every month of every year, so that no point represents a full record of 14 or 15 points. In this area coverage was best on the line extending southwestward from Point Conception. Also, coverage in November, December, and January is less than in other months. Though complete regularity was not achieved, the coverage seems adequate in general to describe the average monthly flow in each month of the year.

It is clear from figure 8 that in January the offshore flow is to the southeast, but that within 50 miles of Point Arguello there is a coastal countercurrent carrying water northward past Point Arguello. In the region of the Channel Islands this countercurrent is about 70 miles wide. Besides these main features there is some apparent meandering in the northwestern part of the area. This may be an artifact of the irregularity of coverage rather than a real feature, but eddies are common in the individual months and will be discussed later.

In February the coastal countercurrent seems much weaker, and very little flow northward past Point Arguello is indicated: most of the northward-flowing water appears to turn southward instead of continuing past Point Arguello.

In March the only vestige of the Countercurrent is seen inside the Channel Islands: no northward flow past Point Conception is indicated.

In April the countercurrent has completely disappeared. In this period, which has been covered particularly well, the isopleths are quite smooth, indicating that any eddy-like structures that might have appeared in individual months have not been regular enough in position to remain after the data have been averaged.

In March and April, while the Countercurrent has weakened and disappeared, the California Current has been strengthened, as indicated by the stronger gradient of geopotential topography. This strengthening continues through May and June (fig. 9), both of which, however, show some evidence of a weak eddy inside the Channel Islands.

In July the California Current is at its strongest. At this stage the eddy inside the Channel Islands has become quite well developed.

August and September (figs. 9 and 10) are much the same as July, but the California Current is weakening slightly and the eddy is still developing.

In October the eddy intensifies still further and in November and December the flow extends northward past Point Conception and can properly be called the Countercurrent again.

The southeastward-flowing California Current obtains throughout the year, but is most intense in the period from May through October. The countercurrent at the surface is not continuous. It is best developed in the period from November through January. It declines in February and March, does not appear at all in April. In May and June it exists only as a weak eddy inside the Channel Islands. The eddy becomes quite strong in July and continues to grow until it finally develops into the countercurrent in November.

The calculated geostrophic speeds at representative sections are shown in figure 11. As the maps indicated, the northward flow past Point Conception (section A) occurs from October through January, at average speeds up to 16 cm/sec (higher speeds have been calculated from the drift bottle results). Through the rest of the year flow near Point Arguello is to the south. South of Point Arguello and within the Channel Islands

(section B) the northward-flowing eddy is apparent from July through January, but, as off Point Arguello, some strong flow to the south is seen in March, April, and May, at speeds up to 10 cm/sec.

Offshore (sections C and D) the flow is nearly always to the south, but the same sense of seasonal variation is seen: the southward flow is strongest in June and July, weakest in January and February. The range of variation, however, is much less.

The results of these calculations of geostrophic flow may be compared with other estimates of the currents. The various drogue and GEK studies and most particularly the drift bottle program confirm the validity and the usefulness of the geostrophic approximation.

A comparison of drogue and GEK measurements with the computed geostrophic flow was made in the area just north of Point Arguello in October 1958 and January 1959 (Reid and Schwartzlose, 1962). The results confirmed the northward flow and the usefulness of the geostrophic approximation.

Drogue measurements in the area of the Channel Islands in October of 1958 (Brown, 1962) show the presence of the countercurrent.

Larger scale comparisons of drogue measurements with the geostrophic current have been made off Baja California (Reid, Schwartzlose and Brown, 1963) and seem to confirm the general usefulness of the geostrophic approximation where the currents are reasonably strong.

The most effective comparison of these average surface current charts can be made with the results of the drift bottle program. This program has been carried out since 1954 and some of its results have been discussed by Schwartzlose (1963). He found (p. 18) from the recovery of drift bottles that "the southern California counterclockwise eddy was present most of the year. The months it commonly was not present were March, April, and May."

He found that no drift bottles released in April off Southern California were recovered north of their release position, and that of those released in March or May many more moved southward than northward. He found that some bottles released near Point Arguello during the countercurrent season were recovered off Washington and Oregon, having moved northward at speeds greater than 0.3 knots.

II.A.2. Subsurface current. The geostrophic flow at 200 m depth is represented in figures 13-15 by the topography of the 200-decibar surface relative to the 500-decibar surface. The horizontal gradient of this quantity is proportional to the speed of the geostrophic flow and the direction of flow is given by the arrows. The figures represent the average of measurements made in the period from 1950 through part of 1964: limitations in data are the same as for figures 8-10.

At 200 m depth there is a Countercurrent carrying water northward past Point Arguello throughout the year. It is at all times wider than the surface Countercurrent, though its own width as well as its speed, seem to vary systematically with the season.

In January (fig. 13) the Countercurrent is about 90 miles wide, and the California Current itself appears only on the outer edge of the figure.

Some weakening and narrowing occur in February and March, and the Countercurrent appears to be weakest in April and May. In June (fig. 14) the Countercurrent strengthens, as does the California Current, but the Countercurrent remains fairly narrow. July, August and September (fig. 15) are much the same as June, with a strong but narrow Countercurrent and a strong California Current. In October and November the Countercurrent widens again, and in December and January the Countercurrent is widest.

The flow at 200 m is usually weaker than the surface flow, and its

range of seasonal variation is also less. The northward-flowing Counter-current at 200 m is weak in April and May, when the surface flow is nearly everywhere to the southeast, and is fairly strong (figs. 14 and 15) through the rest of the year, when there is northward flow at the surface either as an eddy inside the Channel Islands or as a countercurrent carrying water northward past Point Arguello.

The calculated geostrophic speeds at representative sections are shown in figure 16. In the inshore sections the northward flow is weakest in April and May and fairly strong (though erratic in the northern section) in the rest of the year. The strength of the northward flow at 200 m is somewhat less than that of the surface flow, and its seasonal range is much less.

The offshore sections (C and D) lie at the outer edge of the 200-m countercurrent, overlapping the southward flow, and the speed is quite weak throughout the year. The same sense of seasonal variation is seen, with the strongest southward flow in early summer and the weakest southerly flow (or slight northerly flow) in late fall and winter.

No direct comparisons of the 200-m geostrophic flow with drogue trajectories have been made near Point Arguello, but coastal measurements near 36°N with drogues (Reid, 1962b) confirm the northward flow at depth and coastal measurements with drogues near 30°N (Reid, 1963) not only confirm the deep northward flow but compare very favorably with the geostrophic flow calculated from concurrent observation of the density structure.

II.A.3. The deeper transport. From Point Arguello the ocean bottom slopes steeply downward, reaching depths of more than 3.5 km within 100 km of the coast. South of Point Arguello the bottom topography is quite complex, with many islands, basins, ridges, and banks: to the northward the

slope is much more regular.

The shallower flow can be measured and described by calculations based upon the water density and observations with drogues and drift bottles. At successively greater depths the flow indicated by these methods is much weaker and, correspondingly, much harder to measure.

Density measurements will reflect the flow in the upper 1000 m quite well (Reid, 1961 and 1963) in water as deep as 1000 m, but must be augmented with drogues in shallower water (i.e., 200 m, etc.). But below 1000 m depth the transport is so slow that the density gradients are within the margin of error of our measurement techniques. Transport at great depth appears to be so slow that drogues are apparently too much affected by the drag of the upper waters on the float and wire (Brown, 1962). Oscillatory flow also confuses the interpretation of movements over short periods (Knauss, 1962a).

Other information on the quite local flow has been given by Emery (1954), who examined the water properties in 14 basins off Southern California. He found that the "temperatures indicate that the bottom water of most basins must have travelled from basin to basin in a general north-westerly direction while that of the outermost basins came directly from the open sea on the west" (Emery, 1954, p. 1). This direction of flow of the bottom water is imposed by the bottom topography: the various basins east of the great submarine ridge extending southeast from Santa Rosa Island and Santa Cruz Island have deeper connections to the south than across the ridge. The Santa Barbara basin has a deeper connection to the west, and its deeper waters derive from the sea to the west rather than from the southeast. Deeper water from off Point Arguello could reach the inner basins only after having passed south of the ridge (at least to 32°N) and



turning inshore and to the northwest.

The basin water, then, reveals only the consequences of the quite local bottom topography, not an indication of the general offshore flow.

## II.B. Temperature and salinity.

### II.B.1. Distribution of temperature and salinity at various depths.

The distribution of heat and salt in the California Current has been described in general terms by Reid, Roden and Wyllie (1958) and some non-seasonal variations have been discussed by Reid (1960). A more recent set of maps at the 10-meter level has been provided in the CalCofi Atlas No. 1 (Calif. Coop. Oceanic Fish. Invest., 1963). Average maps for January and June at depths from 0 to 150 m are shown in figures 17-24. The averages have been made from the data collected in the period from 1950 through part of 1964.

In January the surface and 10 m temperature and salinity (fig. 17) are high near the coast, decreasing offshore. Temperature decreases for the first 40 or 50 miles offshore and then increases again, but salinity decreases monotonically offshore throughout the area studied. A minimum in salinity is encountered at about 200 miles offshore (fig. 6), and beyond this salinity increases toward the west.

The higher values inshore in January are a consequence of the California Countercurrent, which is strong at the surface in January and carries northward water which is warmer and more saline than the California Current water offshore.

This effect is also seen at the greater depths (figs. 18-20) with two minor differences. The width of the zone of warmer water inshore becomes somewhat greater at greater depths, as the width of the northward-flowing current increases (figs. 8 and 13). At 100 m, 150 m, and 200 m depth the

band of cold water is colder in the south, and at 150 m the coldest part is associated with the most saline water (fig. 20). This is the densest water seen at that level and its characteristics indicate that it has risen from somewhat greater depths as a result of the intensified geostrophic circulation during that month. The cold and saline area of figure 20 is seen to correspond to the lowest value of geopotential anomaly on the January average surface current chart (fig. 8).

In June (fig. 21) the surface and 10-m temperatures are only a little different from those in January, though these months do represent extremes in other respects. Along the coast just north of Point Arguello they are lower in June than in January. This can occur because January is not the month of lowest surface temperature nor is June the month of highest temperature: minimum temperatures in this region occur from February through May and maximum from July through September or October. Also, June is a period of strong upwelling and the very low temperatures near the coast north of Point Arguello occur as a result of upward motion of the deeper colder water.

The cold tongue extending southeastward from Point Arguello thus obtains in June, even when the Countercurrent is not present at the surface and the inshore eddy is very weak or absent.

Salinity at the surface and at 10 m (fig. 21) is markedly higher in June in the inshore areas, and the distribution clearly indicates its origin from below, rather than from the south.

At 30 and 50 m depth (fig. 22) the temperature and salinity differences between January and June are more extreme: June is much colder and more saline in the inshore areas. Also the cold tongue extending southeastward from Point Arguello lies closer inshore in June than the cold axis between

the California Current and Countercurrent does in January. The most marked difference, however, is in the values themselves: at 50 m the inshore water is about 3°C colder and 0.3 ‰ more saline in June because of upwelling and because of the difference in the sense of the inshore flow. Flow toward the south requires the densest water inshore for geostrophic balance, and this is achieved by the maintenance of the cold, saline water at higher levels in those months when the flow is southward.

These same features obtain also at 75 m (fig. 23). At 100 m the contrast in temperature values is less, but the difference in position of the cold tongue is much more extreme. The tongue barely reaches the Channel Islands in June but in January it is well offshore, with its axis about 60 miles off Point Arguello. Likewise, in June the high salinity water at 100 m clearly originates at or north of Point Arguello: in January it appears to come from the south.

At 150 m (fig. 24) the contrast in temperature values is less marked still, and the patterns of the isotherms in June and January begin for the first time to resemble each other. This is the depth of transition to the Countercurrent that obtains throughout the year. There is still a notable seasonal variation, however, as can be seen from the salinity at 150 m in January and June.

At 200 m the ridge of colder water between the Current and Countercurrent dominates the thermal structure, and the salinity decreases monotonically offshore. This is much the same as was seen in the average January conditions.

II.B.2. Vertical sections. The systematic seasonal variation in the geostrophic flow at the surface and at 200 m has been discussed in a previous section. These seasonal variations of the wind-driven flow require

some internal redistribution in the density structure if the quasi-geostrophic balance is to be maintained (as it apparently is: see the section on currents). The redistribution of the density structure results in changes of temperature and salinity which are not necessarily related to the local seasonal exchange of heat and water through the sea surface. The changes are brought about by both horizontal and vertical displacement of the water.

The distribution of temperature and salinity along a line extending southwestward from Point Arguello is shown in figures 25-29 for January, April, July and October. In all seasons the deeper water is warmer and more saline at the inshore end: this has been taken to indicate that this water is coming from lower latitudes, and hence moving northward.

The deeper water is also less dense inshore than in the middle of the section. Therefore it is the temperature (which increases inshore) that controls the density structure, and the downward curve of the 6 to 9°C isotherms at the inshore end of the section can be taken as a good indicator of the horizontal density and pressure gradients, and hence the intensity of the Countercurrent. These isotherms slope downward least intensely in April (fig. 27), when the Countercurrent at 200 m is weakest and when the surface northward flow has disappeared. The slope of these isotherms is much stronger in the other seasons, when the Countercurrent at 200 m is well developed.

The downward slope of the isotherms is not confined to the deeper values, but extends all the way to the surface in the inshore area in January (fig. 25), reflecting the northward flow even in the surface waters. The shape of the isotherms suggests that the Countercurrent is present below about 100 to 125 m in all seasons, and that its width increases with increasing depth.

II.B.3. Seasonal variations at particular positions. In response to the changing intensity of the flow the deeper isotherms appear to move up and down at the inshore end of the line: they are shallowest in April and May (fig. 30). This does not necessarily reflect only an upward movement of deeper water, however: the colder water could come either from below or from the offshore, colder water. If it came from below it is likely that it would be the most saline water also, but it is not: therefore it represents, at least to a major extent, the presence of offshore cooler water of moderate salinity, replacing the Countercurrent water that ordinarily is found in the inshore region.

The highest salinity is found in the inshore region in the period May through August, with its peak in June or July. The temperature at that time is only moderate, however, indicating, by the reasoning of the above paragraph, that the water has not merely risen directly from below. Higher salinity at moderate temperature is consonant with an upward movement of water from the south, rising toward the surface as it moves northward.

The highest temperature at the surface in the inshore water occurs in the September-December period. Further offshore the maximum occurs earlier, but the effect of the June and July upwelling is to retard the warming by mixing in large quantities of cooler water from below. At greater depths inshore the seasonal maximum occurs in December and January, as a result of the stronger countercurrent in that period.

Offshore (fig. 31) the vertical excursions of the isotherms are less extreme: neither reversal of flow nor upwelling occur at this end of the section. From data farther offshore than this section it appears that the California Current is stronger in summer and that some deepening of the deeper isotherms may result: this is suggested in figure 31 but the data

are not so conclusive as those inshore.

II.C. Oxygen and nutrient distribution.

II.C.1. Oxygen. The distribution of dissolved oxygen in the area of the California Current has been discussed by Reid, Roden and Wyllie (1958) and more recently by Reid (in press) for the entire Pacific Ocean.

Since oxygen from the atmosphere dissolves in greater quantity in colder less saline water, the surface waters of the California Current are fairly high in oxygen concentration. Since the mixed layer of the ocean is in constant contact with the atmosphere the value of oxygen in the surface waters is nearly always quite near the saturation value for the temperature and salinity, regardless of consumption or production in the mixed layer (Reid, 1962c). Beneath the mixed layer the replenishment by vertical diffusion from the upper layer is limited by the stability of the water column and processes of lateral replenishment (by water having sunk from the surface in high latitudes) are limited by the distance of the sources and the consumption that take place in transit: for these reasons the deeper values of oxygen are generally lower than those at the surface.

The California Current receives oxygen-rich water (4.5 to 7 ml/L) from the relatively cold West Wind Drift at the surface. At great depth another supply comes from the northward-flowing bottom water, of about 3.5 ml/L. The water of the 200-m Countercurrent is relatively low in oxygen (as it is high in temperature and salinity) since it contains a large mixture of water from the equatorial region, where subsurface values less than 0.2 ml/L are found over large areas. As a result the water of the California Current system beneath the surface layer are generally much lower inshore than offshore. This is clearly illustrated in Reid, Roden and Wyllie (1958) in their figures 5(c) and 13: the very lowest values in the Point Arguello

region are found in the deep cold tongue (the boundary between the California Current and the 200-m Countercurrent, where the deeper, denser waters lie at somewhat shallower depths referred to in section II.B.1.).

The seasonal variation of oxygen in the upper 150 m (above which it is most marked) is seen in figure 32, which is representative of the area near Point Arguello. The surface values follow the seasonal variation of surface temperature, being highest in the cold period (March-May) and lowest in late fall. A curious feature is that beneath the upper few meters (about 20 meters in this case) the high values attained in March, when the mixed layer is thickest and coldest, continue throughout October, though the surface values give off oxygen to the atmosphere when they are heated in summer: beneath the summer thermocline an oxygen maximum is seen. Reid (1962c) has shown that this situation obtains throughout the California Current system, and indeed over all of the North Pacific that is subject to substantial seasonal overturn and temperature variation.

Beneath the mixed layer the oxygen varies, as do the temperature and salinity, as a consequence of the variations in flow discussed in section II.B.3.: The deeper waters rise nearest the surface in April-June as a result of the upwelling and the change from northward to southward flow above 150 m. Since the deeper waters are poorer in oxygen the oxygen concentration at 75 to (at least) 150 m is lowest in April to June. It is emphasized that this change in oxygen concentration appears to be a consequence of a physical readjustment of the water masses, not a direct result of seasonal changes in the biological processes.

II.C.2. Nutrients. The general distribution of inorganic phosphate-phosphorus in the California Current has been discussed by Reid, Roden and Wyllie (1958) and Reid (1962d).

Phosphate, like the other plant nutrients, is consumed in the lighted zone of the ocean and regenerated at depth by decay. It is generally in lower concentration in the mixed layer than below it because the upward diffusion of phosphate, like the downward diffusion of oxygen, is limited by the stability of the water column. The upward transfer of phosphate, then, is much enhanced by the upwelling that occurs along the coast of California as a consequence of the prevailing northwesterly winds. The California Current is rich in phosphate not only because of the upwelling but because of the relatively high concentration of the water entering from the West Wind Drift, which is itself an area of surface divergence and upward transfer of deep water. A third factor in enriching the water immediately beneath the mixed layer is the adjustment of the water masses toward geostrophic equilibrium: the southward flowing water must have the densest water, of deepest origin, on its inshore edge, and the northward flowing water must have the densest water on its offshore side: the "ridge" of denser water that rises near the surface (figs. 20-23) between these two currents maintains a relatively high concentration of phosphate. This feature is clearly illustrated in figure 5d of Reid, Roden and Wyllie (1958) and discussed further by Reid (1962d) for the entire Pacific Ocean.

At the surface it is the upwelling that most severely affects the variation of phosphate. In figure 33 is seen the average variation near Point Arguello. It is relatively low (though not in terms of mid-ocean values) in the Countercurrent period but rises abruptly in April and remains high throughout the period of intense upwelling off Point Arguello. Although the data for this graph are rather sparse they indicate a wide range of variation about this mean, partly as a **result** of year-to-year variations but possibly as a result of very short-period fluctuations in the rate of upwelling



or of consumption by plants.

Farther offshore the mean values are lower and the range of variation is much reduced.

### III. RESULTS OF THE MORE CLOSELY SPACED OBSERVATIONS OFF POINT ARGUELLO IN JANUARY AND JUNE OF 1964.

#### III.A. January 1964.

##### III.A.1. Current.

III.A.1.a. Surface current. The surface flow of the California Current in January 1964 is seen in figure 34. The area near Point Arguello is seen in greater detail in figure 35 (which also shows the trajectories of the drogues released during the cruise) and the recoveries of drift bottles are shown in figure 36.

In general the flow was similar to that in most of the Januarys observed since 1949. The Countercurrent is well developed in the northern part of the area but is hardly apparent in the area off Baja California. Compared with the January flow in 1958 (fig. 1), for example, it is much reduced.

The closer spacing of the data in the area of Point Arguello (fig. 35) will show greater detail than that seen in the average flow (fig. 8). Also, the effect of the non-seasonal variations have been reduced in the averaging process, so a smoother chart is to be expected. It seems reasonable to infer, however, that the inshore Countercurrent was stronger in January 1964 (fig. 35) than in the mean January chart (fig. 8) though not necessarily stronger than the flow in January 1958.

The drogues (fig. 35) were released in the inshore area in order to get direct current measurements where the water is shallowest and the

geostrophic approximation likely to be least useful. They show an excellent agreement with the calculated geostrophic flow at the surface.

Likewise the drift bottles (fig. 36) recovered from the releases in January 1964 seem to fit the pattern of surface geostrophic flow. Recoveries from those released inshore were nearly always from north of the release point: recoveries from those farther offshore and south of the Channel Islands were in general agreement with the surface flow shown on figure 34.

III.A.1.b. Subsurface current. The deeper flow in January 1964 (fig. 35) is much like the surface flow, since this is in the season of the inshore Countercurrent. At 100 m and below the northward flow is slower but somewhat wider than at the surface.

### III.A.2. Temperature and salinity.

III.A.2.a. Horizontal distribution. The distribution of temperature and salinity at the surface, 50, 100, 150 and 200 m depth is shown in figures 37-39. Except for the greater detail in January 1964 the distribution of surface temperature is very much like the mean January temperature (fig. 17): the area may be as much as half a degree warmer inshore in January 1964. The surface salinity in January 1964 is definitely higher than the mean: this is consonant with the slightly higher temperature and the slightly stronger surface Countercurrent (section III.A.1.).

At 50 m depth the inshore temperatures in January 1964 are higher than the mean but the cold tongue is somewhat colder: this may indicate an intensification of the Countercurrent in 1964 or it may reflect only the extra detail given by the more closely spaced stations. The salinity at 50 m is much higher in the January 1964 map than in the mean: this seems to indicate an intensified Countercurrent as well as an increase in amount of detail.

At 100 m depth (fig. 38) January 1964 is definitely warmer inshore and about the same as the average offshore. The 100-m salinity also is higher inshore than the mean (fig. 19) and about average offshore. At 150 and 200 m depth (figs. 38 and 39) the temperature in January is still above average (fig. 20) inshore but the salinity is of about average value, though more detail is shown.

III.A.2.b. Vertical sections. A vertical section of temperature and salinity in a line extending southwestward from Point Arguello is shown in figure 40 (position of the section is shown in figure 26). At the inshore end of the section the isotherms from 6 to 10°C lay deeper in 1964 than in the January average (fig. 31), in some cases by almost 100 m. Offshore they lay at about the average depth. The January 1964 salinity was more nearly like the average except for the inshore surface layer, which was about 0.20‰ high.

III.B. June 1964.

III.B.1. Current.

III.B.1.a. Surface current. The surface flow of the California Current in June 1964 is seen in figure 41. The area near Point Arguello is seen in greater detail in figure 42 and the recoveries of drift bottles are shown in figure 43.

In general the flow at the surface in June 1964 (fig. 41) is much like the flow in most of the other Junes observed since 1949. The most significant feature of the June flow is the presence of more meanders and eddies, particularly near and north of Point Arguello, than are found in January. The seasons are different not only in the strength of flow and the sense of the inshore flow, but in that summer is a period of intense upwelling in the northern area. This upwelling does not occur as a smooth and regular

feature all along the coast but at least in part as a series of eddies generated at the coast and carried offshore, spinning counterclockwise (cyclonically) as they drift southward with the flow. The more intense the grid of observations the more of these eddies are observed. The average current maps for June-August (fig. 9) are not based on very close grids, and the averaging process smooths out the presence of these eddies, which are of different sizes and do not always follow exactly the same track. As a result the June-August maps (fig. 9) are smooth. But in June of 1964 the grid was tight and an eddy was observed in considerable detail in the northwestern part of the area.

The eddy inside the Channel Islands is clearly present in June 1964 (fig. 42). It may be more strongly developed than the average (fig. 9) or it may only appear so as a result of the greater detail displayed by the closer observations. Likewise, the offshore southward flow is shown. But the significantly different feature is the cyclonic eddy-like feature.

The recoveries of drift bottles released near Point Arguello are indicated in figure 43. Only one was recovered north of Point Arguello and this was found six months after release: it may have gone aground in the south and then been carried northward much later in the year. Most of the recoveries were made south of the release point, as would be expected from the calculated geostrophic flow at the surface.

III.B.1.b. Subsurface current. The eddy is still apparent at 100 m depth (fig. 42): at 150 and 200 m depth the flow is not substantially different from the average June flow (fig. 14).

III.B.2. Temperature and salinity.

III.B.2.a. Horizontal distribution. The distribution of temperature and salinity at the surface, 50, 100, 150 and 200 m depth in June

1964 is shown in figures 44-46. The June 1964 surface temperature distribution (fig. 44) is of course much more complex than the mean (fig. 21). The surface waters are generally colder than the average, particularly in the north, in the region of the eddy. Surface salinity is generally higher, indicating more than the average effect of upwelling, and the northern eddy shown in the surface current (fig. 42) is clearly seen to be characterized by a patch of more saline as well as colder water, sure evidence of its sub-surface origin.

At 50 m depth the June 1964 temperature (fig. 44) is everywhere lower and the salinity everywhere higher than the average, but in both properties the greatest difference from the average is found in the patch of upwelled water at the center of the northern eddy.

Likewise at 100 m depth (fig. 45) the June 1964 map shows slightly colder and more saline water everywhere, but extreme values in the eddy.

At 150 and 200 m depth (fig. 45) the temperature and salinity in June are much like the average (fig. 24): it is more complex because of the extra observations but the values are nearly the same. The main strength of the northern eddy seems to have been confined above 150 m depth.

III.B.2.b. Vertical sections. A vertical section of temperature and salinity in June 1964 in a line extending southwestward from Point Arguello is shown in figure 47 (position of the section is shown in figure 26). This can be compared with the July average sections (fig. 28) since figures 30 and 31 indicate the average June and July values are fairly close.

As in January 1964 there are some differences in absolute values but the principal difference is in the additional detail, with the effect of the eddying upwelled water dominant in the upper 200 m. From the salinity section (fig. 47) in particular it appears that some major deviation from

the seasonal pattern occurred in June 1964 at depths as great as 300 or 400 m: this may be a part of the effect of the eddy of upwelled water (which is extreme above 150 m depth) or it may not be related directly to the overlying water. The speed of the flow is much greater above 100 m depth than below, so that a vertically continuous feature from the surface to 300 or 400 m may not remain vertically continuous for more than a very few days: after the original impetus the upper part may drift southward leaving the deeper part behind. This deep disturbance, at 300 to 400 m may be a relic of a previous eddy that has passed by or it may be a feature of internal readjustment that is not related at all directly to the surface eddies.

The flow at 200 m (fig. 35) in January of 1964 does not indicate so severe a difference from the mean as the salinity section (fig. 47) suggests. The salinity and temperature deviations in the greater depths act in opposite sense (i.e., lower salinity with lower temperature, etc.) upon the density distribution. This means that the redistribution does not necessarily require a large energy input. The low-salinity, low-temperature area at about 200 to 400 m depth on the section (fig. 47) rather suggests an influx of offshore water from about the same depth (water of about such values can be seen at the offshore end of the mean July vertical section (fig. 28). Likewise, the anomalously warm and saline water at about 200 to 400 m depth in June 1964 has almost the same characteristics as the inshore water on the mean section. An east-west readjustment of water of about the same density has occurred: the mechanism is obscure.

### III.C. Oxygen and nutrient distribution in January and June 1964.

Until recently only a few observations of nutrient concentration had been made in this area: there is not a well-defined average of phosphate

(and none at all of silicate) against which the observations in January and June can be examined. The general relation of oxygen and nutrients to the upper and deeper levels of the ocean has been discussed in section II.C. and the maps of oxygen, phosphate, and silicate (figs. 48-53) can be seen to fit into the general description quite well. The distribution of dissolved oxygen, inorganic phosphate-phosphorus, and silicate at 0, 100 and 200 m depth for January and June 1964 are shown in figures 48-53.

In January 1964 the surface Countercurrent obtains and little upwelling occurs: the temperatures are highest inshore (fig. 37) and as a result the oxygen concentration is lowest inshore. Phosphate at the surface appears to be slightly lower and silicate slightly higher in the countercurrent.

At 100 m depth (fig. 49) the oxygen is seen to be low and both phosphate and silicate high in the countercurrent water (fig. 35).

At 200 m depth (fig. 50) the lowest values of oxygen, and the highest values of phosphate and silicate are found on the ridge of denser water at the boundary between the Countercurrent and the California Current (see section II.C.1.).

In June 1964 when coastal upwelling was occurring and an offshore eddy of upwelled water was seen, the lowest values of oxygen at the surface (fig. 51) were found in the newly-upwelled water extending southward from Point Arguello. This was very cold water, and the low values of oxygen indicate undersaturation: the water had not yet been in contact with the atmosphere long enough to come into equilibrium from its previous low subsurface values. The offshore eddy water had become saturated, however.

The newly-upwelled water at the surface was higher in both phosphate and silicate (fig. 51): the enrichment was more obvious near the Channel Islands than in the offshore eddy.

At 100 m depth (fig. 52) the water both near the Channel Islands and in the offshore eddy shows its deeper origin by lower values of oxygen and higher values of both phosphate and silicate.

At 200 m depth (fig. 53) the lowest values of oxygen and the highest values of phosphate and silicate are found inshore.

Oxygen, phosphate, and silicate all show notable differences between their January 1964 and June 1964 distributions. Oxygen is lower and phosphate and silicate higher in the upwelled water found in June at both 0 and 100 m depth. At 200 m depth upwelling is less effective, yet a substantial change occurs. In January when the deep Countercurrent is well developed the ridge of deeper water between the Countercurrent and the California Current is well developed and shows the lowest oxygen and the highest phosphate and silicate at that depth (fig. 50). But in June the Countercurrent has weakened and the California Current has strengthened: geostrophic balance requires an upward movement of denser water to the 200 m level, and it is inshore in the Countercurrent, not in the ridge between the currents, that the lowest oxygen values and the highest phosphate and silicate values occur (fig. 53).

#### IV. COMMENT ON THE EDDIES OF UPWELLED WATER

The eddy observed in June 1964 had some characteristics like those of the eddy off Baja California in October 1959 described by Reid, Schwartzlose and Brown (1963). Both were cyclonic, about 40 or 50 miles in diameter, and confined well above 200 m; the density difference was a result of colder, more saline water in the eddy. They differ in that the June 1964 eddy was distinguished from its surroundings by colder, more saline water in the mixed layer: the eddy off Baja California in October of 1959 was not



distinguished by the properties in the mixed layer or by the depth (40 m) of the mixed layer: its extreme feature was the steeper vertical gradients in the pycnocline (50-100 m) that made the water between 50 and 150 m colder and more saline than the surrounding waters in that depth range.

Perhaps these differences are a result of the different "age" of the eddies. Presumably that off Point Arguello was newly upwelled water. That off Baja California was much farther from shore: if it had originated from coastal upwelling then it had certainly traveled farther from its point of origin than had the Point Arguello eddy. Possibly lateral mixing with the adjacent waters had reduced the extreme values in the mixed layer, with the geostrophic balance being maintained entirely by the horizontal gradients at the depth of the pycnocline.

These eddies are of particular interest and significance in terms of the lateral mixing and turbulent diffusion of properties in the ocean. A mixing scale of 40 to 50 miles is suggested by each of these: other eddies have been observed, but with a wider grid the scale cannot be so nicely judged, and many may have escaped the network entirely.

## V. DISPOSITION OF THE WATERS IN THE POINT ARGUELLO REGION

### V.A. Flow and dilution.

The trajectories of the waters departing the Point Arguello region are indicated by drift bottles, drogues, calculated geostrophic flow, and the nature of various water masses.

V.A.1. The surface flow. The surface flow is indicated for some distance along the coast by the recoveries of drift bottles. Schwartzlose (1963) has shown that a high percentage of those released within 20 miles of the coast will be found on the beaches, either nearby or at great distances

to the north or south. Of those released farther offshore only a few are recovered: the rest drift offshore and presumably sink after some weeks or months as a result of marine growth upon their surfaces. Therefore the lack of recoveries from the Hawaiian Islands, etc., does not indicate that water from the California area does not eventually pass these Islands.

V.A.2. The California Current water. The surface and shallow waters of the offshore California Current can be traced (Reid, in press) by their low salinity through the North Equatorial Current and the North Equatorial Countercurrent (into which they mix laterally: they do not extend in a recognizable form south of the equator). In the central Pacific between the equator and about 20°N a salinity minimum lying at various depths from 75 to 200 m beneath the surface is clearly water that has come from the West Wind Drift, passing southward along the coast of Washington, Oregon, California and Baja California, turning southwestward at about 20°N. During the flow it mixes with both deeper and overlying less dense waters and the salinity and temperature have been substantially altered by the time it reaches the central Pacific: a large amount of dilution has occurred.

V.A.3. The California Countercurrent water. The nearshore subsurface waters move northward throughout the year: the relatively saline, warm, and nutrient-rich waters appearing beneath the surface off Oregon, Washington, and British Columbia have been transported northward along the coast of California. They also are subject to substantial dilution (as their decreasing values of temperature and salinity indicate) by mixing with the overlying cold low-salinity water.

V.A.4. The basin water. Water within the deep basins off southern California might be thought to be fairly immobile and free from exchange with the overlying waters. Emery (1954) however has pointed out

that the oxygen concentration of most of the water within these basins remains about equal to the concentration at the sill depth of the basin: only quite near the bottom may the oxygen decrease. Since oxygen is consumed within the basins but not regenerated, this may be taken to imply that substantial exchange with sill-depth water (of the same potential density) does take place, effectively renewing the oxygen concentration of the water except within a few meters of the bottom, where the bottom-dwelling organisms and the sediment may cause some depletion.

V.B. The effect upon other water masses.

These indications of flow are only the more obvious evidences of the effect of California Current water. The effect of these waters upon those which surround them (both laterally and vertically) must be equal to the effect of the other waters in diluting those of the California Current. The scale upon which such mixing takes place in the open ocean is not well understood. Closely-spaced measurements that reveal transient eddies of the kind discussed above have not been made in the open ocean, but eddies of this scale (or larger or smaller) may well obtain.

It has been pointed out above that although the California Current waters have been diluted as they flow, they are recognized over great distances in some cases. The sudden disappearance of the shallow salinity minimum at the equator does not signify that no California Current water moves across it, but only that at the level of the recognizable California Current water intense vertical mixing takes place in or below the Equatorial Undercurrent. The salinity minimum disappears as a feature in this process but the waters that emerge to the south are nevertheless lower in salinity because of an admixture of the California Current water.

Likewise, waters far to the west and to the southeast of the California

Current contain some mixture of the California Current waters: the proportions are uncertain, since the effects of exchanges through the sea surface and with the deeper waters must also be considered. Such calculations are also inhibited by the fact that there is no "pure" California Current water: it is itself a mixture of the surrounding water masses altered somewhat by vertical exchange.

REFERENCES

- Bien, G. S., N. W. Rakestraw and H. E. Suess, 1960. Radiocarbon concentration in Pacific Ocean water: Tellus 12(4), 436-443.
- Brown, D. M., 1962. Results of current measurements with drogues, 1958-1961: Scripps Inst. Oceanogr. Data Rep., SIO Ref. 62-27, 64 pp.
- California Cooperative Oceanic Fisheries Investigations, 1963. CalCOFI Atlas of 10-meter Temperatures and Salinities 1949 through 1959, Atlas No. 1, 297 plates.
- Emery, K. O., 1954. Source of water in basins off Southern California: J. Mar. Res. 13(1), 1-21.
- Knauss, J. A., 1962a. Observations of internal waves of tidal period made with neutrally-buoyant floats: J. Mar. Res. 20(2), 111-118.
- Knauss, J. A., 1962b. On some aspects of the deep circulation of the Pacific: J. Geophys. Res. 67(10), 3943-3954.
- Prestwich, Joseph, 1875. Tables of temperatures of the sea at different depths beneath the surface, reduced and collated from the various observations made between the years 1749 and 1868, discussed: Philosoph. Trans. of the roy. Soc. 165, Part II, 587-674, pl. 65-68.
- Reid, J. L., Jr., 1956. Observations of internal tides in October 1950: Trans. Amer. Geophys. Union 37, 278-286.
- Reid, J. L., Jr., 1958. A comparison of drogue and CEK measurements in deep water: Limnol. & Oceanogr. 3(2), 160-165.
- Reid, J. L., Jr., 1960. Oceanography of the northeastern Pacific Ocean during the last ten years: In Calif. Coop. oceanic Fish. Invest. Reps., 1 January 1958 to 30 June 1959, Mar. Res. Comm., Calif. Fish Game, 1, 77-90.

- Reid, J. L., Jr., 1961. On the geostrophic flow at the surface of the Pacific Ocean with respect to the 1000-decibar surface: Tellus 13(4), 489-502.
- Reid, J. L., Jr., 1962a. Observations of inertial rotation and internal waves: Deep-Sea Res. 9, 283-289.
- Reid, J. L., Jr., 1962b. Measurements of the California Countercurrent at a depth of 250 meters: J. Mar. Res. 20(2), 134-137.
- Reid, J. L., Jr., 1962c. Distribution of dissolved oxygen in the summer thermocline: J. Mar. Res. 20(2), 138-148.
- Reid, J. L., Jr., 1962d. On the circulation, phosphate-phosphorus content and zooplankton volumes in the upper part of the Pacific Ocean: Limnol. & Oceanogr. 7(3), 287-306.
- Reid, J. L., Jr., 1963. Measurements of the California Countercurrent off Baja California: J. Geophys. Res. 68(16), 4819-4822.
- Reid, J. L., Jr., in press. Intermediate waters of the Pacific Ocean: Johns Hopkins Oceanographic Studies, no. 2.
- Reid, J. L., Jr., and R. J. Lynn, 1964. The distribution of water properties at deep and abyssal depths beneath the California Current: Final Report to the U. S. Atomic Energy Commission, UCSD-34P97-1, 19 pp., 9 figs.
- Reid, J. L., Jr., G. I. Roden and J. G. Wyllie, 1958. Studies of the California Current system: Calif. Coop. oceanic Fish. Invest., Progr. Rep. 1 July 1956 to 1 Jan. 1958. Mar. Res. Comm., Calif. Fish Game, 28-56.
- Reid, J. L., Jr., and R. A. Schwartzlose, 1962. Direct measurements of the Davidson Current off Central California: J. Geophys. Res. 67(6), 2491-2497.

- Reid, J. L., Jr., R. A. Schwartzlose and D. M. Brown, 1963. Direct Measurements of a small surface eddy off northern Baja California: J. Mar. Res. 21(3), 205-218.
- Schwartzlose, R. A., 1963. Nearshore currents of the western United States and Baja California as measured by drift bottles: Calif. Coop. oceanic Fish. Invest. Rep. 9, 15-22.
- Sverdrup, H. U. and R. H. Fleming, 1941. The waters off the coast of Southern California March to July, 1937: Scripps Inst. Oceanogr. Bull. 4(10), 261-378.
- Wooster, W. S. and G. H. Volkmann, 1960. Indications of deep Pacific circulation from the distribution of properties at five kilometers: J. Geophys. Res. 65(4), 1239-1249.
- Wüst, Georg, 1937. Bodentemperatur und Bodenstrom in der Pazifischen Tiefsee: Veröff. Inst. Meeresk. Univ. Berlin, N. F., A. Geogr.-Naturwiss., 35, 1-56.

DATA SOURCES

- Scripps Institution of Oceanography, Univ. Calif., 1957. Oceanic Observations of the Pacific: 1949. Berkeley and Los Angeles, Univ. Calif. Press, 363 pp.
- Scripps Institution of Oceanography, Univ. Calif., 1960a. Oceanic Observations of the Pacific: 1950. Berkeley and Los Angeles, Univ. Calif. Press, 536 pp.
- Scripps Institution of Oceanography, Univ. Calif., 1963a. Oceanic Observations of the Pacific: 1951. Berkeley and Los Angeles, Univ. Calif. Press, 598 pp.
- Scripps Institution of Oceanography, Univ. Calif., 1965a. Oceanic Observations of the Pacific: 1952. Berkeley and Los Angeles, Univ. Calif. Press, 617 pp.
- Scripps Institution of Oceanography, Univ. Calif., 1965b. Oceanic Observations of the Pacific: 1953. Berkeley and Los Angeles, Univ. Calif. Press, 576 pp.
- Scripps Institution of Oceanography, Univ. Calif., 1965c. Oceanic Observations of the Pacific: 1954. Berkeley and Los Angeles, Univ. Calif. Press, 426 pp.
- Scripps Institution of Oceanography, Univ. Calif., 1962. Oceanic Observations of the Pacific: 1955. Berkeley and Los Angeles, Univ. Calif. Press, 477 pp.
- Scripps Institution of Oceanography, Univ. Calif., 1960b. Oceanic Observations of the Pacific: 1955, the NORPAC Data. Berkeley and Tokyo, Univ. Calif. Press and Univ. Tokyo Press, 582 pp.



Scripps Institution of Oceanography, Univ. Calif., 1963b. Oceanic Observations of the Pacific: 1956. Berkeley and Los Angeles, Univ. Calif. Press, 458 pp.

Scripps Institution of Oceanography, Univ. Calif., 1965d. Oceanic Observations of the Pacific: 1957. Berkeley and Los Angeles, Univ. Calif. Press, 707 pp.

Scripps Institution of Oceanography, Univ. Calif., 1965e. Oceanic Observations of the Pacific: 1958. Berkeley and Los Angeles, Univ. Calif. Press, 804 pp.

Scripps Institution of Oceanography, Univ. Calif., 1965f. Oceanic Observations of the Pacific: 1959. Berkeley and Los Angeles, Univ. Calif. Press, 901 pp.

Scripps Institution of Oceanography, Univ. Calif., 1961a. Data Report, Physical and Chemical Data, CCOFI Cruise 6001, 8 Jan.-13 Feb. 1960. SIO Ref. 61-23, 1-90.

Scripps Institution of Oceanography, Univ. Calif., 1961b. Data Report, Phys. and Chem. Data, CCOFI Cruise 6002, 11 Feb.-3 Mar. 1960. SIO Ref. 62-3, 91-117.

Scripps Institution of Oceanography, Univ. Calif., 1961c. Data Report, Phys. and Chem. Data, CCOFI Cruise 6003, 10-29 Mar. 1960. SIO Ref. 62-5, 118-142.

Scripps Institution of Oceanography, Univ. Calif., 1961d. Data Report, Phys. and Chem. Data, CCOFI Cruise 6004, 29 Mar.-30 Apr. 1960. SIO Ref. 62-6, 143-227.

Scripps Institution of Oceanography, Univ. Calif., 1961e. Data Report, Phys. and Chem. Data, CCOFI Cruise 6005, 13-29 May 1960. SIO Ref. 62-7, 228-248.

- Scripps Institution of Oceanography, Univ. Calif., 1961f. Data Report,  
Phys. and Chem. Data, CCOFI Cruise 6006, 14-30 June 1960. SIO Ref.  
62-8, 249-272.
- Scripps Institution of Oceanography, Univ. Calif., 1962a. Data Report,  
Phys. and Chem. Data, CCOFI Cruise 6007-8, 15 July-29 Aug. 1960. SIO  
Ref. 62-9, 273-313.
- Scripps Institution of Oceanography, Univ. Calif., 1962b. Data Report,  
Phys. and Chem. Data, CCOFI Cruise 6008, 10-22 Aug. 1960, CCOFI Cr.  
6009, 9-21 Sep. 1960, CCOFI Cr. 6009-10, 22 Sep.-22 Oct. 1960. SIO  
Ref. 62-10, 314-375.
- Scripps Institution of Oceanography, Univ. Calif., 1961g. Data Report,  
Phys. and Chem. Data, CCOFI Cruise 6101-2, 5 Jan.-20 Feb. 1961. SIO  
Ref. 61-24, 1-49.
- Scripps Institution of Oceanography, Univ. Calif., 1961h. Data Report,  
Phys. and Chem. Data, CCOFI Cruise 6103, 8-13 Mar. 1961, CCOFI Cr.  
6104-5, 4 Apr.-12 May 1961, CCOFI Cr. 6105, 17-29 May 1961. SIO Ref.  
62-15, 53-107.
- Scripps Institution of Oceanography, Univ. Calif., 1962c. Data Report,  
Phys. and Chem. Data, CCOFI Cruise 6107-8, 12 July-1 Aug. 1961, CCOFI  
Cr. 6108, 13-28 Aug. 1961. SIO Ref. 62-16, 108-175.
- Scripps Institution of Oceanography, Univ. Calif., 1962d. Data Report,  
Phys. and Chem. Data, CCOFI Cruise 6109, 31 Aug.-19 Sep. 1961, CCOFI  
Cr. 6110-11, 10 Oct.-12 Nov. 1961. SIO Ref. 62-17, 179-226.
- Scripps Institution of Oceanography, Univ. Calif., 1962e. Data Report,  
Phys. and Chem. Data, CCOFI Cruise 6201-2, 12 Jan.-19 Feb. 1962. SIO  
Ref. 62-26, 1-50.

- Scripps Institution of Oceanography, Univ. Calif., 1963a. Data Report,  
Phys. and Chem. Data, CCOFI Cruise 6203-4, 15 Mar.-2 May 1962. SIO  
Ref. 63-9, 51-110.
- Scripps Institution of Oceanography, Univ. Calif., 1962f. Data Report,  
Phys. and Chem. Data, CCOFI Cruise 6207-8, 10 July-29 Aug. 1962. SIO  
Ref. 62-23, 1-33.
- Scripps Institution of Oceanography, Univ. Calif., 1963b. Data Report,  
Phys. and Chem. Data, CCOFI Cruise 6210-11, 5 Oct.-18 Nov. 1962, CCOFI  
Cr. 6212, 17-19 Dec. 1962. SIO Ref. 63-25, 143-193.
- Scripps Institution of Oceanography, Univ. Calif., 1963c. Data Report,  
Phys. and Chem. Data, CCOFI Cruise 6301-2, 10 Jan.-23 Feb. 1963. SIO  
Ref. 64-2, 1-54.
- Scripps Institution of Oceanography, Univ. Calif., 1964a. Data Report,  
Phys. and Chem. Data, CCOFI Cruise 6304, 9 Apr.-24 May 1963, CCOFI Cr.  
6306, 25-26 June 1963. SIO Ref. 64-13, 55-123.
- Scripps Institution of Oceanography, Univ. Calif., 1964b. Data Report,  
Phys. and Chem. Data, CCOFI Cruise 6307, 10 July-8 Aug. 1963, CCOFI Cr.  
6309, 3-29 Sep. 1963. SIO Ref. 64-18, 123-163.
- Scripps Institution of Oceanography, Univ. Calif., 1964c. Data Report,  
Phys. and Chem. Data, CCOFI Cruise 6310, 2-29 Oct. 1963, CCOFI Cr.  
6311, 28-29 Nov. 1963, CCOFI Cr. 6311 (El Golfo), 9 Nov.-7 Dec.  
1963. SIO Ref. 65-1, 163-203.
- Scripps Institution of Oceanography, Univ. Calif., 1965. Data Report, Phys.  
and Chem. Data, CCOFI Cruise 6401, 10 Jan.-4 Mar. 1964. SIO Ref. 65-7,  
1-76.

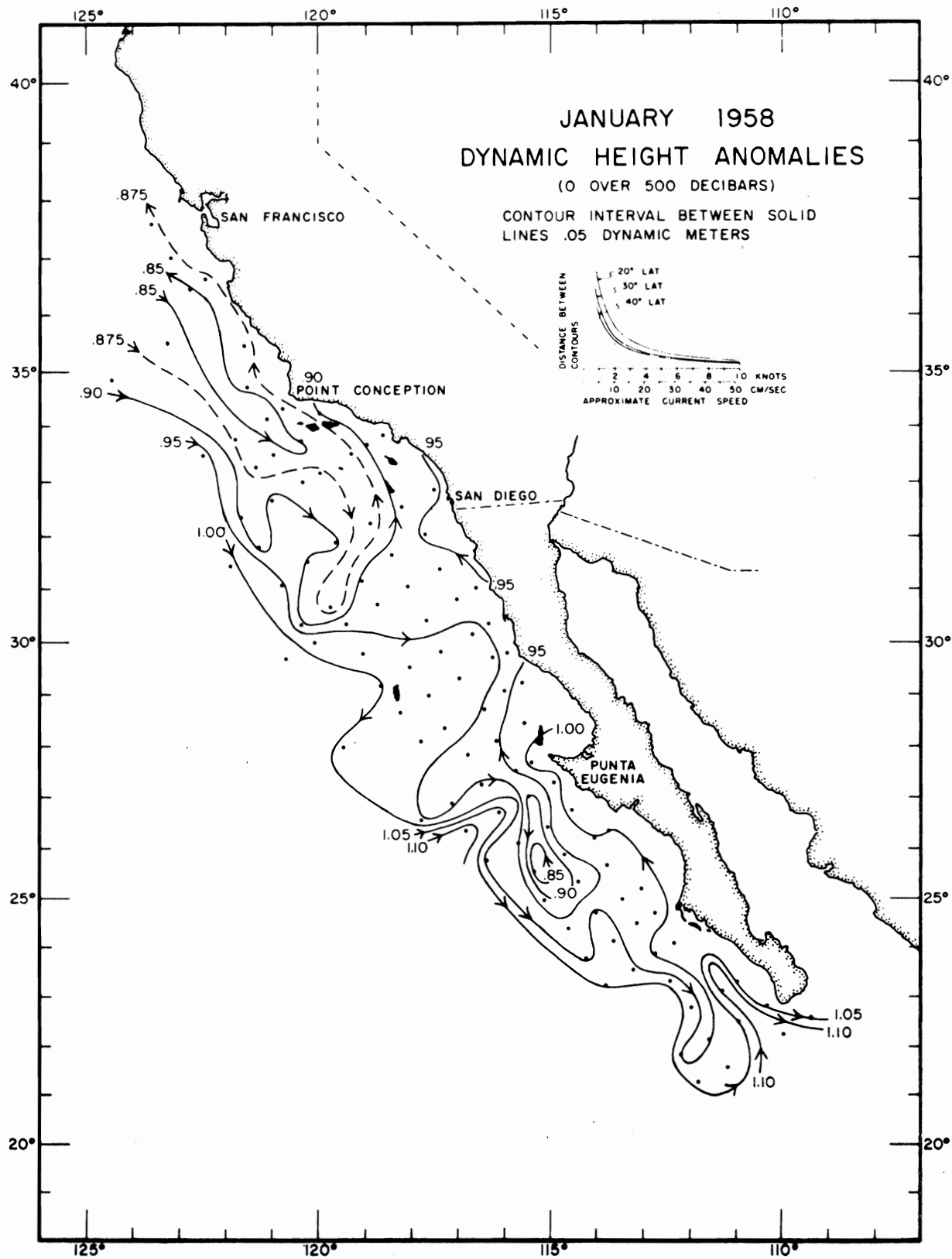


Fig. 1. Surface geostrophic flow in January 1958 (topography of the 0-decibar surface, in dynamic meters, relative to the 500-decibar surface).

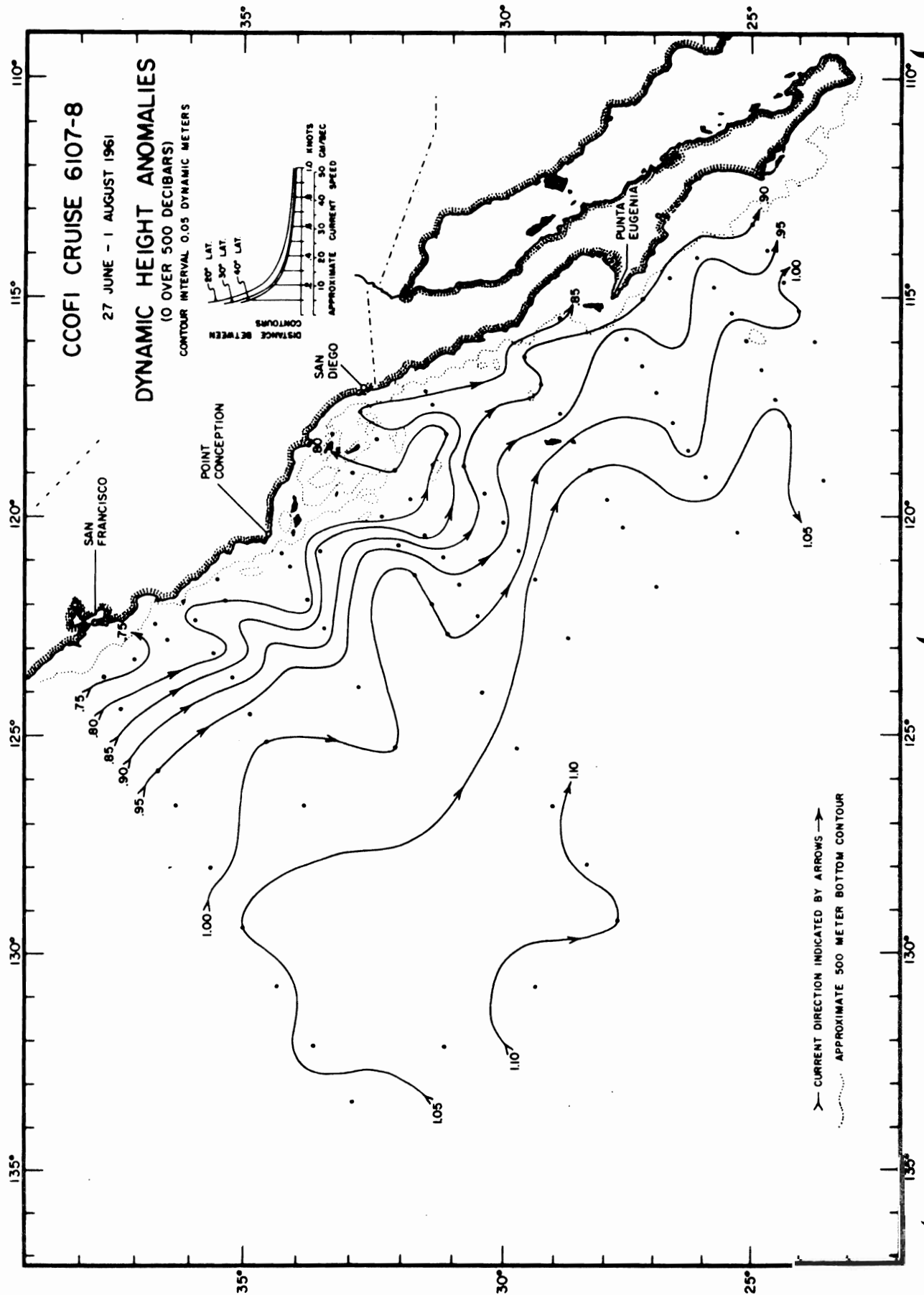


Fig. 2. Surface geostrophic flow in July 1961 (topography of the 0-decibar surface, in dynamic meters, relative to the 500-decibar surface).

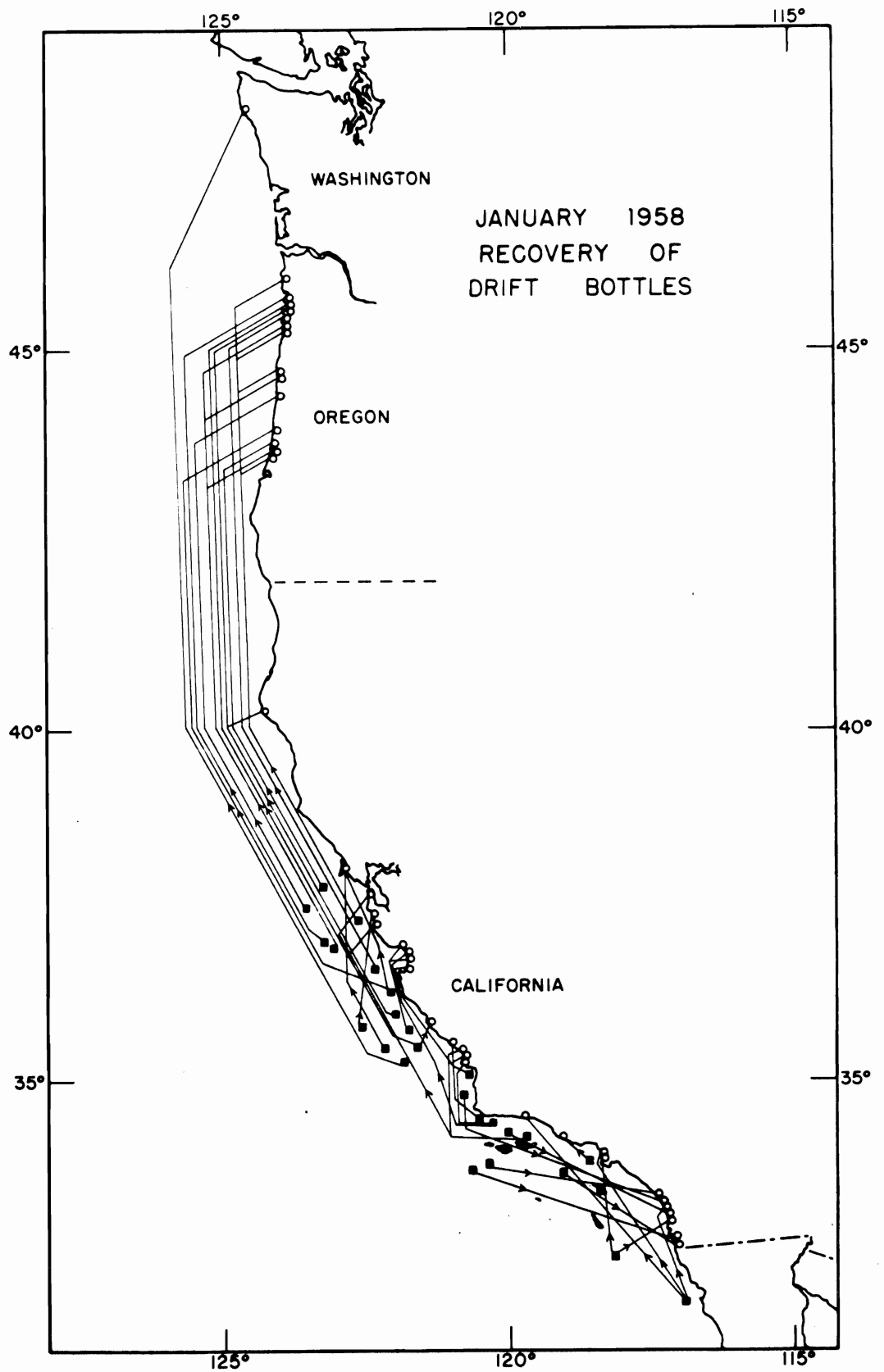


Fig. 3. Recoveries of drift bottles released in January 1958. Black squares show the release points, circles show the recovery points.

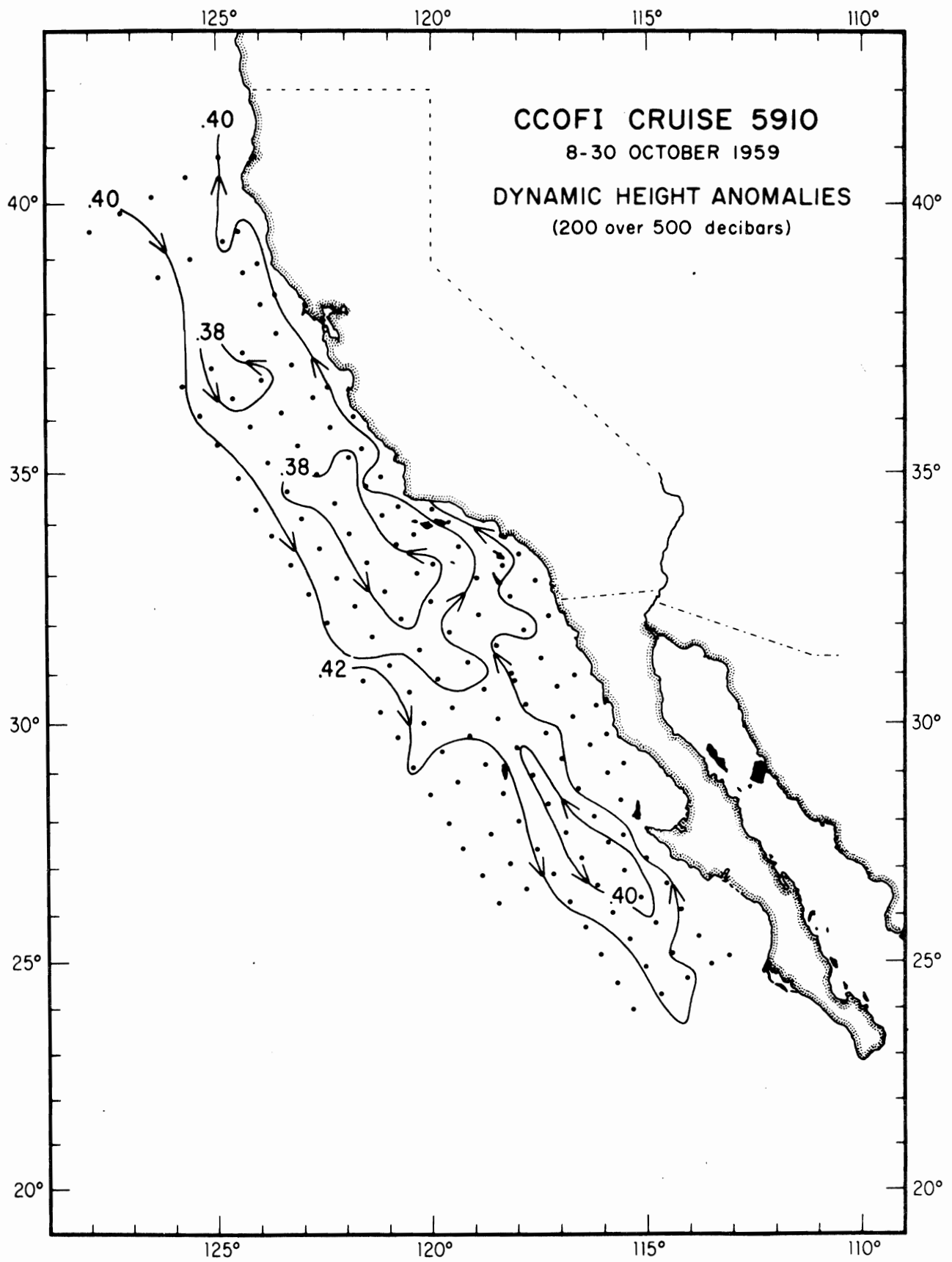


Fig. 4. Geostrophic flow at 200 meters in October 1959 (topography of the 200-decibar surface, in dynamic meters, relative to the 500-decibar surface).

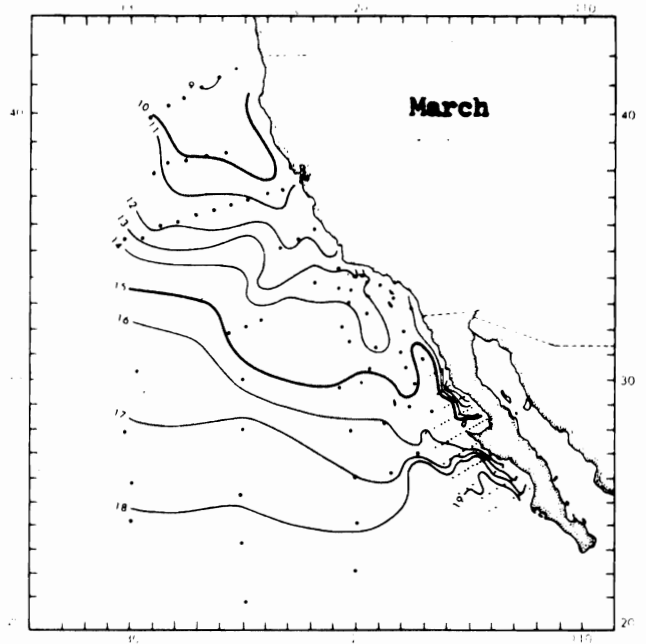
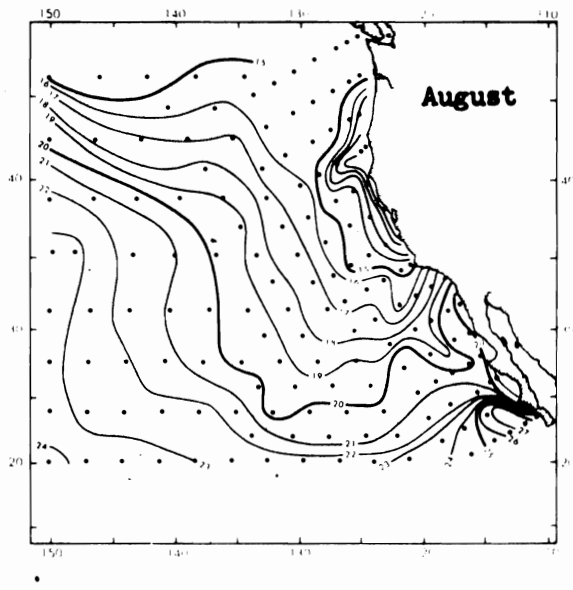


Fig. 5. Temperature ( $^{\circ}\text{C}$ ) at 10 m depth in August 1955 and March (composite).

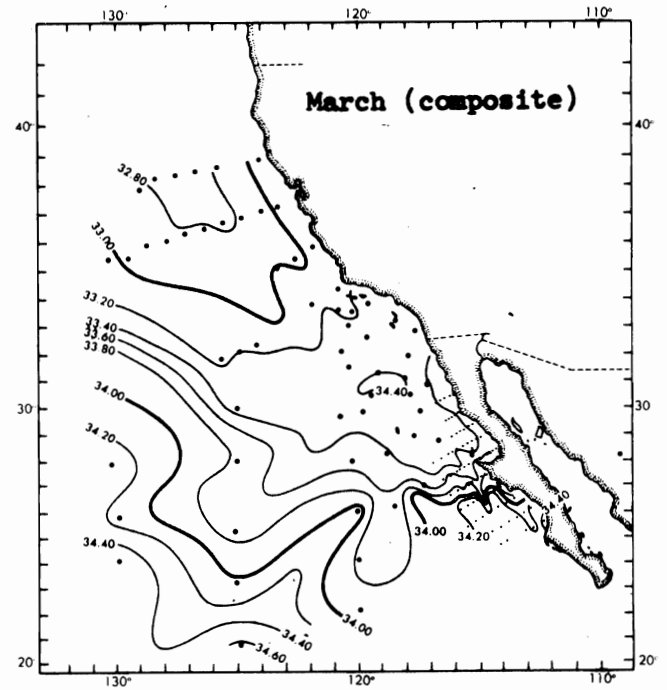
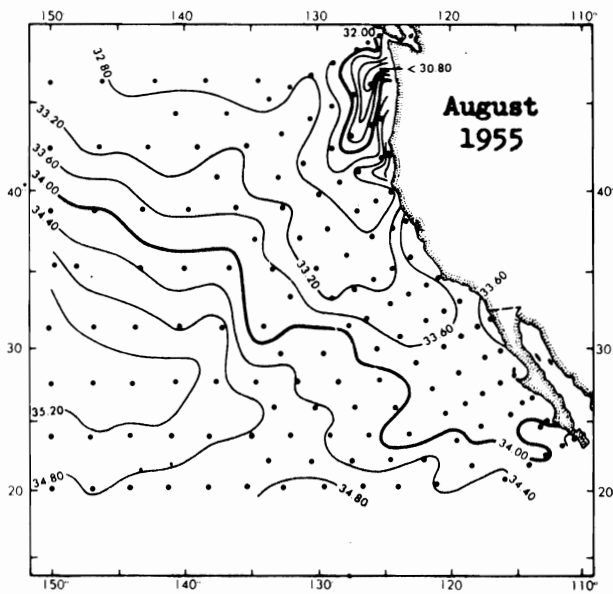


Fig. 6. Salinity ( $\text{‰}$ ) at 10 m depth in August 1955 and March (composite).



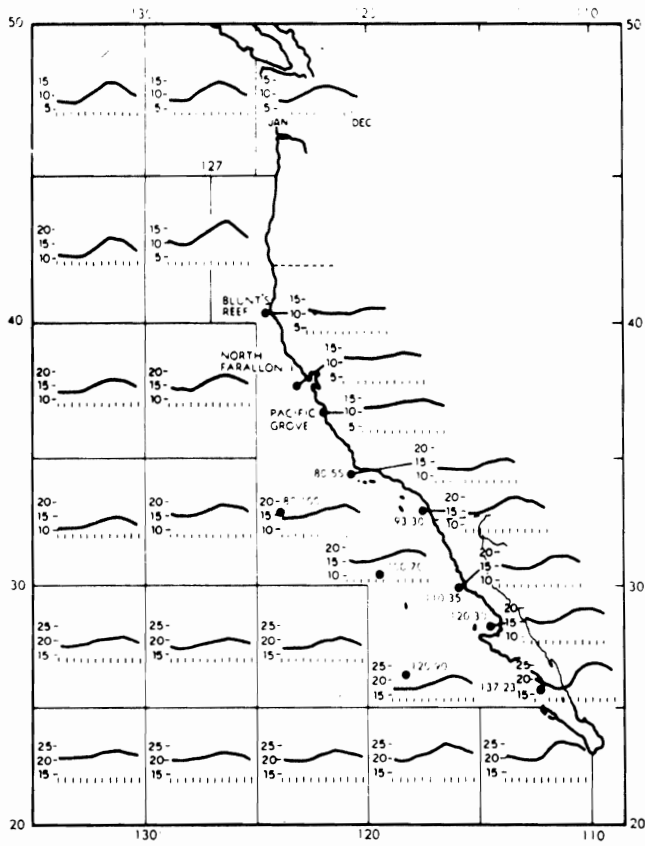
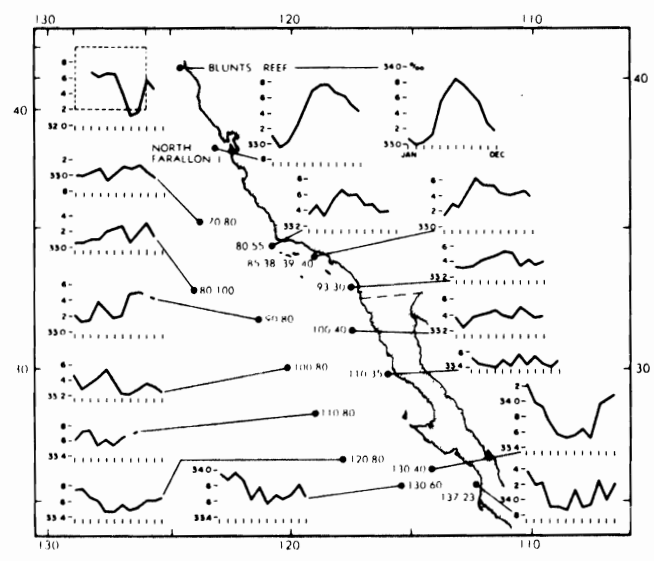


Fig. 7. Seasonal variation of temperature and salinity at the surface off the western coast of North America.

(a) Temperature in degrees Centigrade. Values over five-degree squares are from Robinson (1957); values at Blunt's Reef, North Farallon Island and Pacific Grove are from U.S. Coast and Geodetic Survey (1956); Values at numbered stations are from CCOFI data, 1949-55.



(b) Salinity in parts per mille. Value's at Blunt's Reef and North Farallon Island are from U.S. Coast and Geodetic Survey (1954); all other values are from CCOFI data, 1949-55.

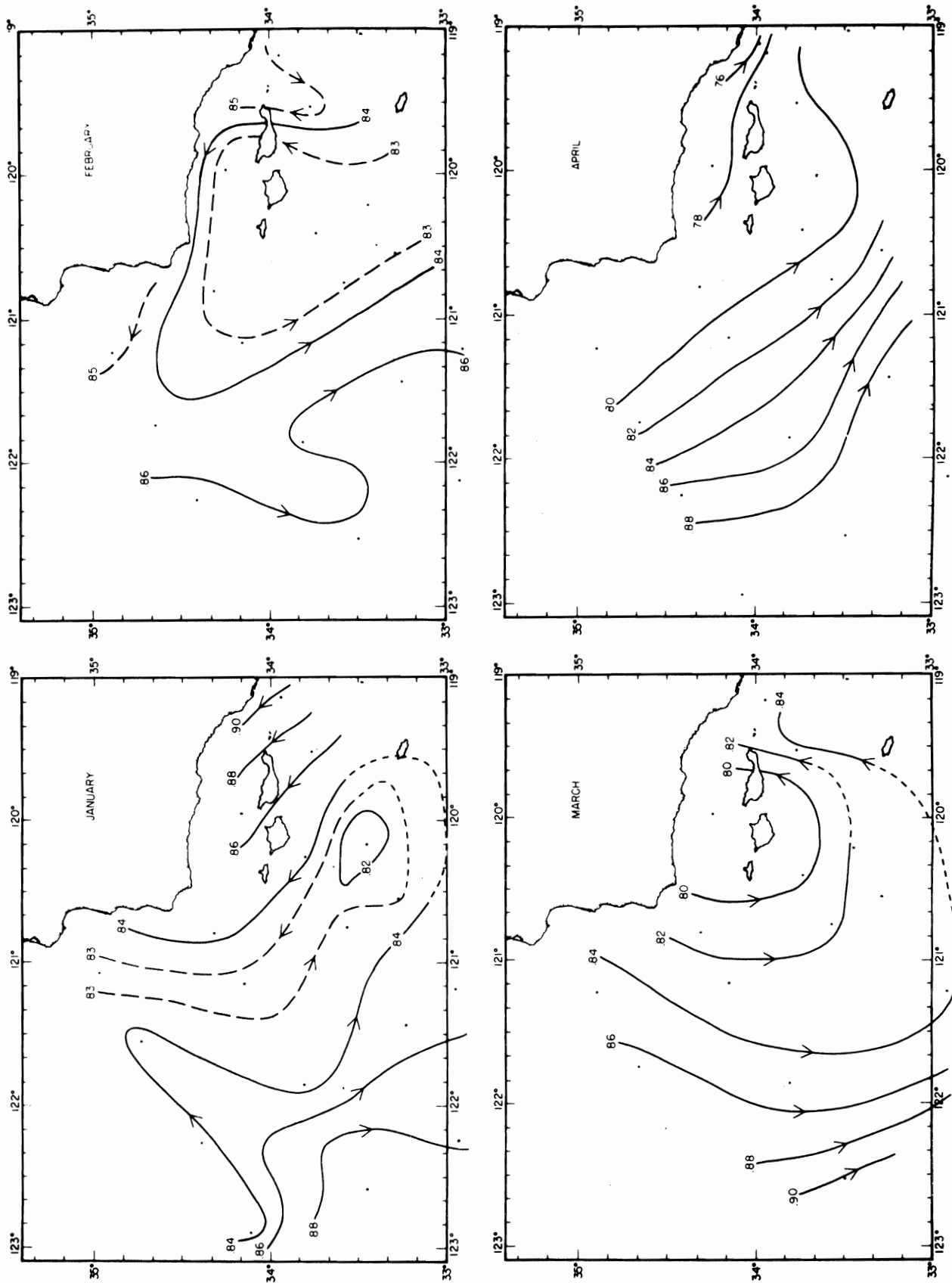


Fig. 8. Average surface geostrophic flow (topography of the 0-decibar surface, in dynamic meters, relative to the 500-decibar surface) in January, February, March, and April.

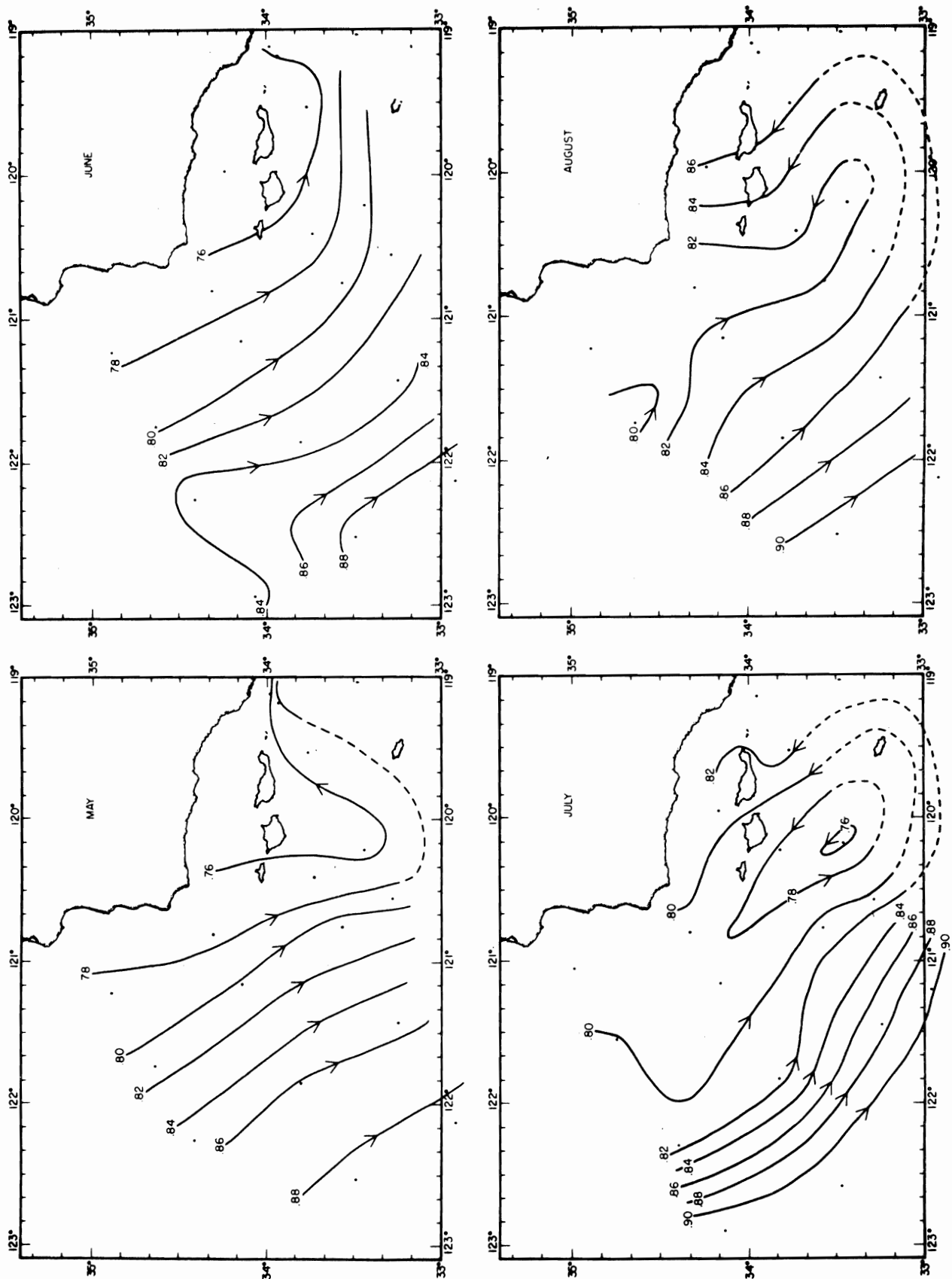


Fig. 9. Average surface geostrophic flow (topography of the 0-decibar surface, in dynamic meters, relative to the 500-decibar surface) in May, June, July, and August.

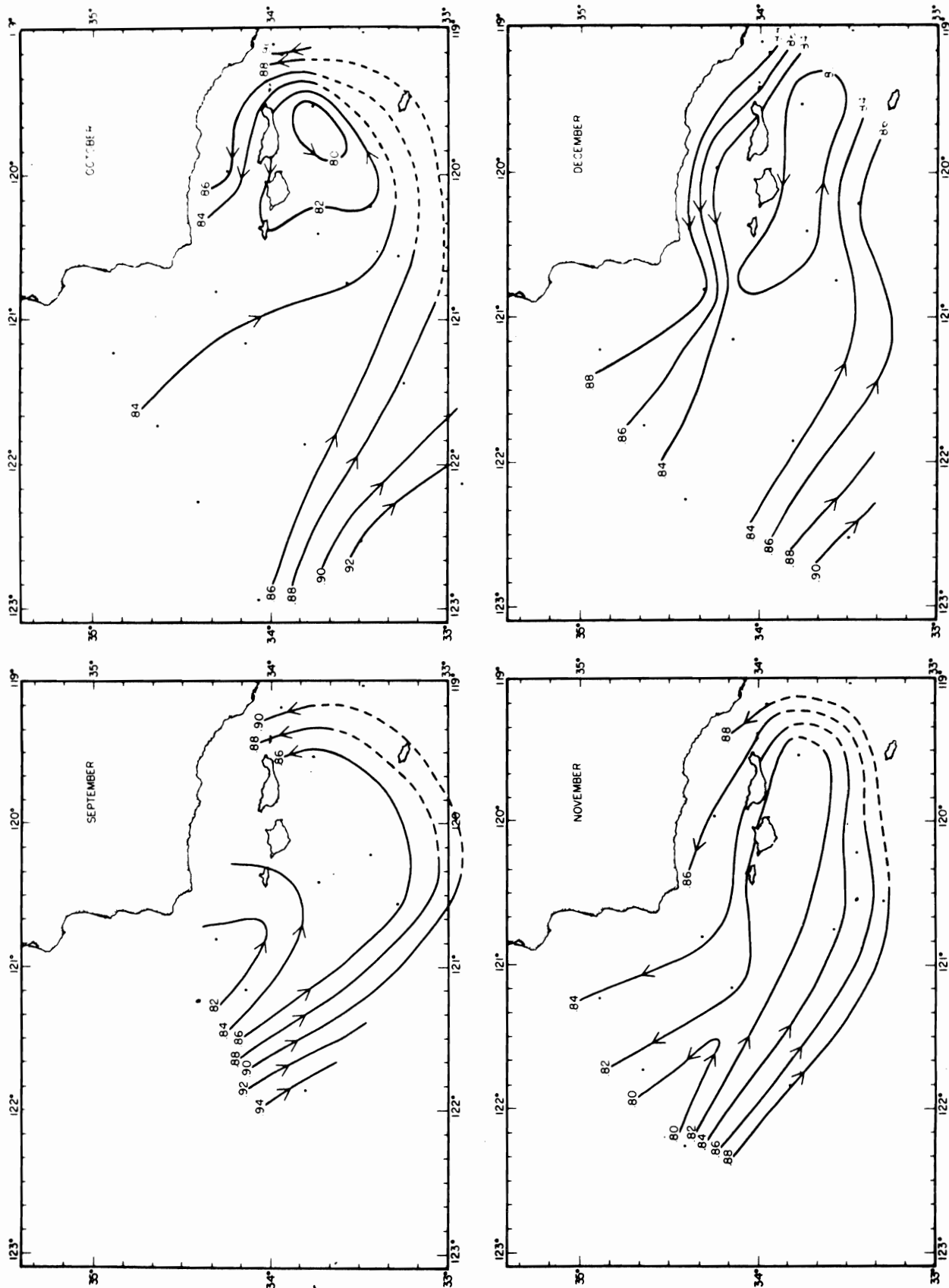


Fig. 10. Average surface geostrophic flow (topography of the 0-decibar surface, in dynamic meters, relative to the 500-decibar surface) in September, October, November, and December.

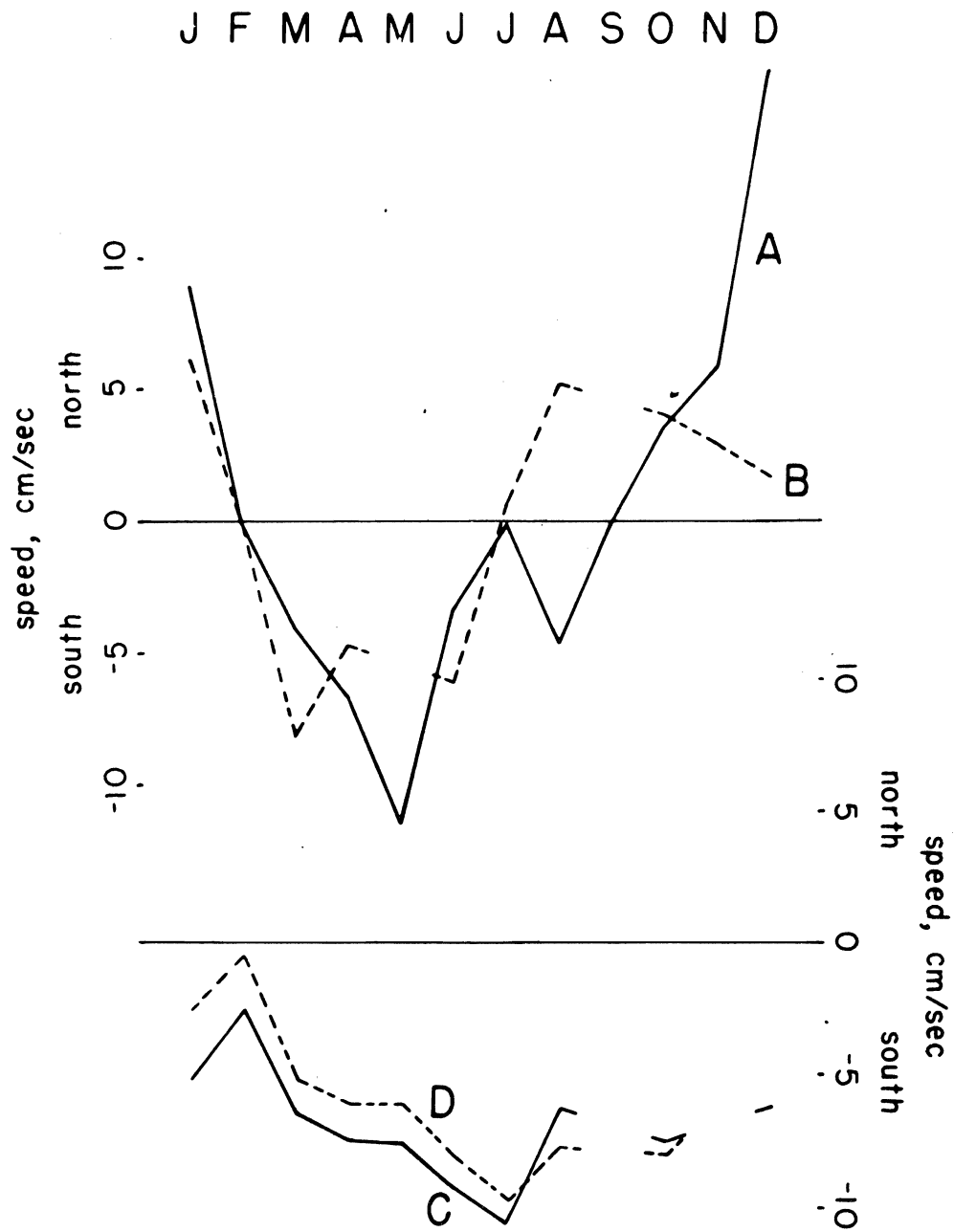


Fig. 11. Average surface geostrophic speed (relative to the 500-decibar surface) calculated across 4 sections. Positions of the sections are shown in fig. 12.

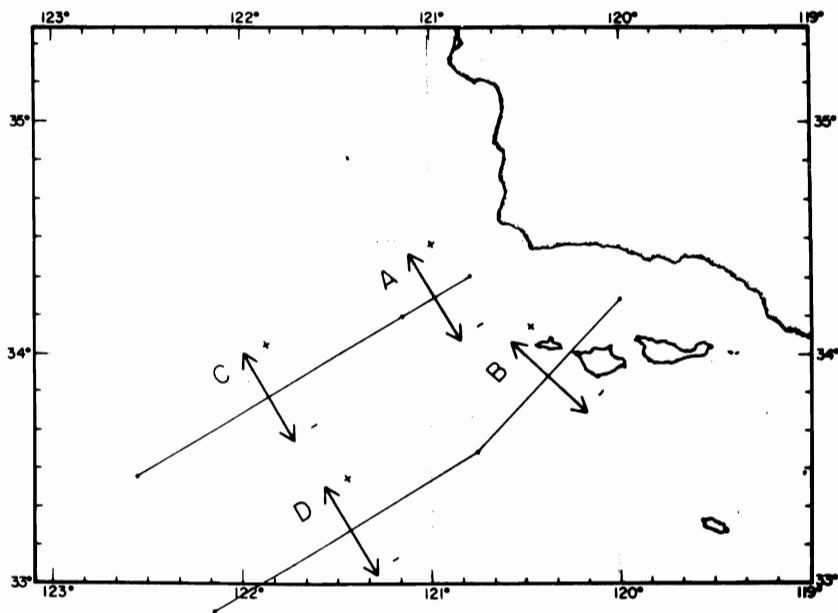


Fig. 12. Positions of the sections used in fig. 11.

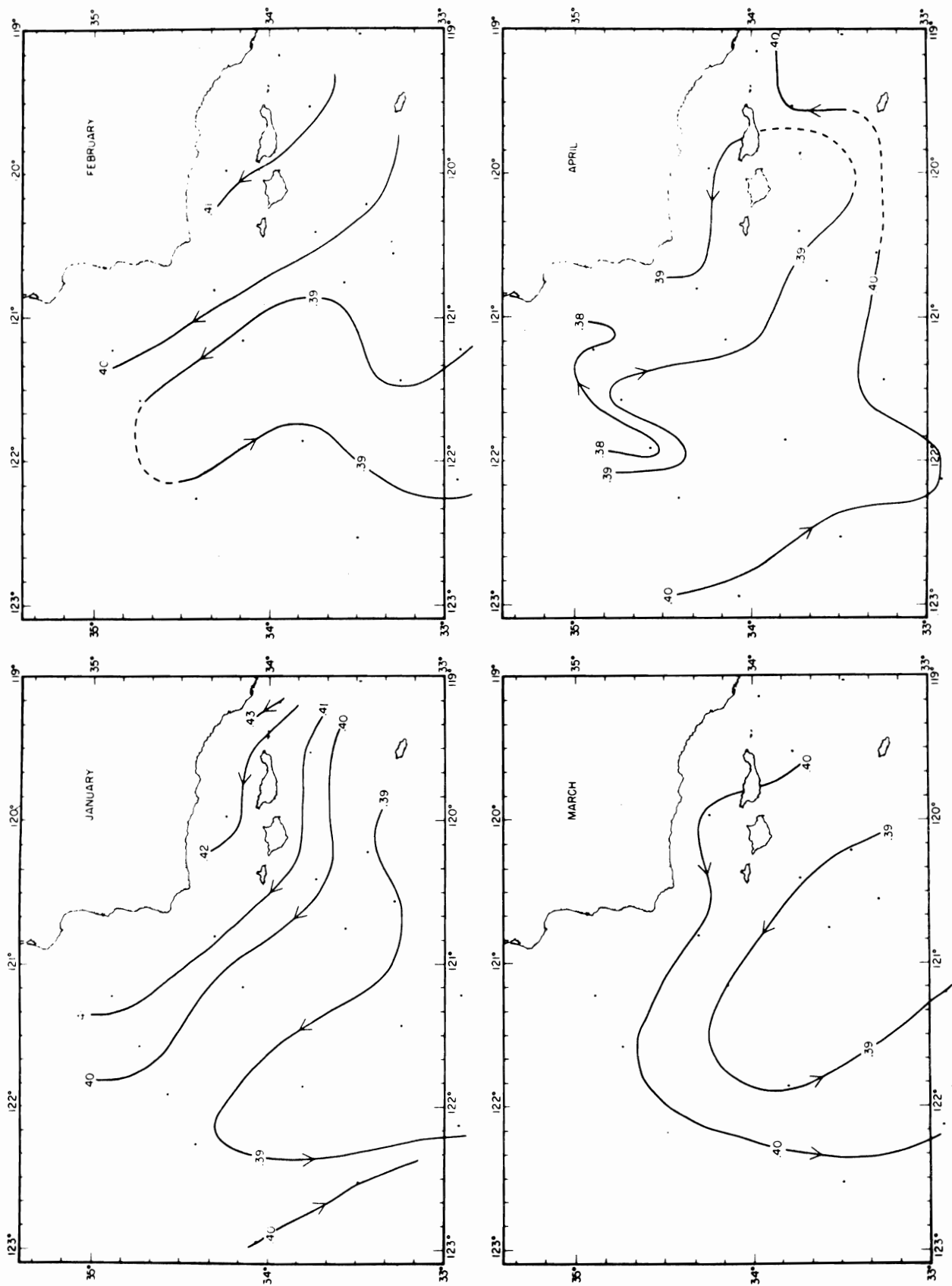


Fig. 13. Average geostrophic flow at 200 m (topography of the 200-decibar surface, in dynamic meters, relative to the 500-decibar surface) in January, February, March, and April.

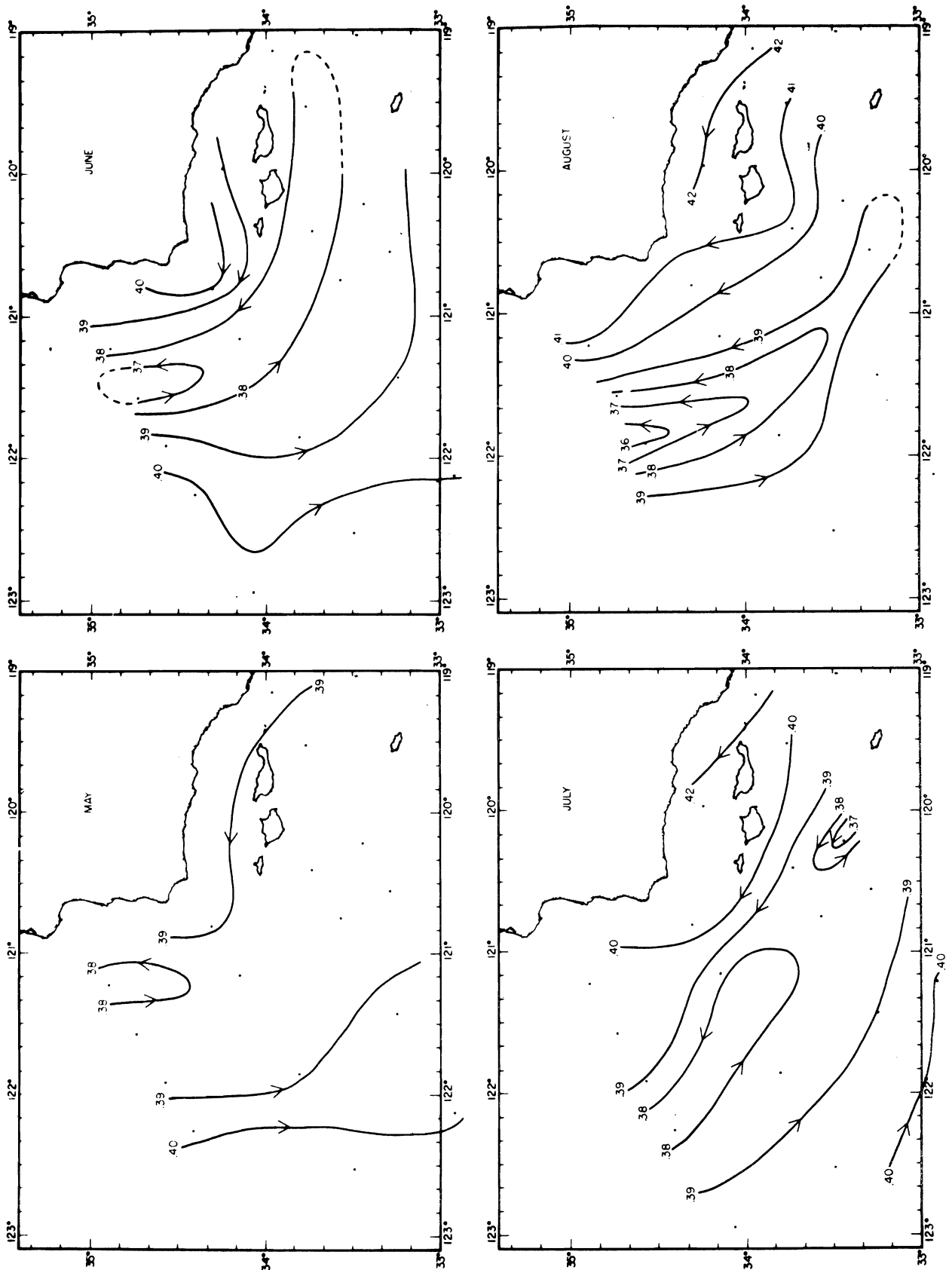


Fig. 14. Average geostrophic flow at 200 m (topography of the 200-decibar surface, in dynamic meters, relative to the 500-decibar surface) in May, June, July, and August.



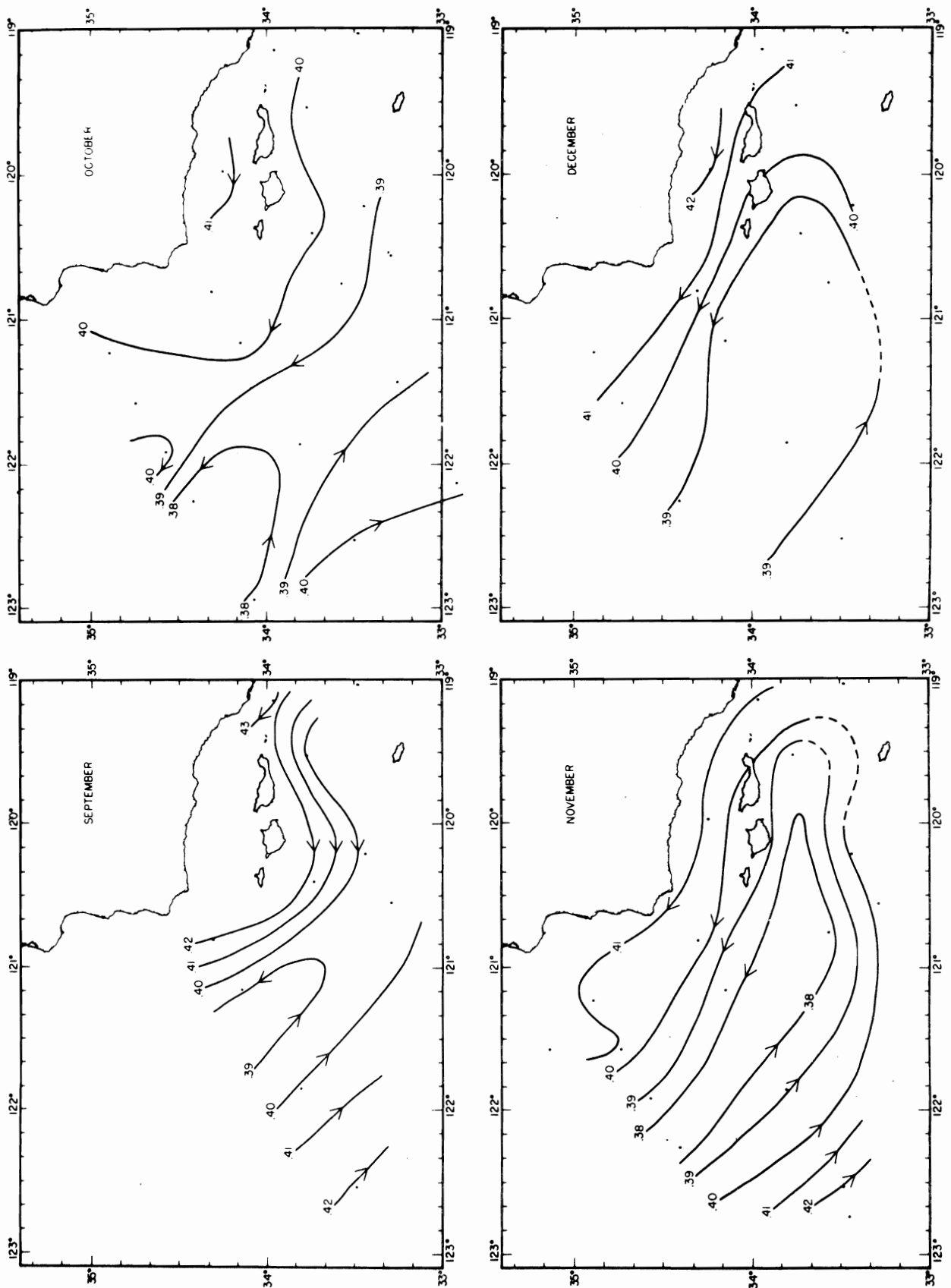


Fig. 15. Average geostrophic flow at 200 m (topography of the 200-decibar surface, in dynamic meters, relative to the 500-decibar surface) in September, October, November, and December.

J F M A M J J A S O N D

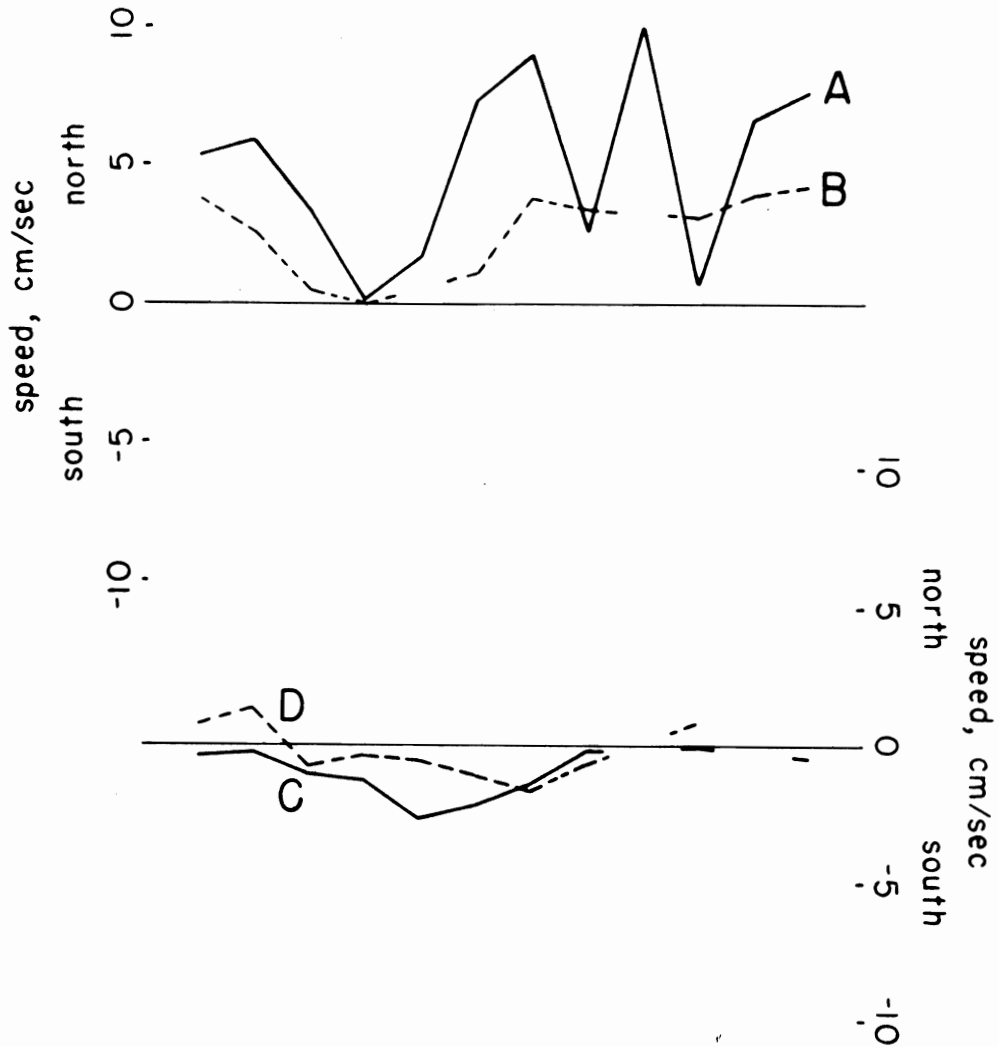


Fig. 16. Average geostrophic speed at 200 m (relative to the 500-decibar surface) calculated across 4 sections. Positions of the sections are shown in fig. 12.

Fig. 17. Average temperature ( $^{\circ}\text{C}$ ) and salinity ( $\text{‰}$ ) at the sea surface and at 10 m depth in January.

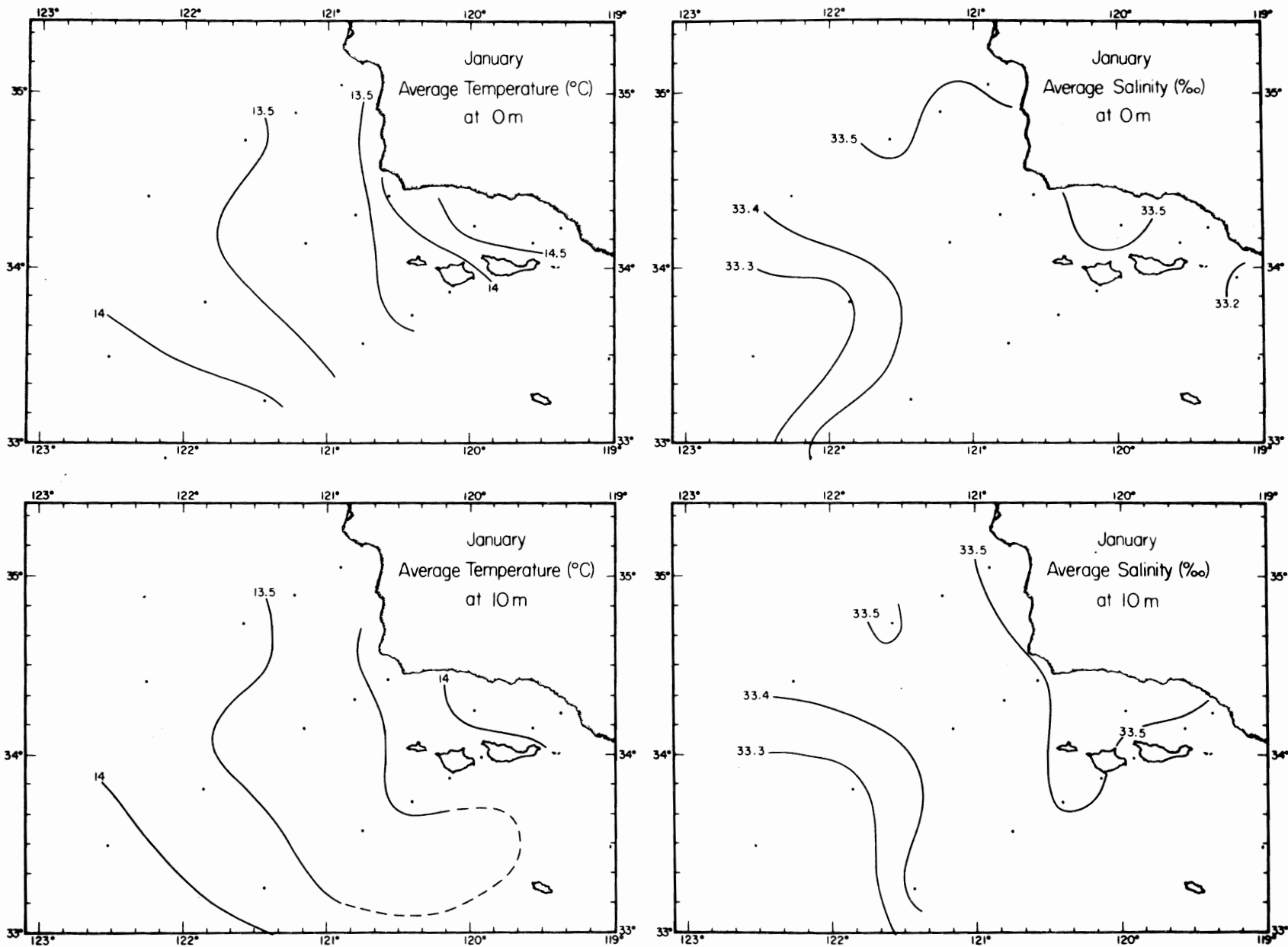


Fig. 18. Average temperature ( $^{\circ}\text{C}$ ) and salinity ( $\text{‰}$ ) at 30 m and 50 m depth in January.

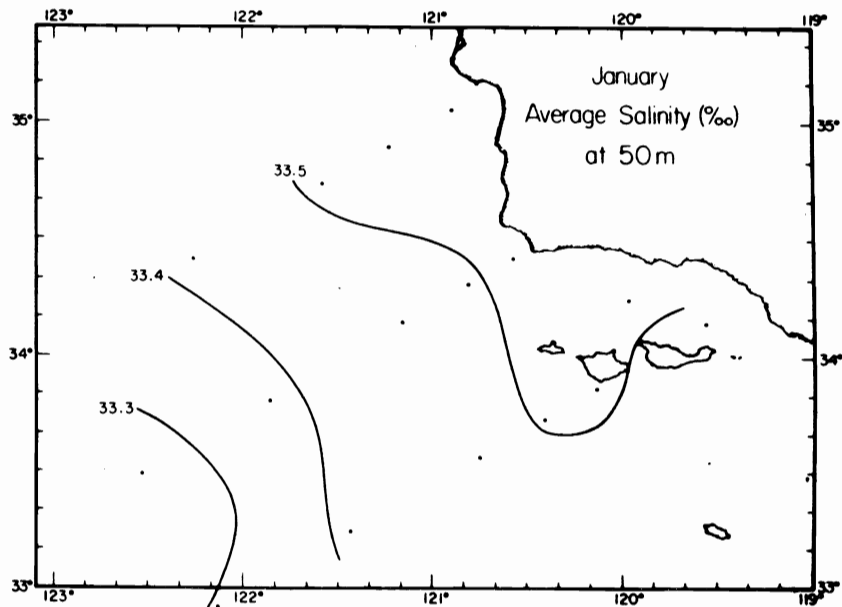
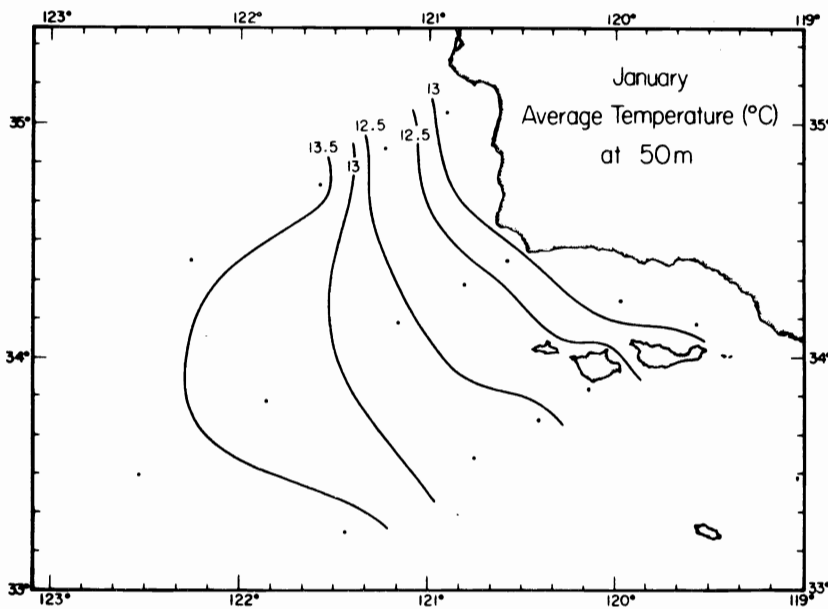
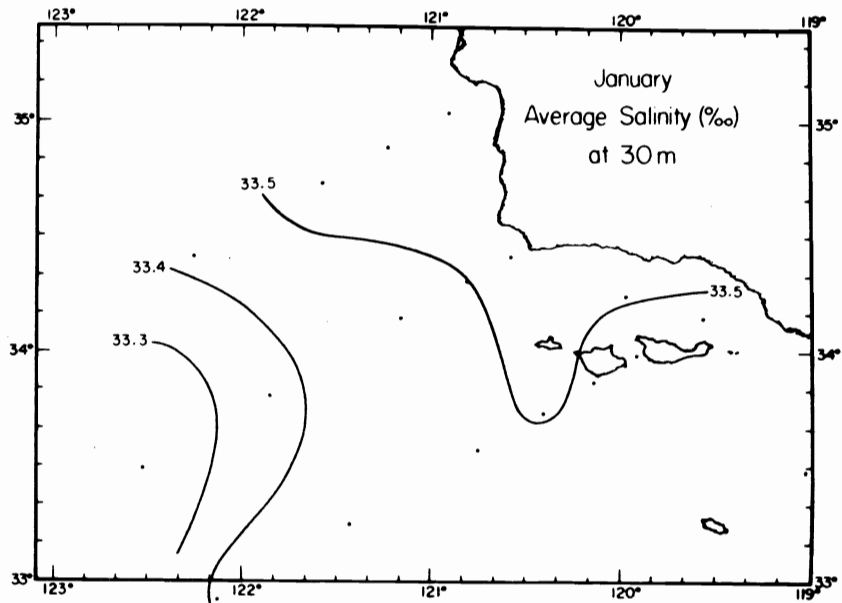
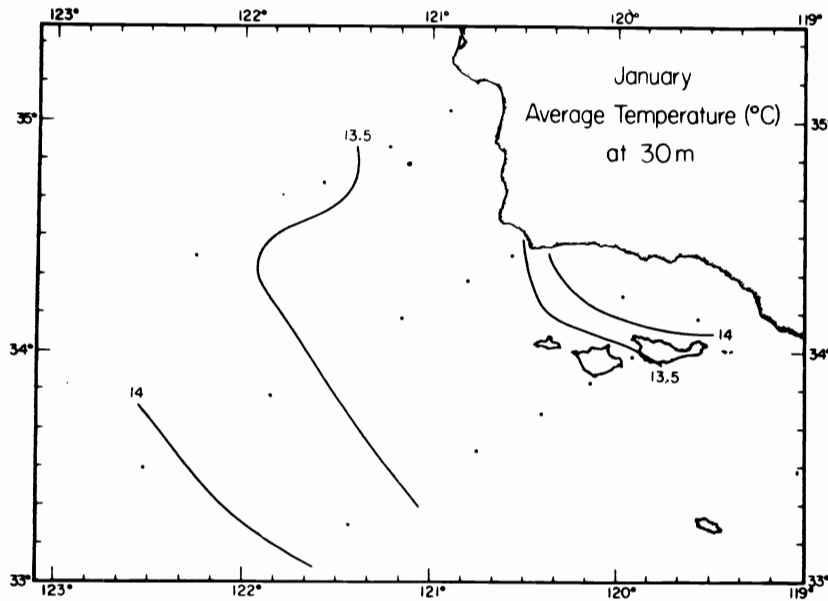


Fig. 19. Average temperature ( $^{\circ}\text{C}$ ) and salinity ( $\text{‰}$ ) at 75 m and 100 m depth in January.

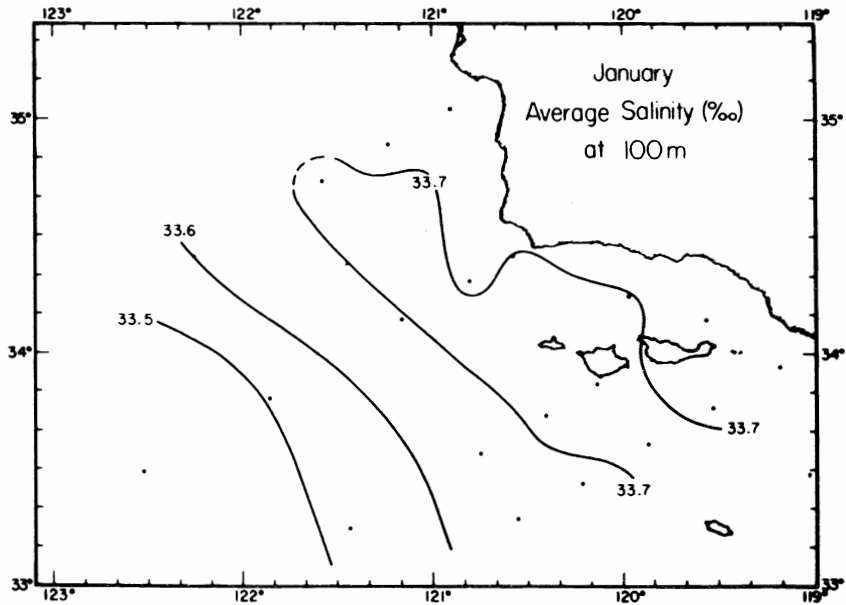
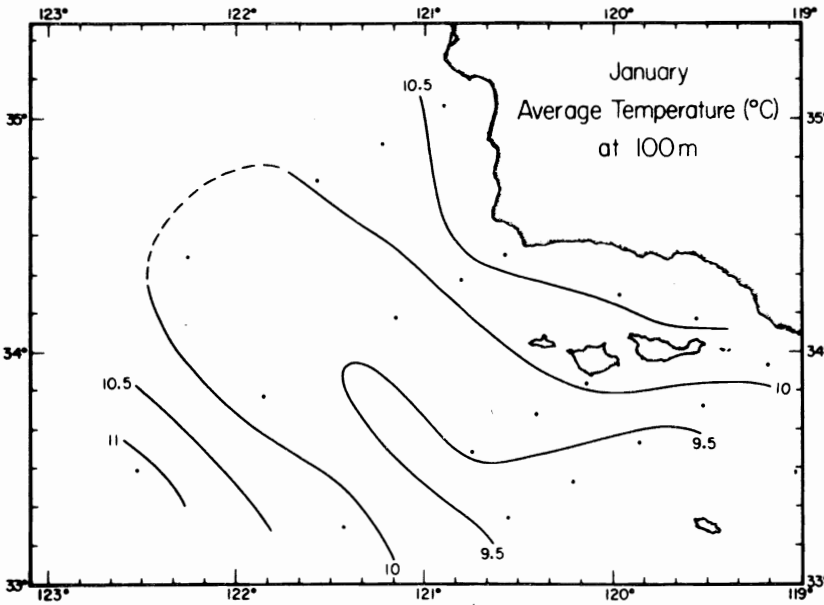
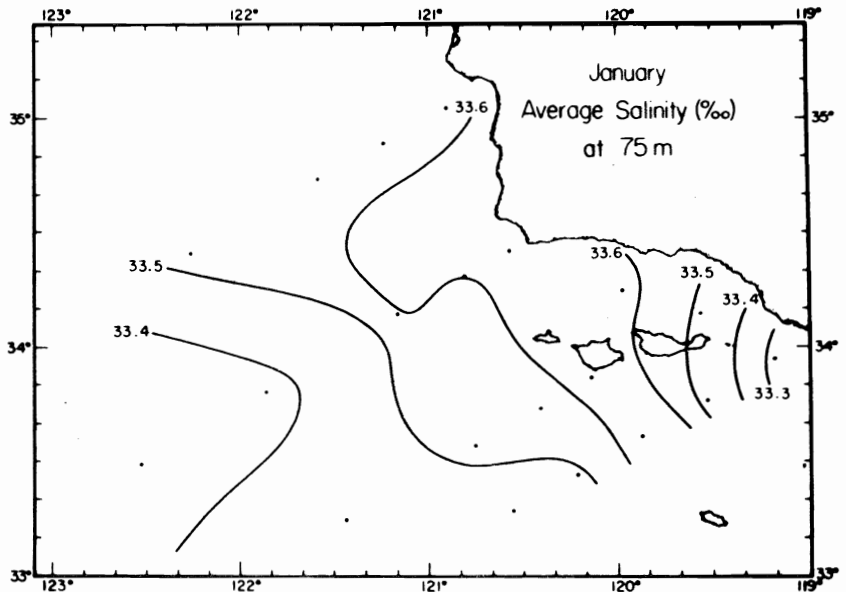
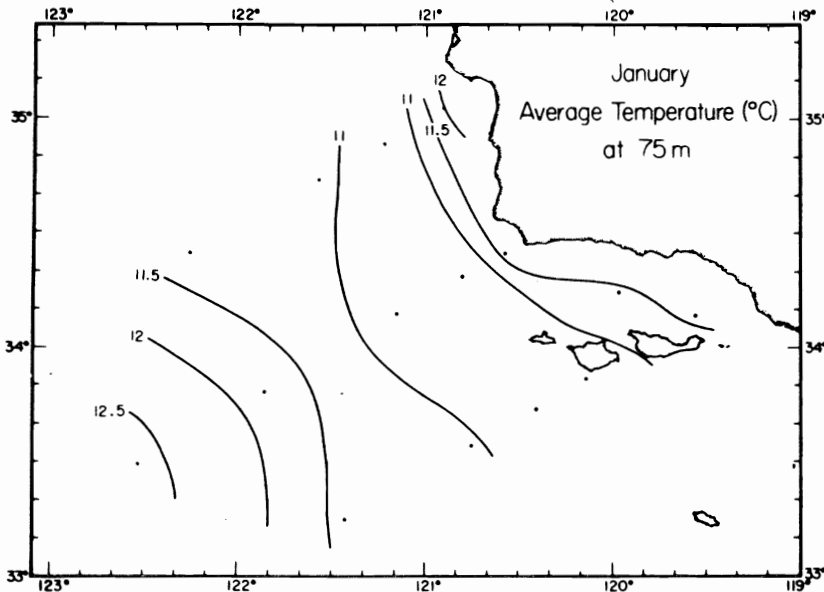


Fig. 20. Average temperature (°C) and salinity (‰) at 150 m and 200 m depth in January.

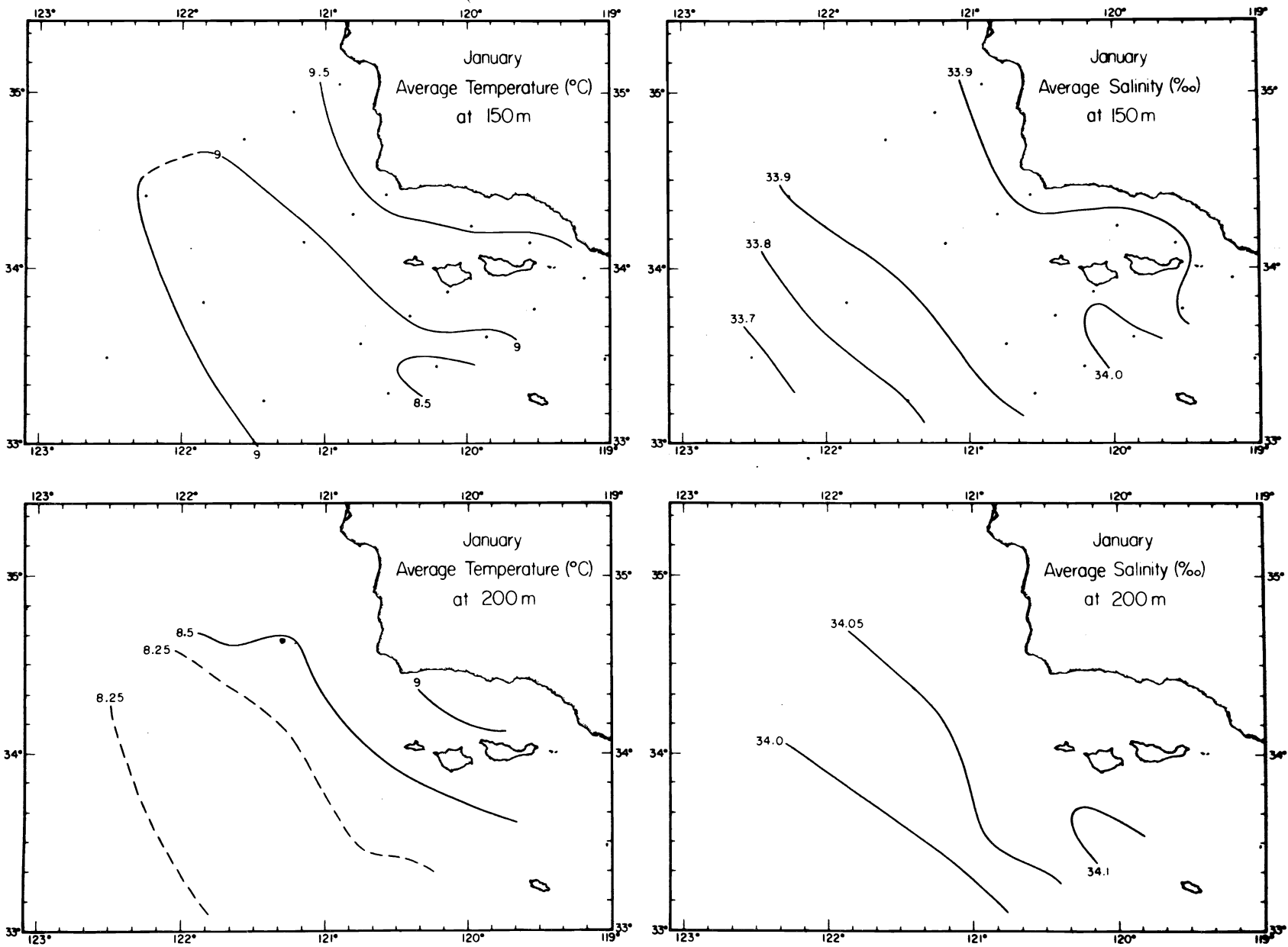


Fig. 21. Average temperature ( $^{\circ}\text{C}$ ) and salinity ( $\text{‰}$ ) at the sea surface and at 10 m depth in June.

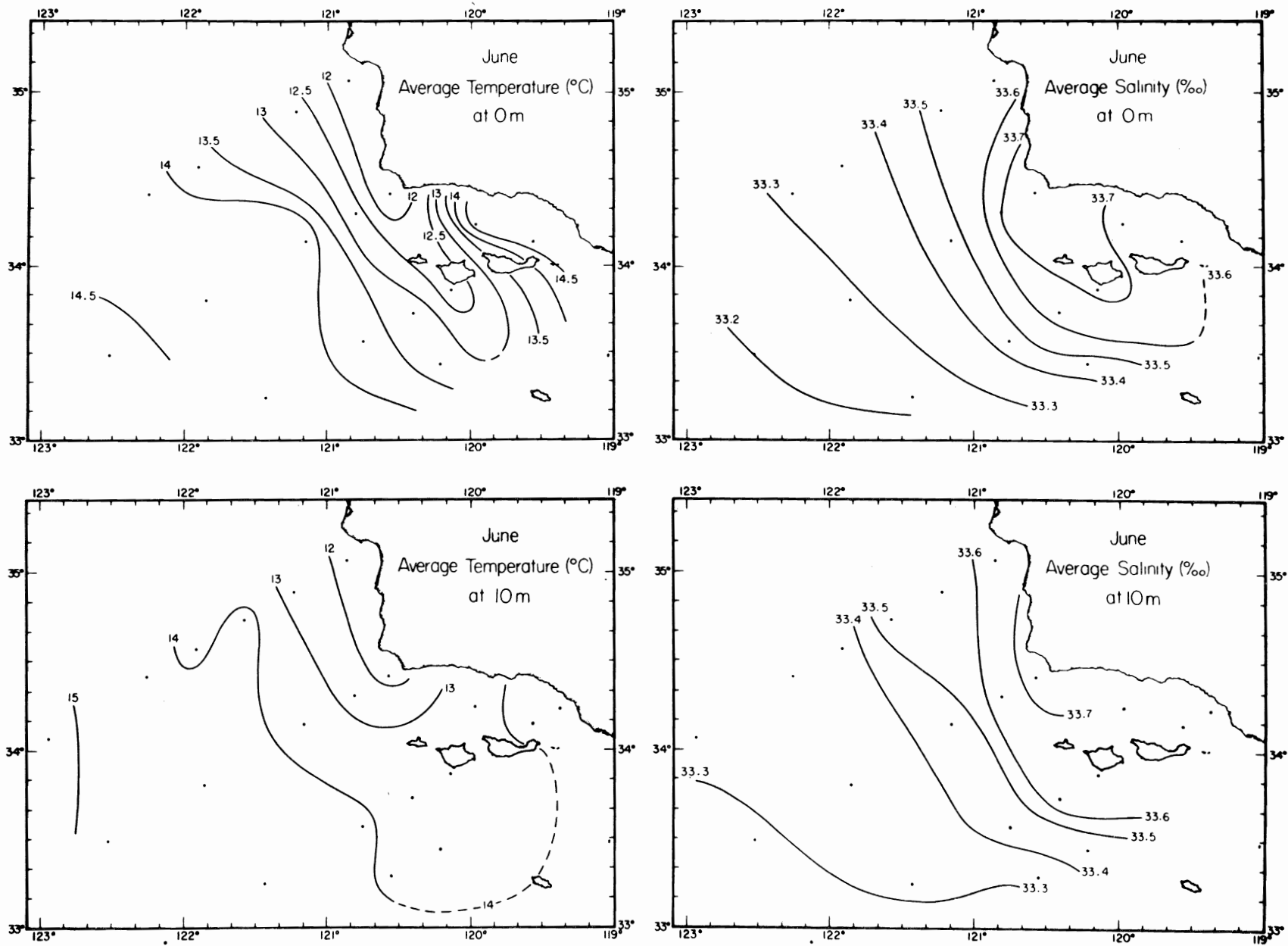


Fig. 22. Average temperature (°C) and salinity (‰) at 30 m and 50 m depth in June.

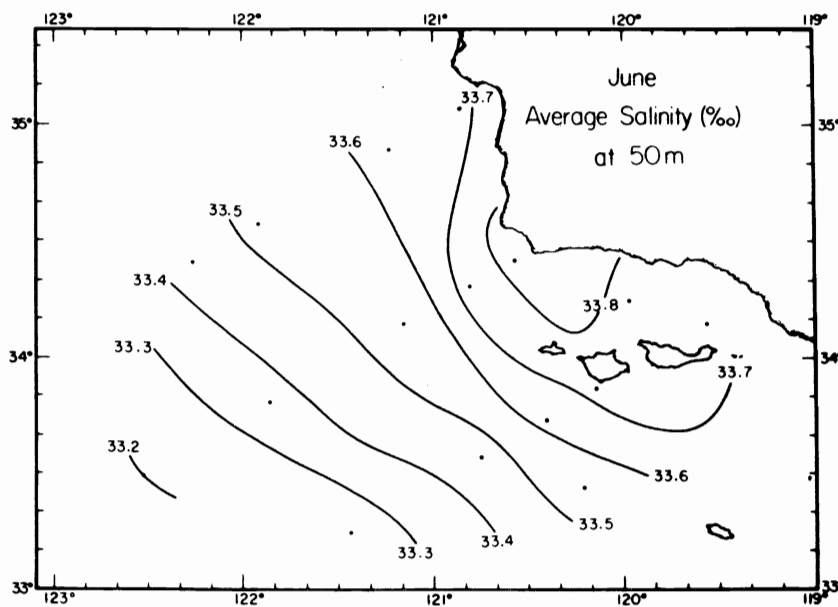
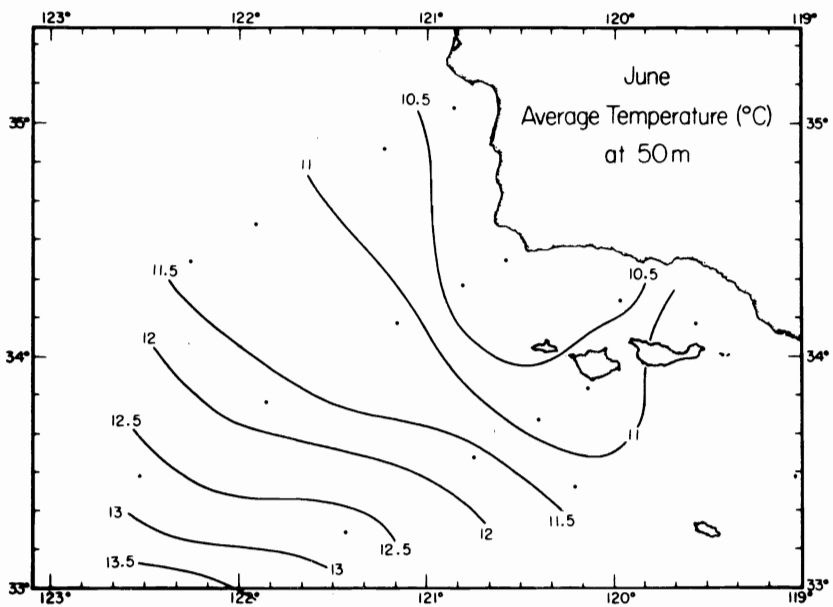
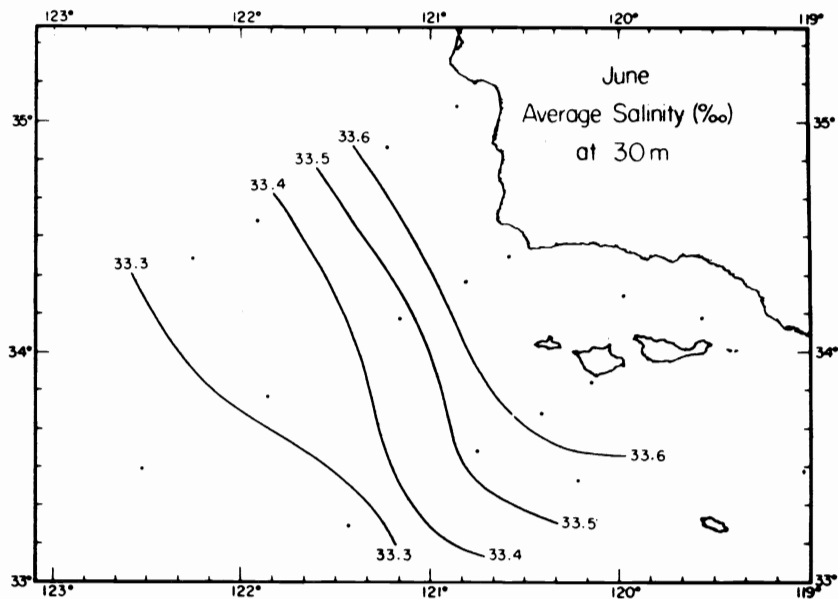
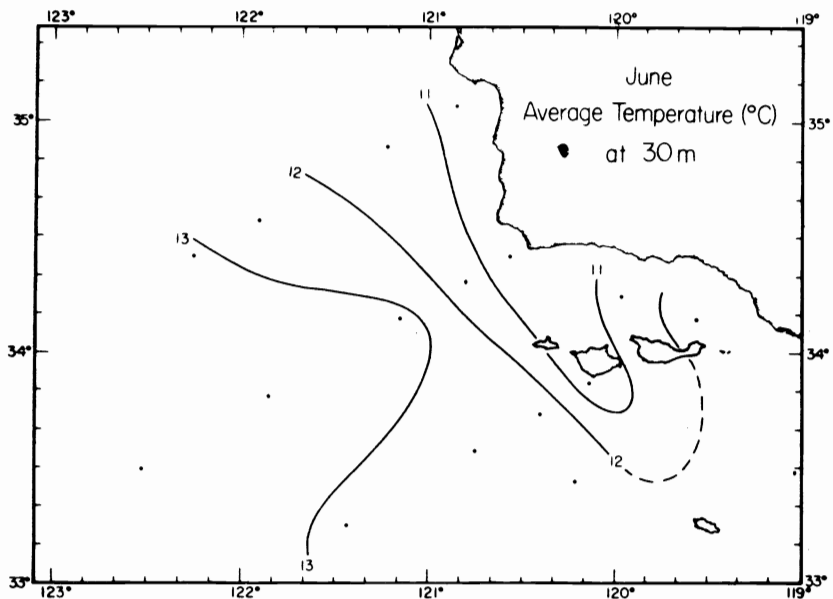




Fig. 23. Average temperature (°C) and salinity (‰) at 75 m and 100 m depth in June.

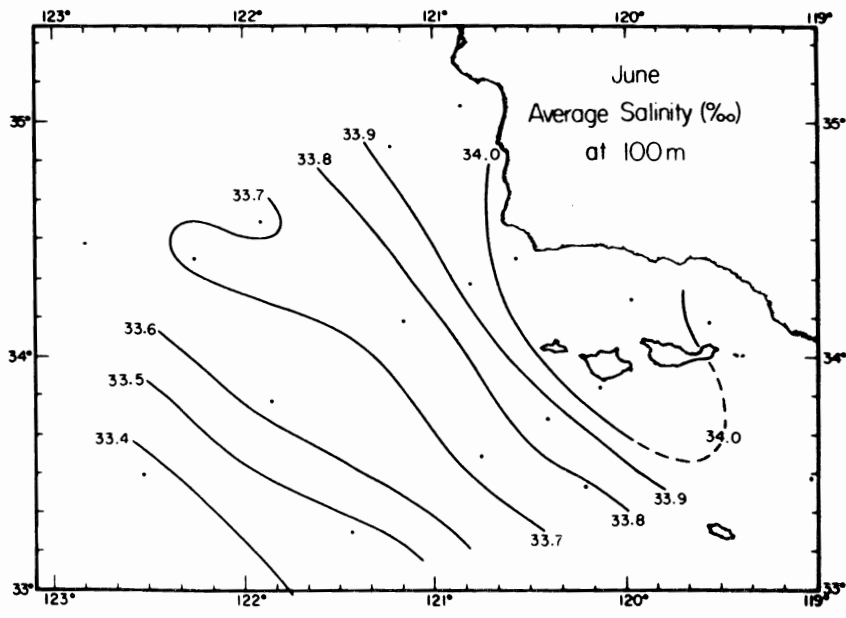
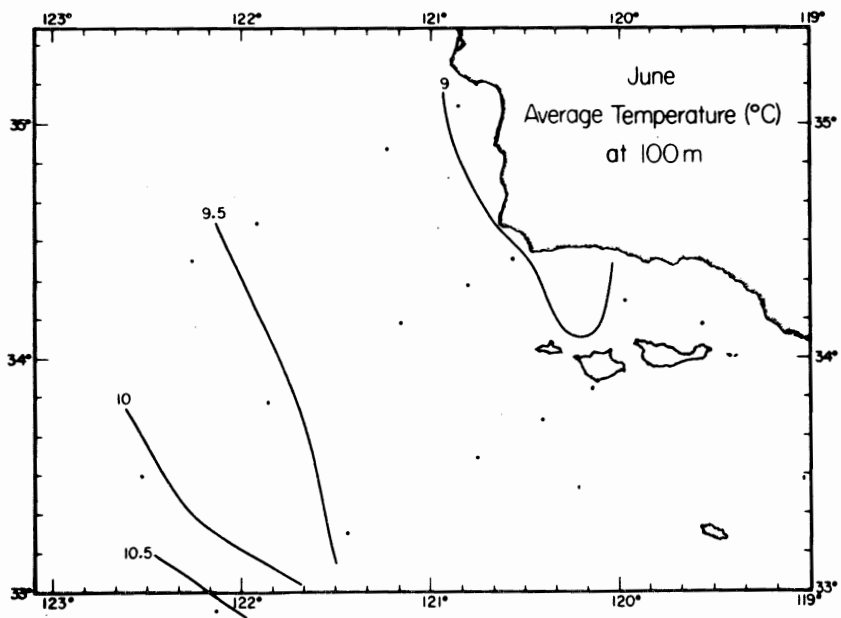
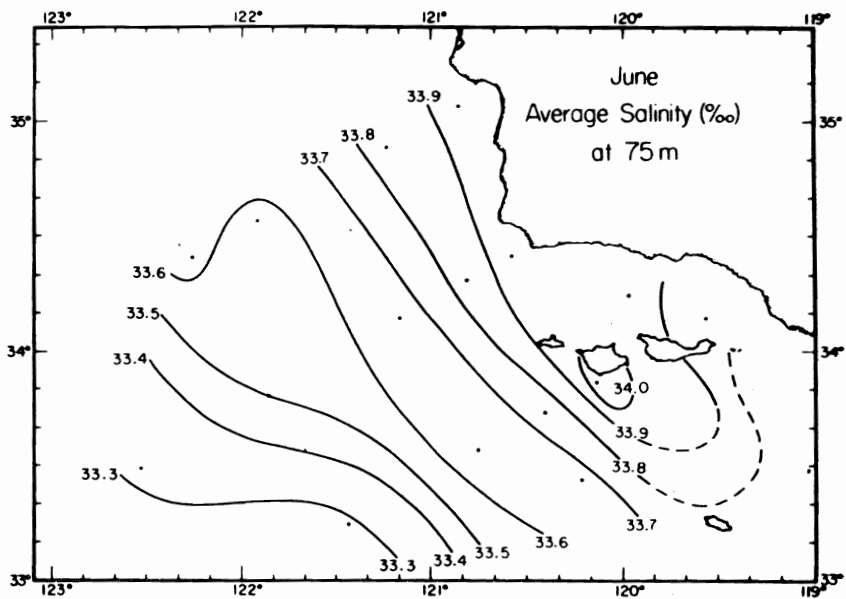
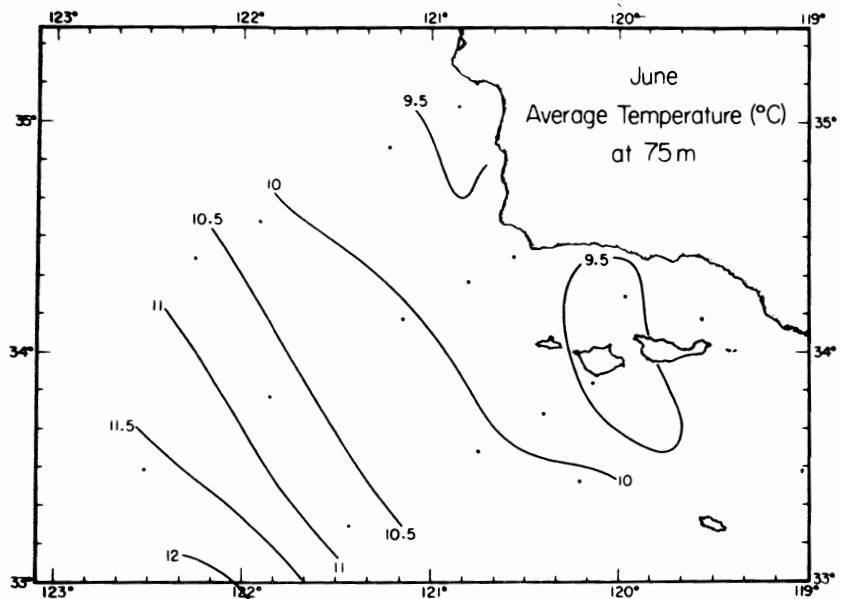
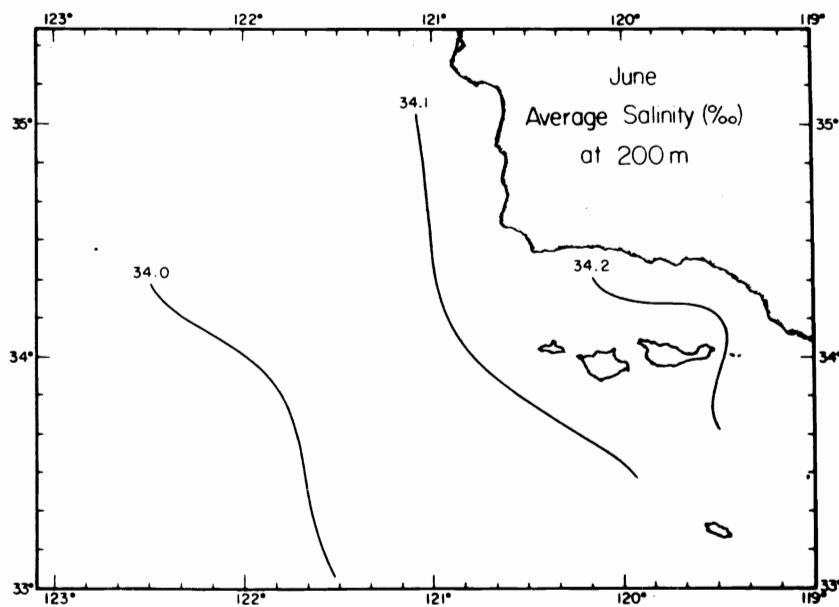
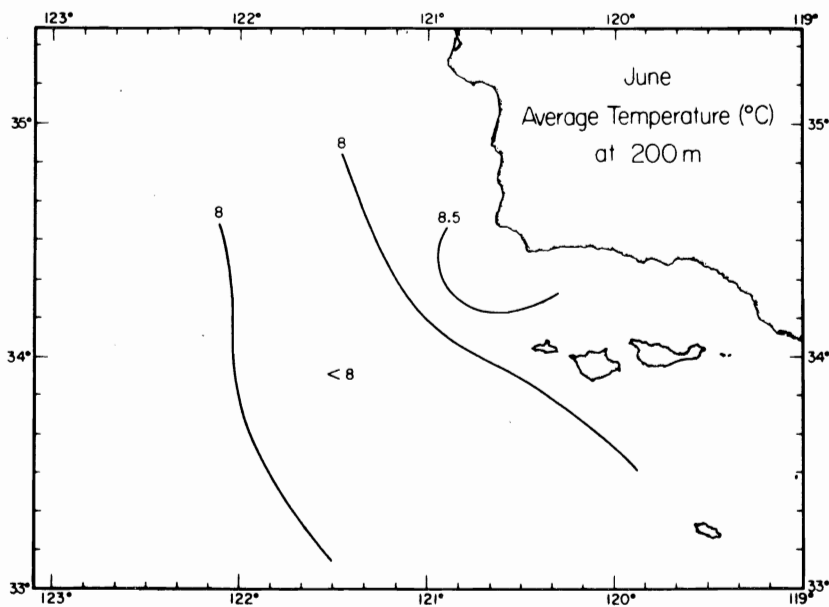
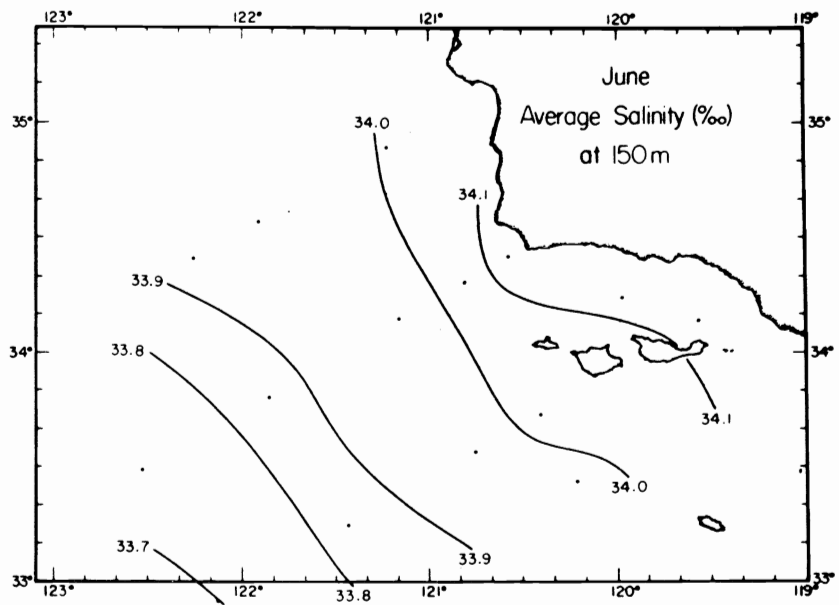
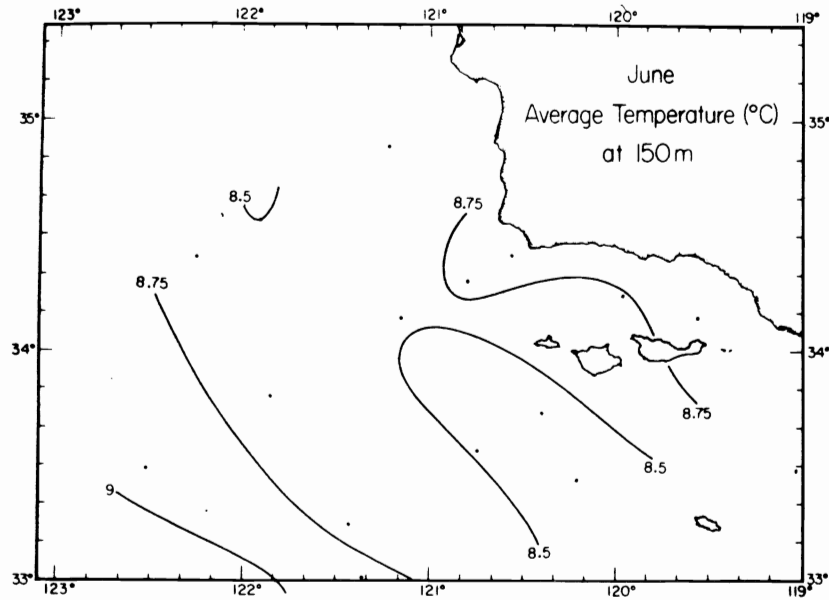


Fig. 24. Average temperature (°C) and salinity (‰) at 150 m and 200 m depth in June.



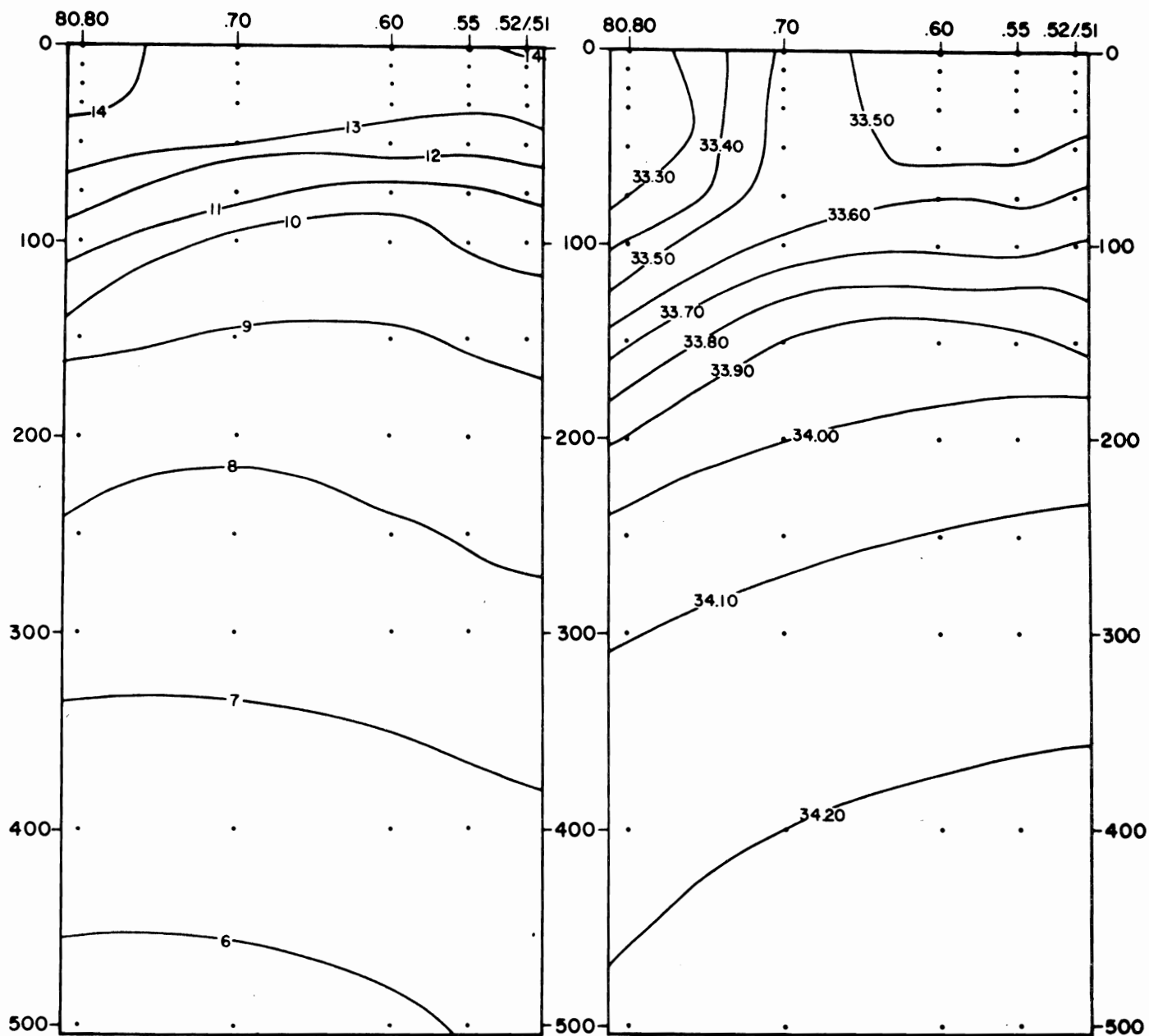


Fig. 25. Average temperature ( $^{\circ}\text{C}$ ) and salinity ( $\text{‰}$ ) in January in a vertical section extending 118 miles from Point Arguello and to a depth of 500 m. Position shown in fig. 26.

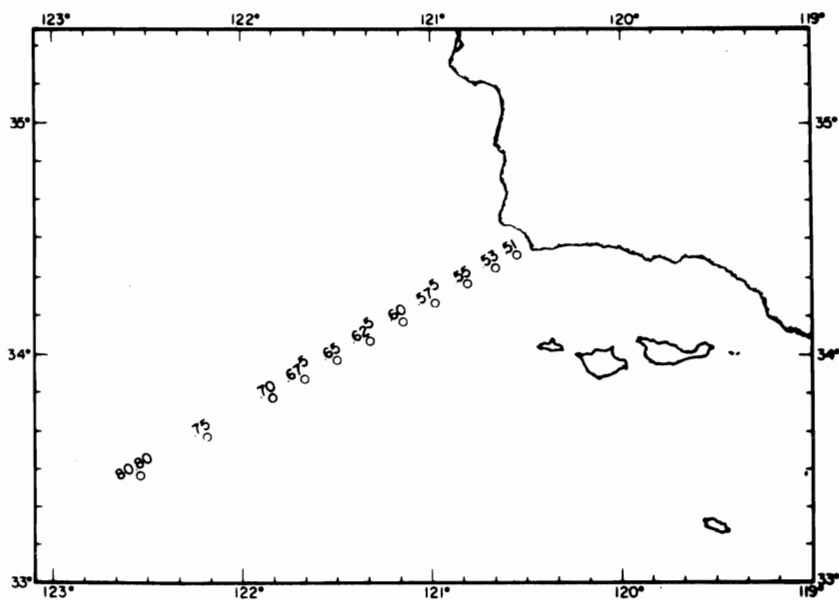


Fig. 26. Positions of stations and vertical sections shown in figs. 25, 27-31, 40 and 47.

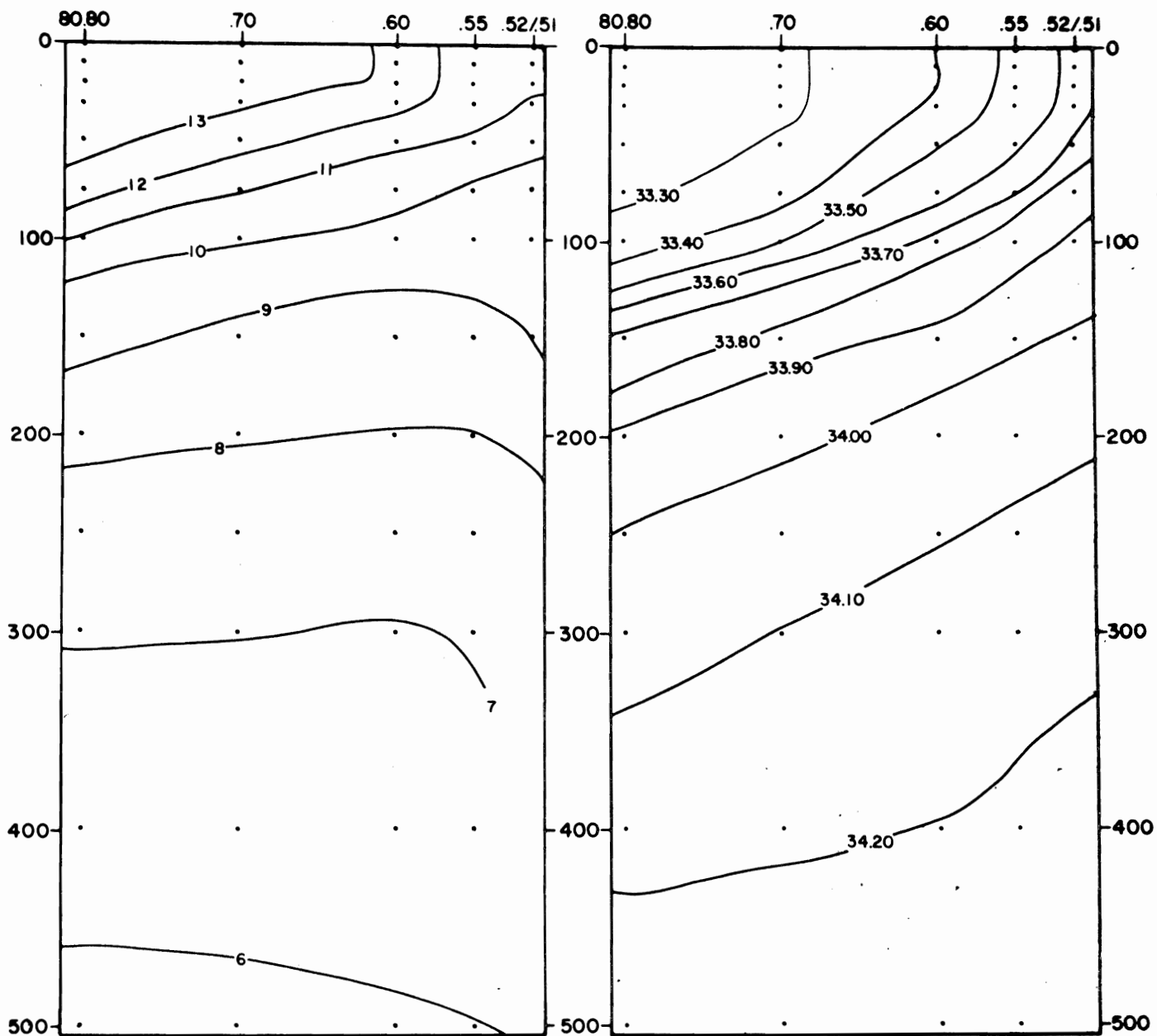


Fig. 27. Average temperature ( $^{\circ}\text{C}$ ) and salinity ( $\text{‰}$ ) in April in a vertical section extending 118 miles from Point Arguello and to a depth of 500 m. Position shown in fig. 26.

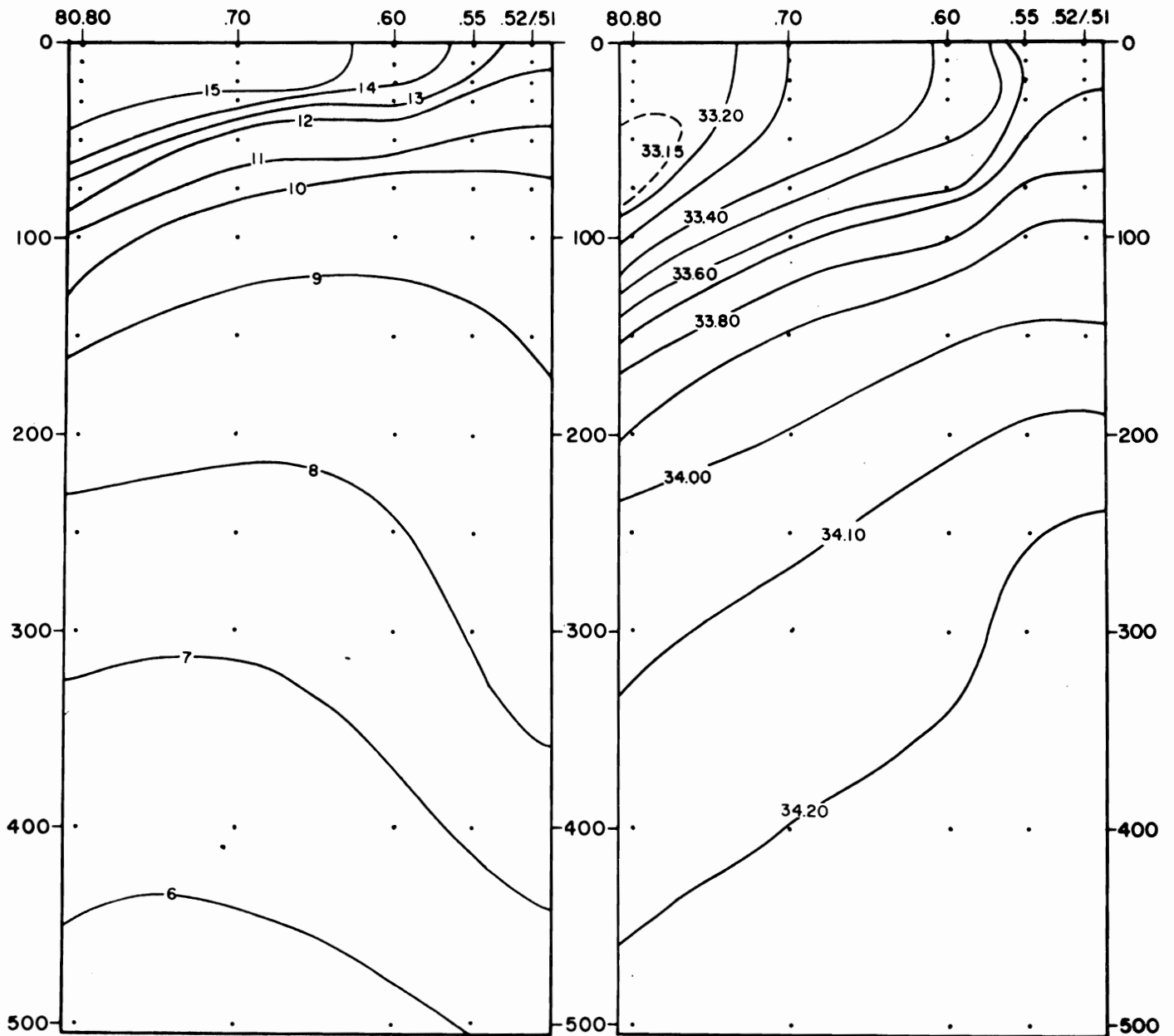


Fig. 28. Average temperature ( $^{\circ}\text{C}$ ) and salinity ( $\text{‰}$ ) in July in a vertical section extending 118 miles from Point Arguello and to a depth of 500 m. Position shown in fig. 26.

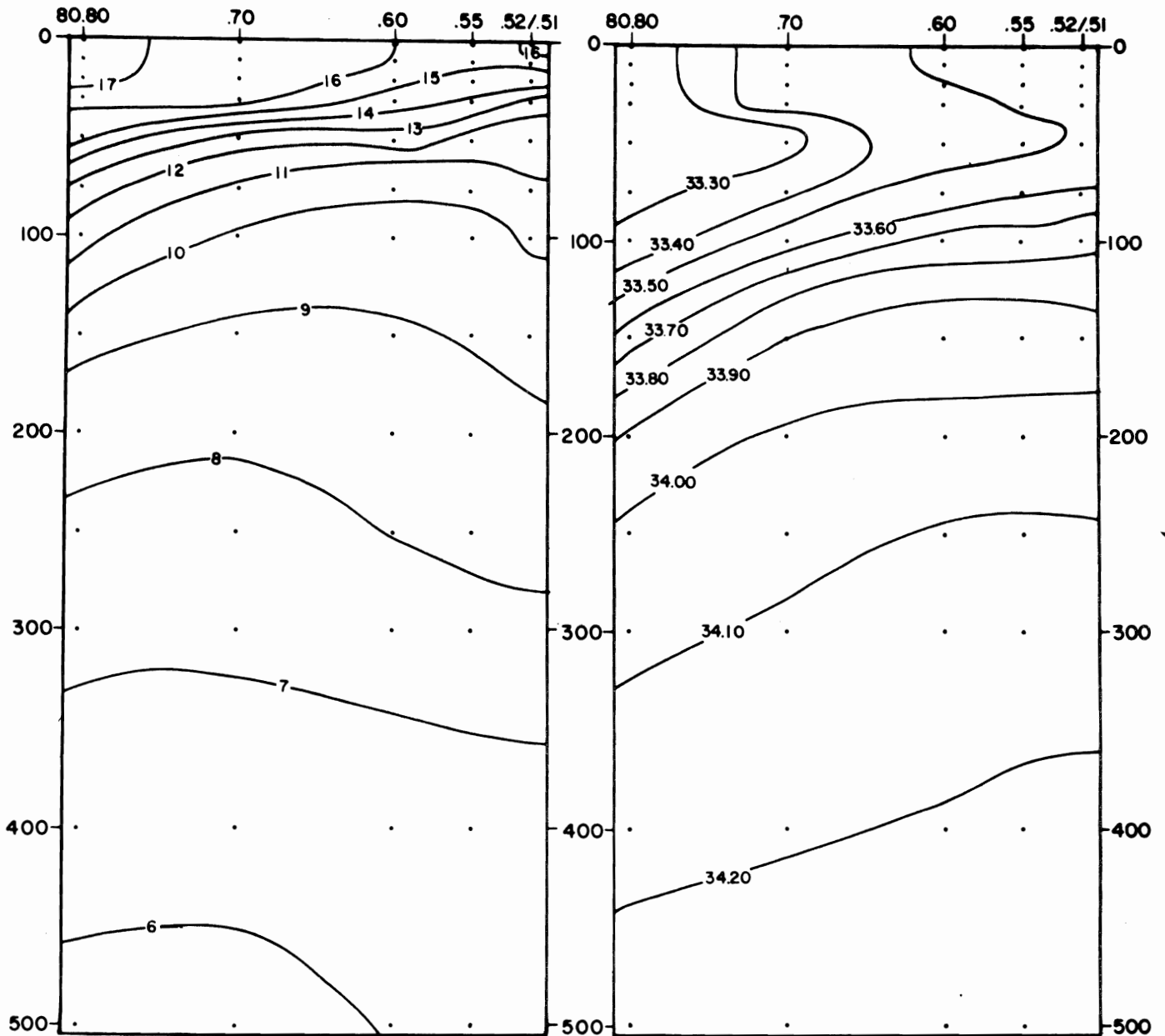


Fig. 29. Average temperature ( $^{\circ}\text{C}$ ) and salinity ( $\text{‰}$ ) in October in a vertical section extending 118 miles from Point Arguello and to a depth of 500 m. Position shown in fig. 26.

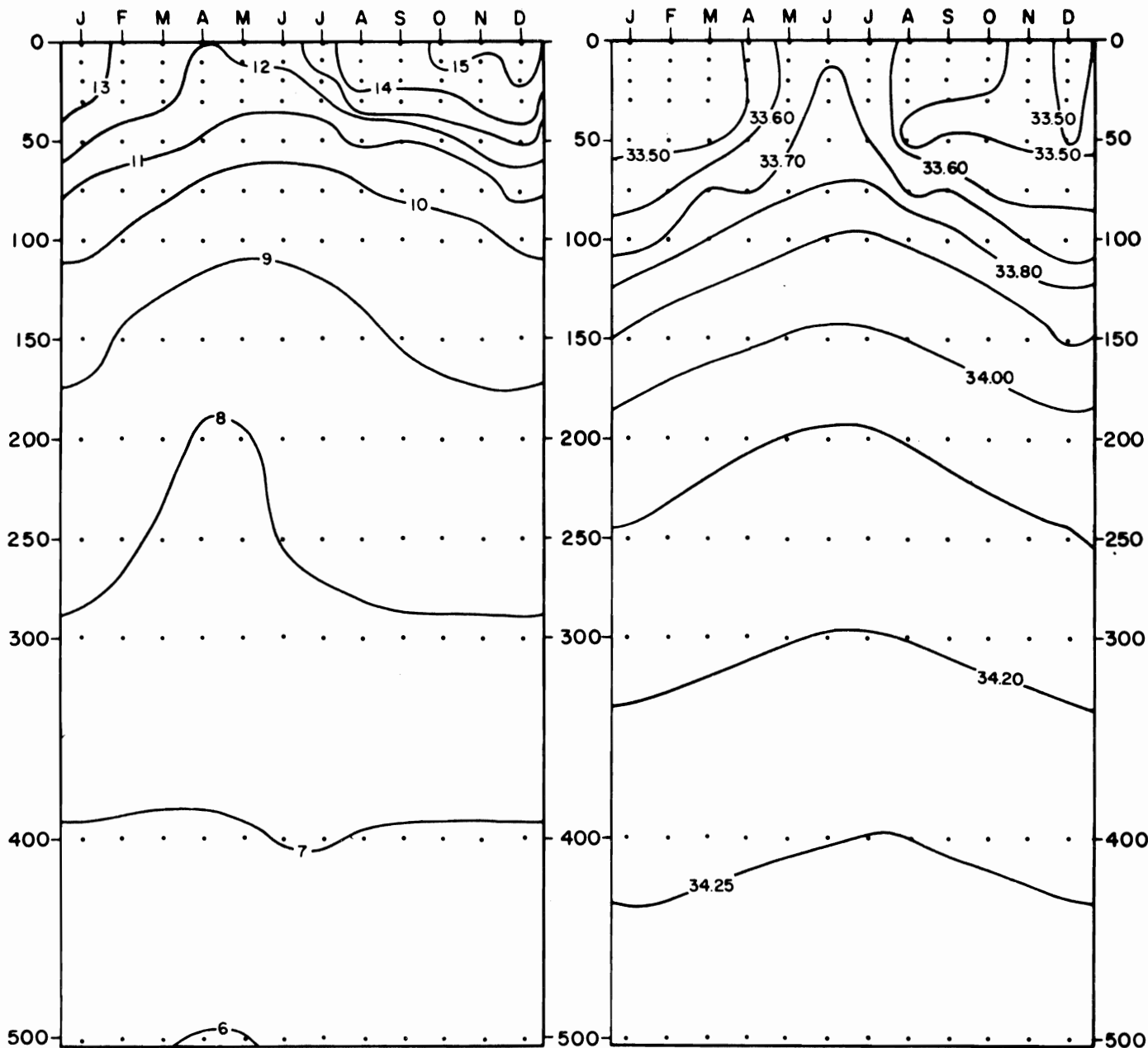


Fig. 30. Average temperature ( $^{\circ}\text{C}$ ) and salinity ( $\text{‰}$ ) in the upper 500 m for each month of the year at a position 18 miles southwest of Point Arguello (the inshore end of the line shown in fig. 26).



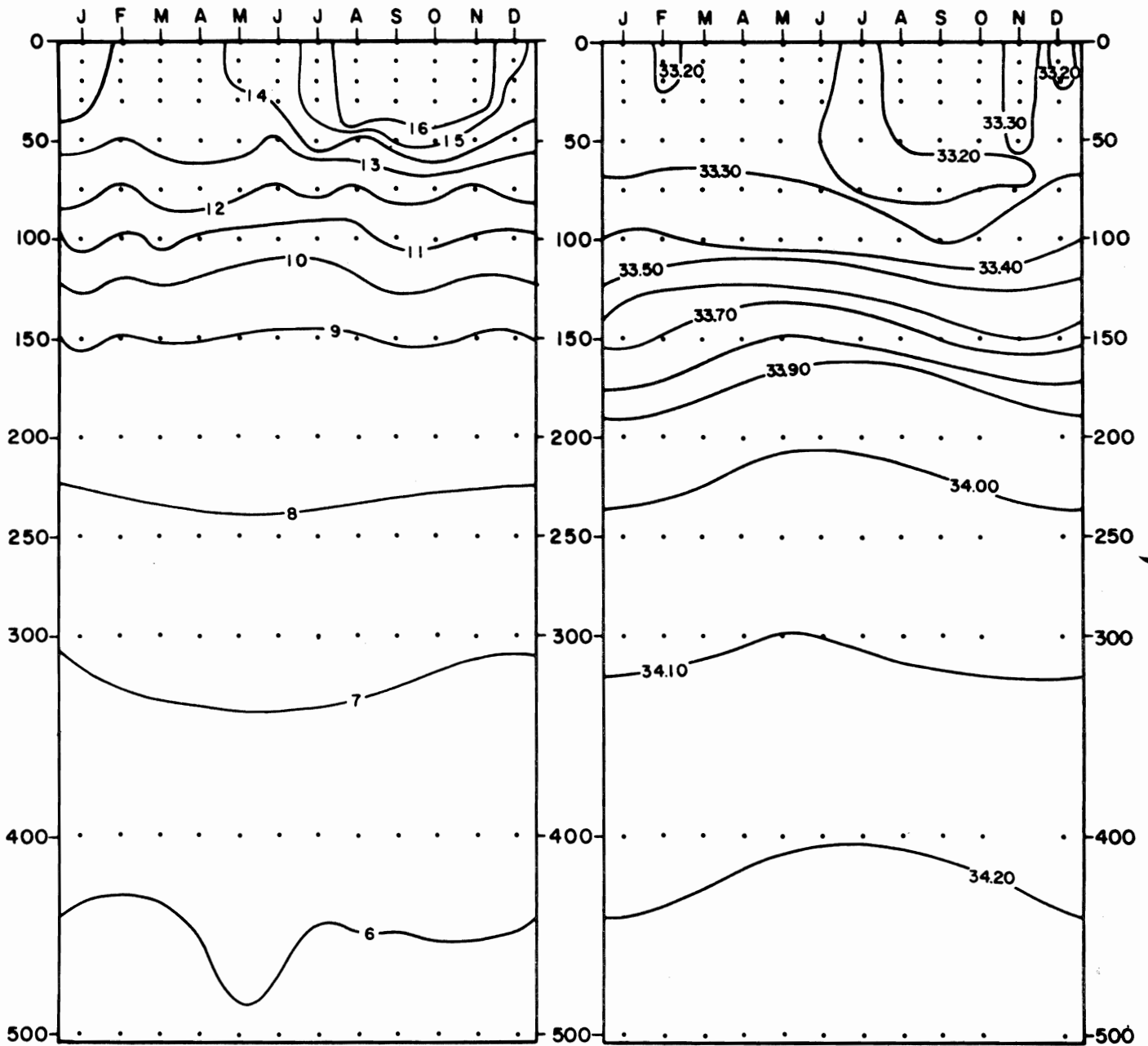


Fig. 31. Average temperature ( $^{\circ}\text{C}$ ) and salinity ( $\text{‰}$ ) in the upper 500 m for each month of the year at a position 118 miles southwest of Point Arguello (the outer end of the line shown in fig. 26).

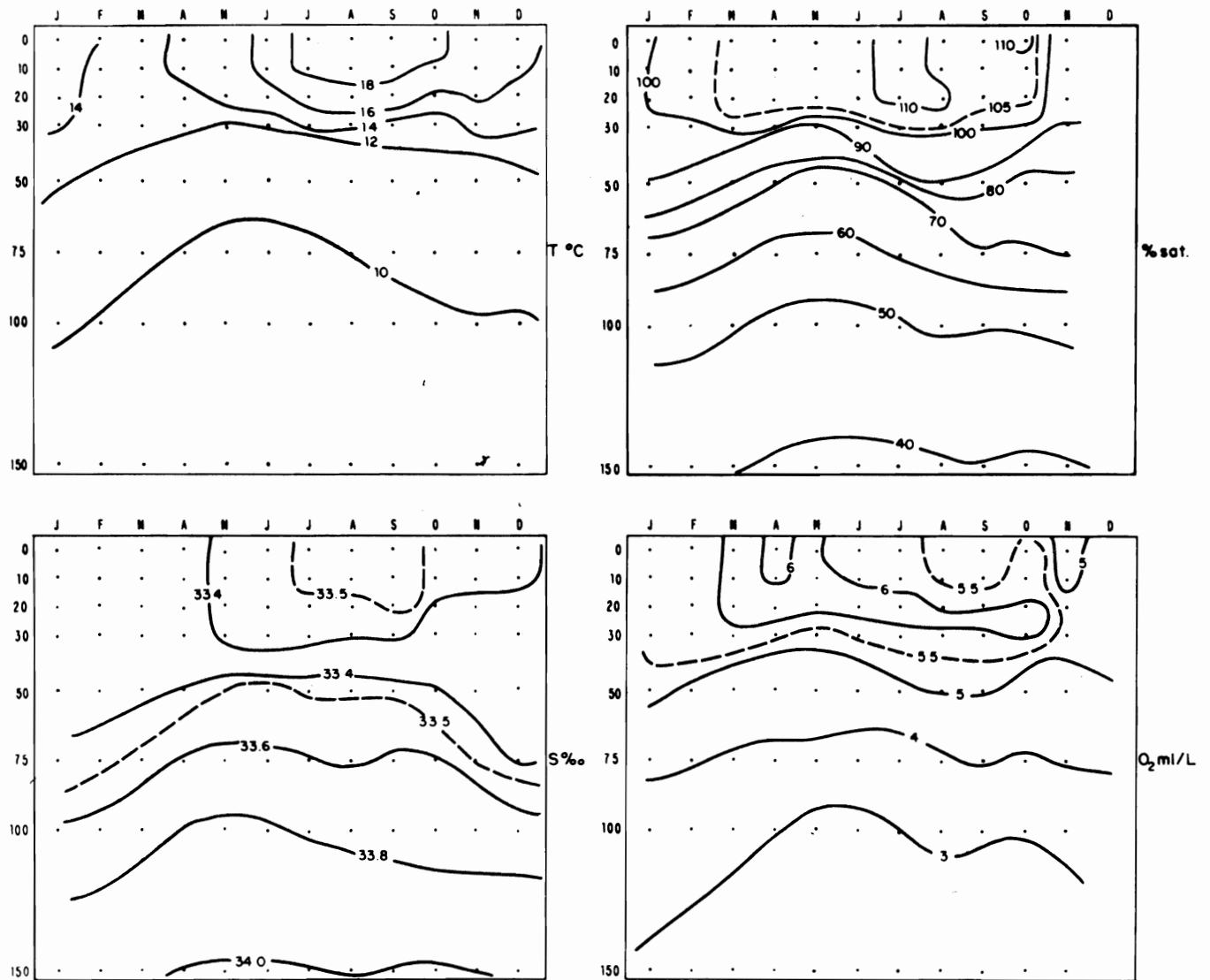


Fig. 32. Average seasonal variation of temperature, salinity, dissolved oxygen and per cent of saturation of dissolved oxygen in the upper 150 m at 33°12'N, 118°24'W (in the Channel Islands area) in the period 1950-1953.

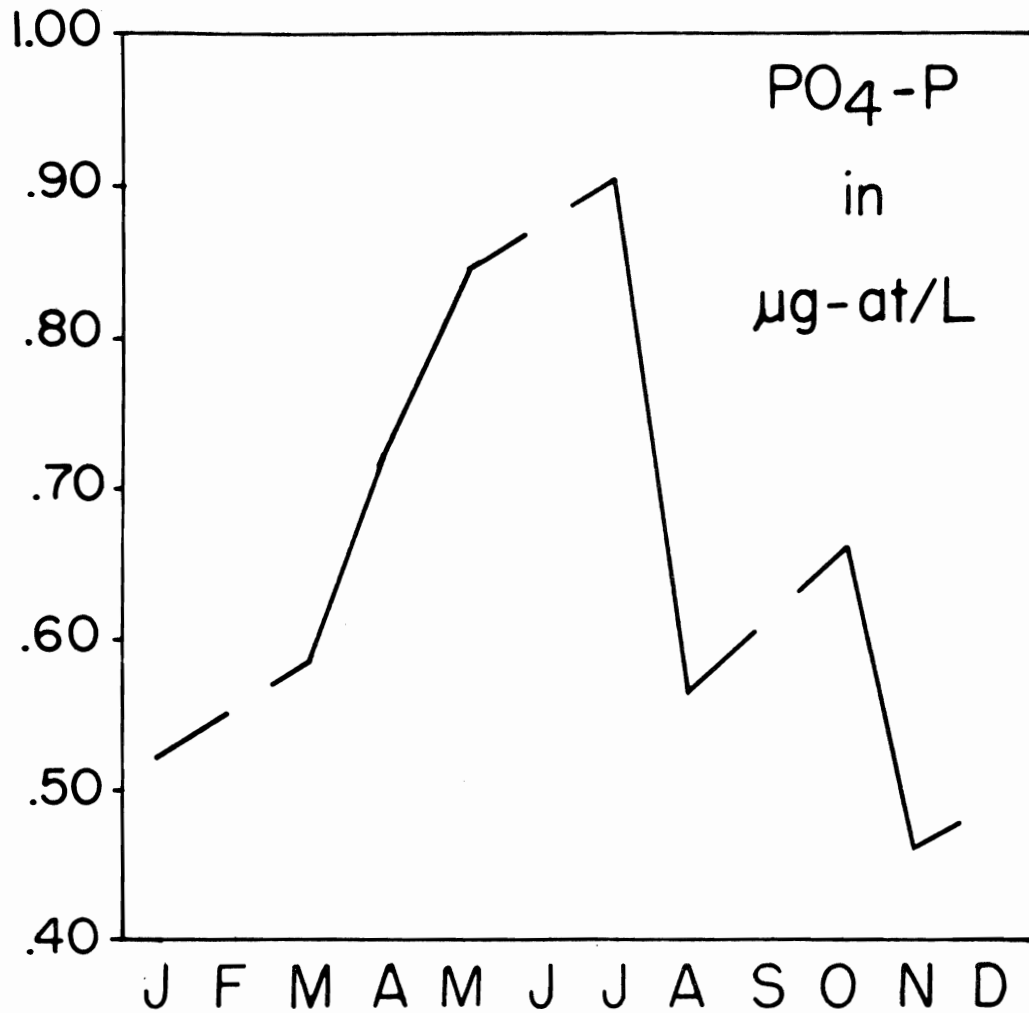


Fig. 33. Average phosphate-phosphorus ( $\mu\text{g-at/L}$ ) at the sea surface at a position 18 miles southwest of Point Arguello, from data collected in various years between 1949 and 1964.

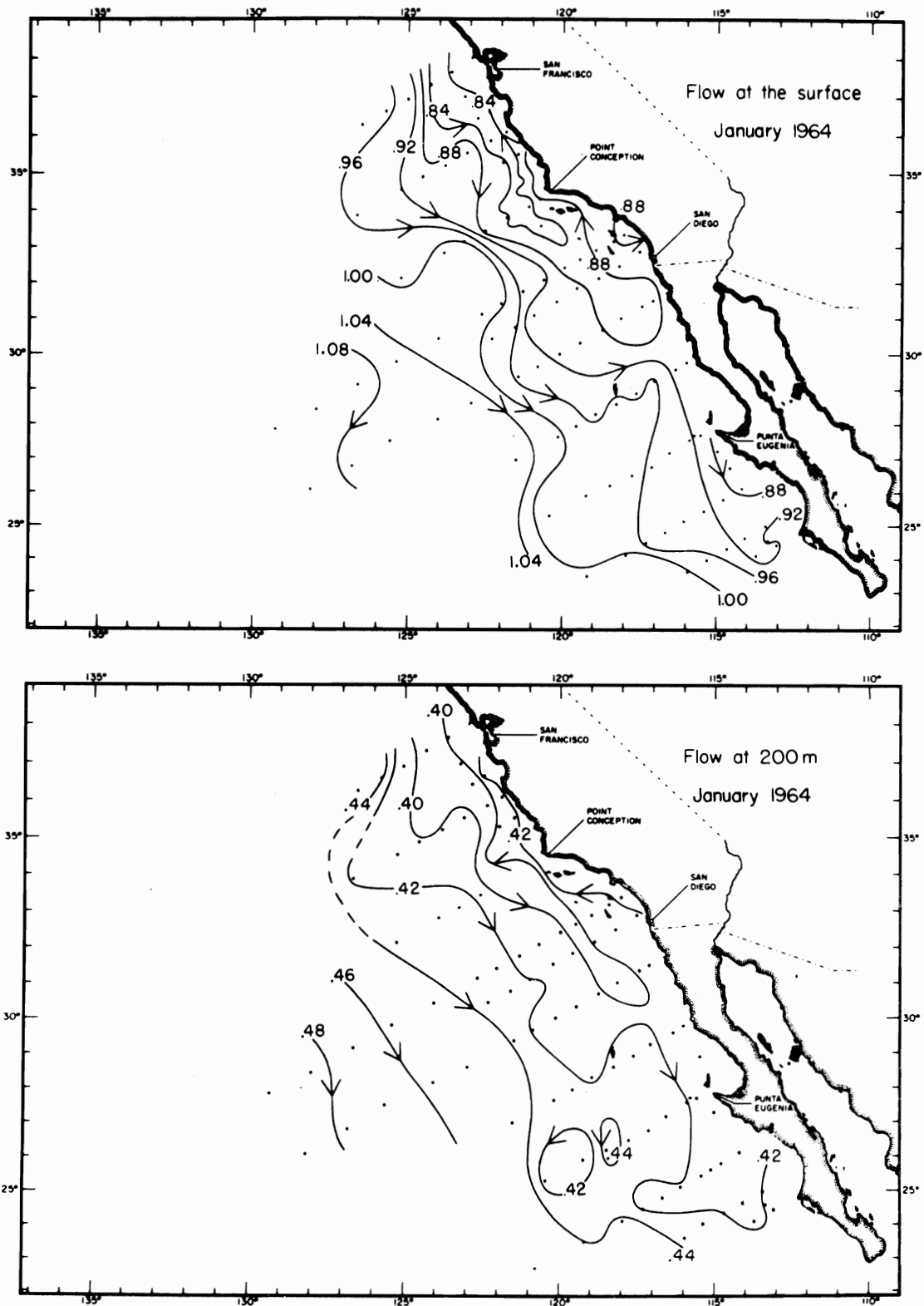


Fig. 34. Geostrophic flow at the surface and at 200 m depth (topography of the 0- and the 200-decibar surfaces relative to the 500-decibar surface, in dynamic meters) of the California Current in January 1964.

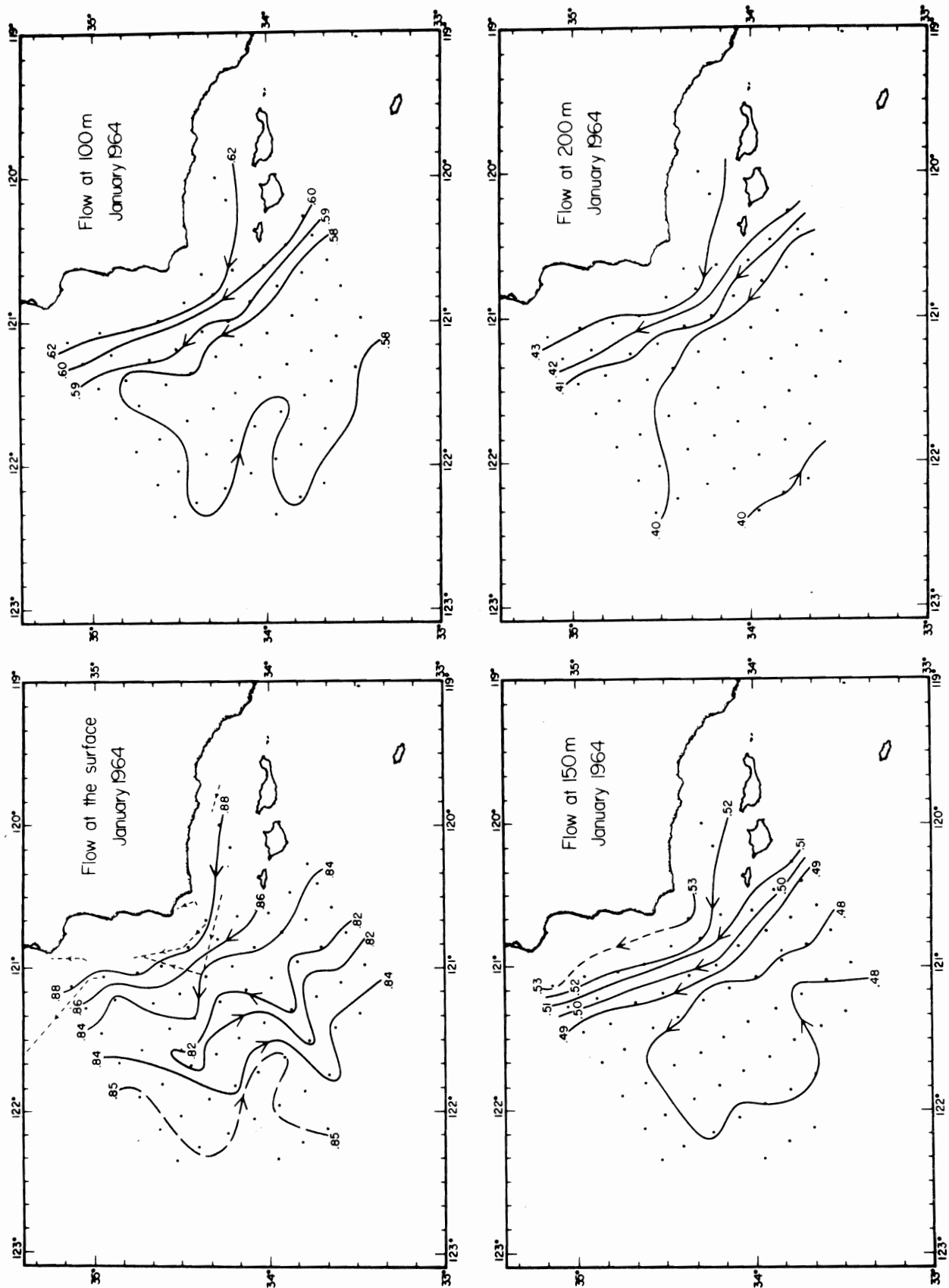


Fig. 35. Geostrophic flow at the surface and at 100, 150, and 200 m depth (topography of the 0-, 100-, 150-, and 200-decibar surfaces relative to the 500-decibar surface) in the region off Point Arguello in January 1964. The dashed lines on the surface chart represent the trajectories of drogues released during this period.

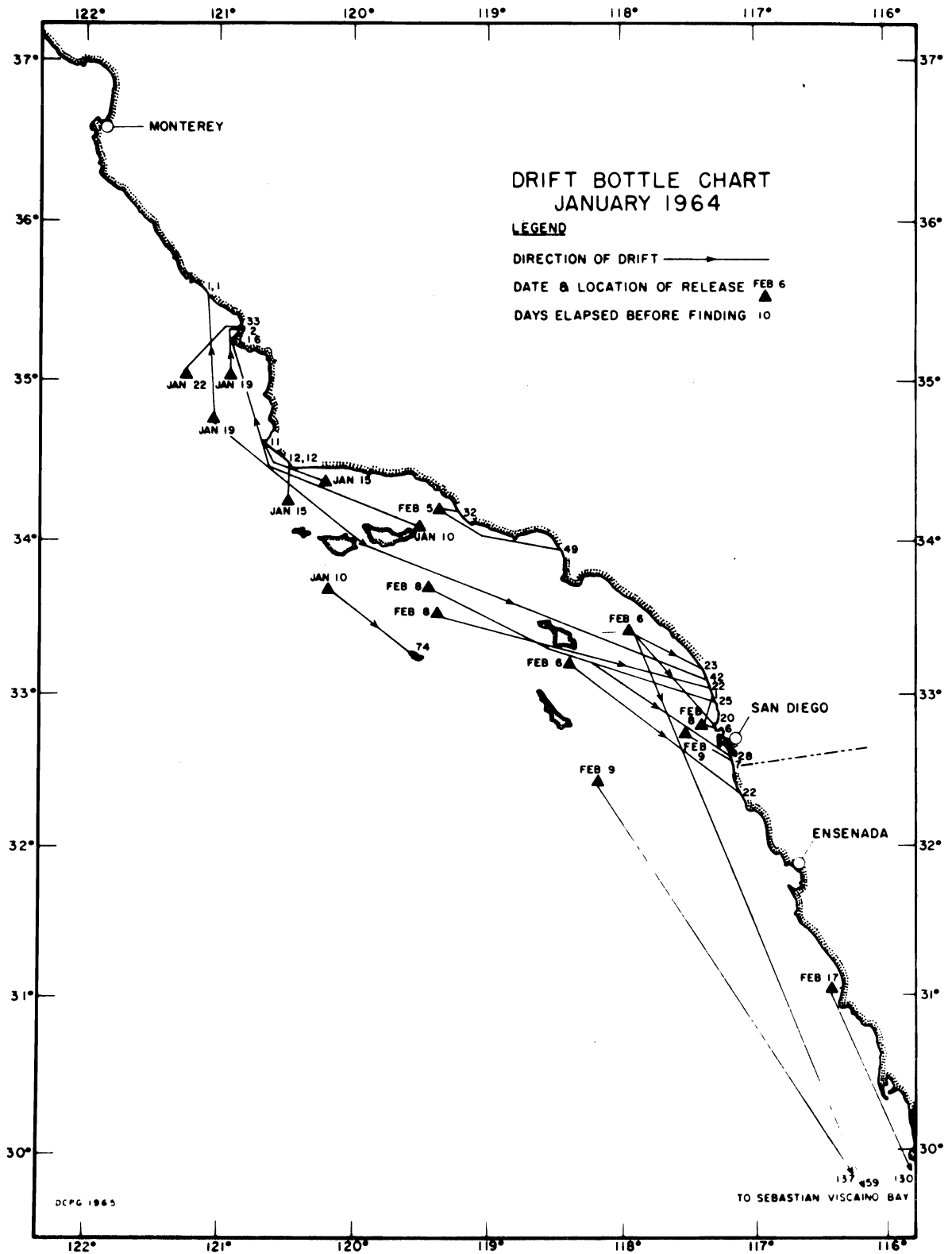
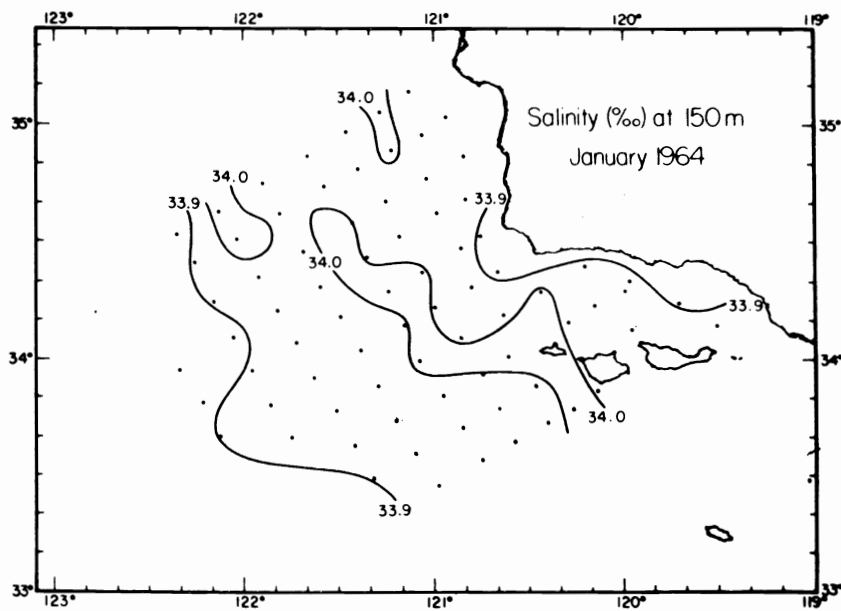
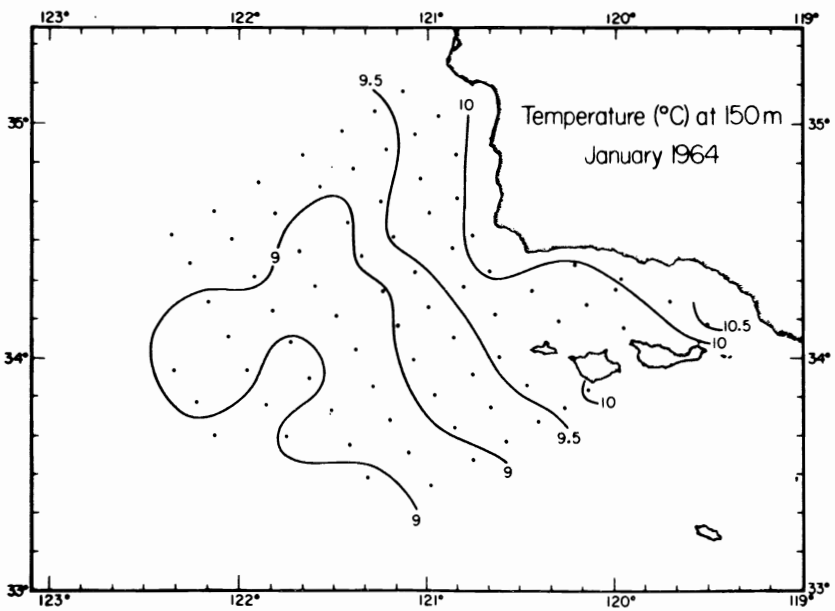
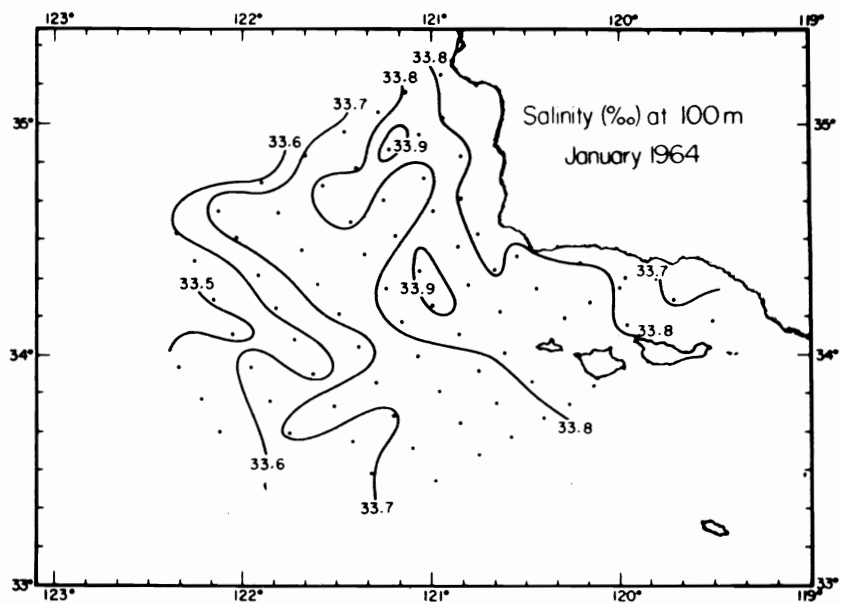
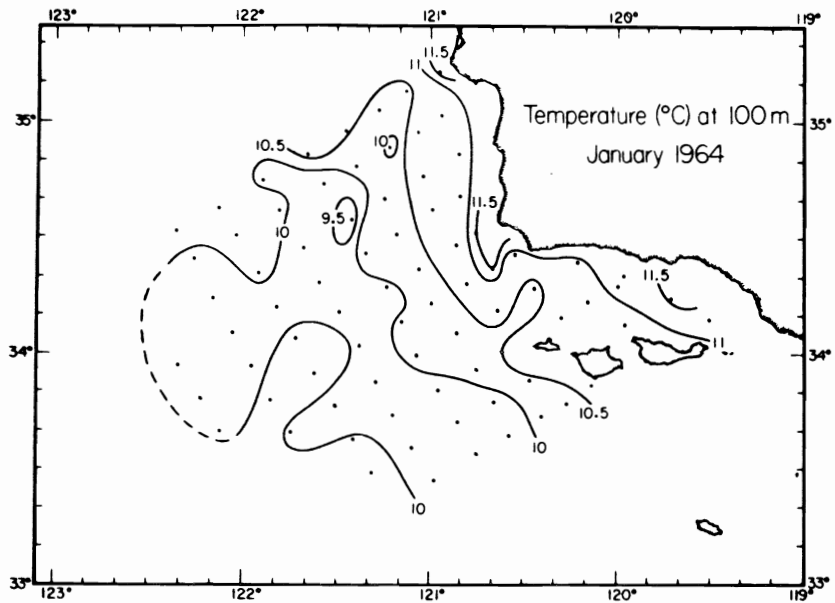


Fig. 36. Recoveries of drift bottles released in January 1964 in the area near Point Arguello.



Fig. 38. Temperature ( $^{\circ}\text{C}$ ) and salinity ( $\text{‰}$ ) at 100 m and 150 m depth in January 1964.





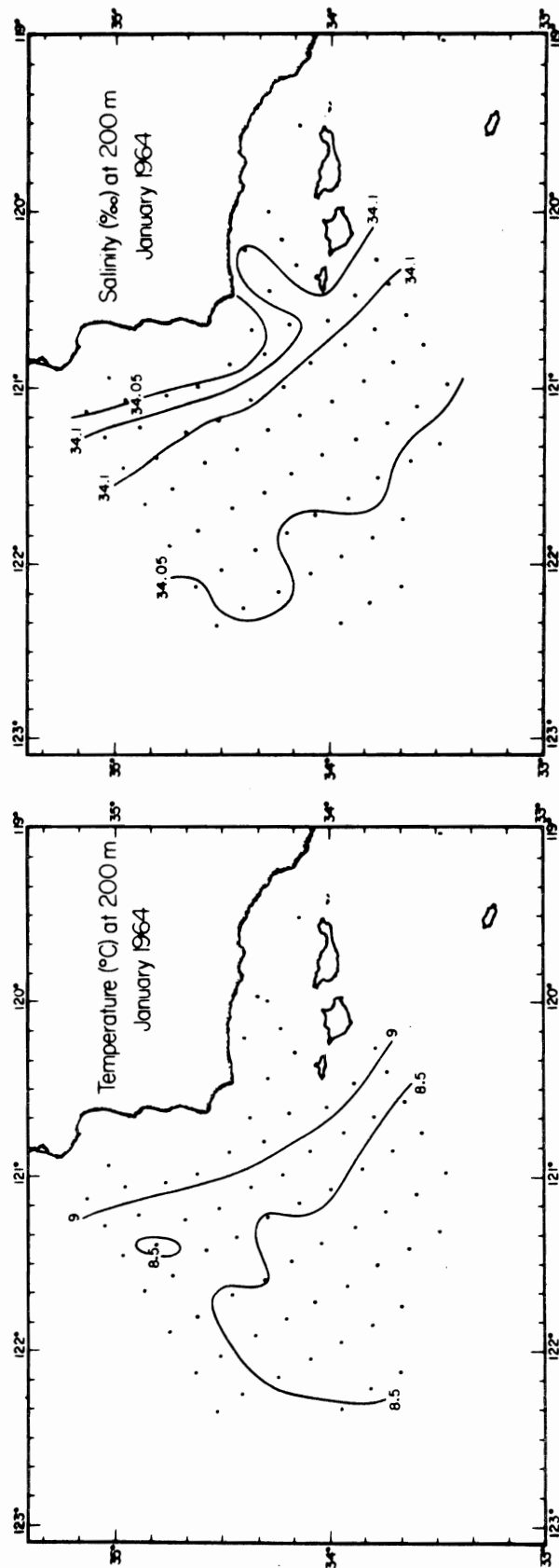


Fig. 39. Temperature (°C) and salinity (‰) at 200 m depth in January 1964.

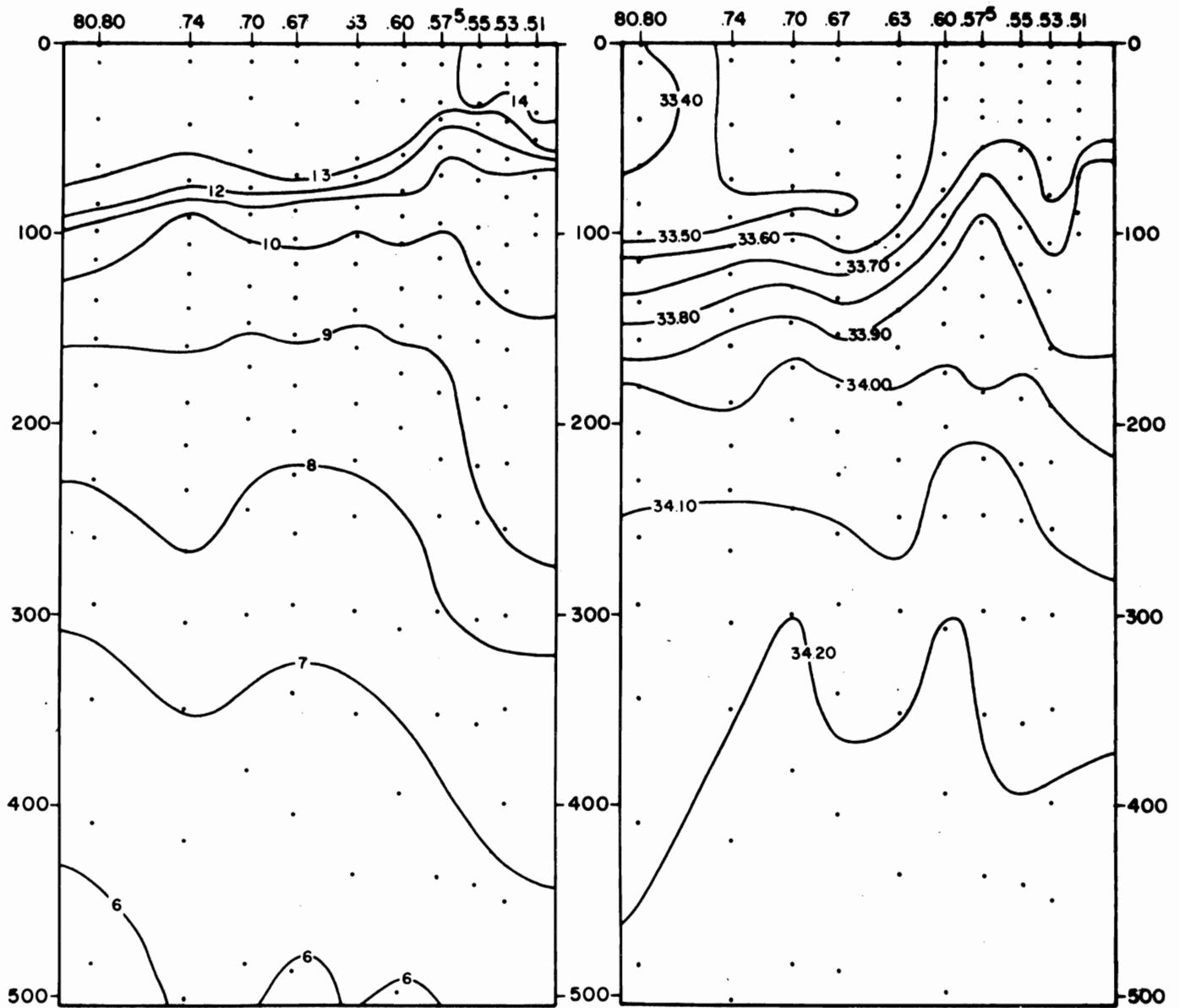


Fig. 40. Temperature ( $^{\circ}\text{C}$ ) and salinity ( $\text{‰}$ ) in January 1964 in a vertical section extending 118 miles from Point Arguello and to a depth of 500 m. Position shown in fig. 26.

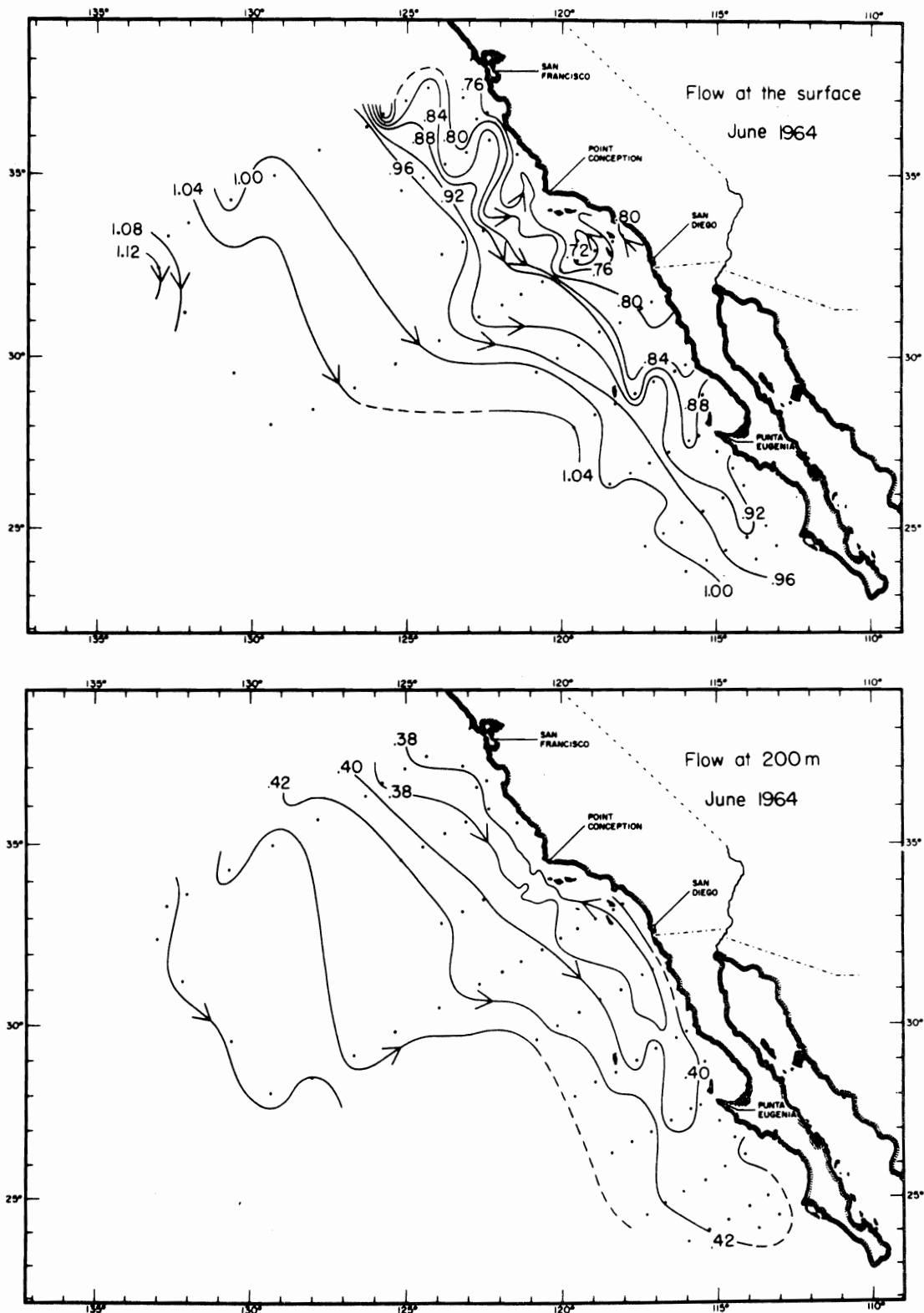


Fig. 41. Geostrophic flow at the surface and at 200 m depth (topography of the 0- and the 200-decibar surfaces relative to the 500-decibar surface, in dynamic meters) of the California Current in June 1964.

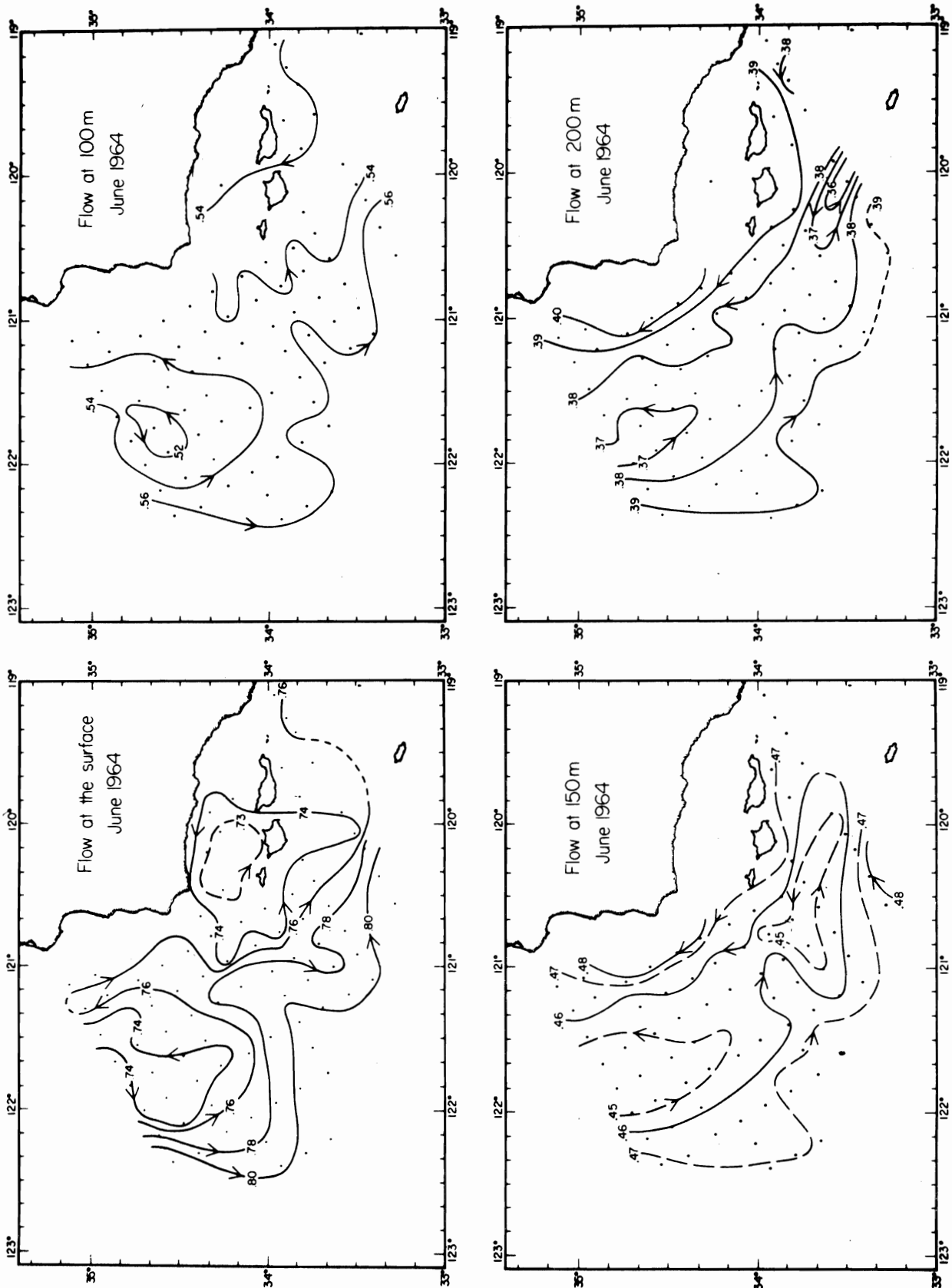


Fig. 42. Geostrophic flow at the surface and at 100, 150, and 200 m depth (topography of the 0-, 100-, 150-, and 200-decibar surfaces relative to the 500-decibar surface) in the region off Point Arguello in ~~January~~ June 1964.



Fig. 44. Temperature ( $^{\circ}\text{C}$ ) and salinity ( $\text{‰}$ ) at the sea surface and at 50 m depth in June 1964.

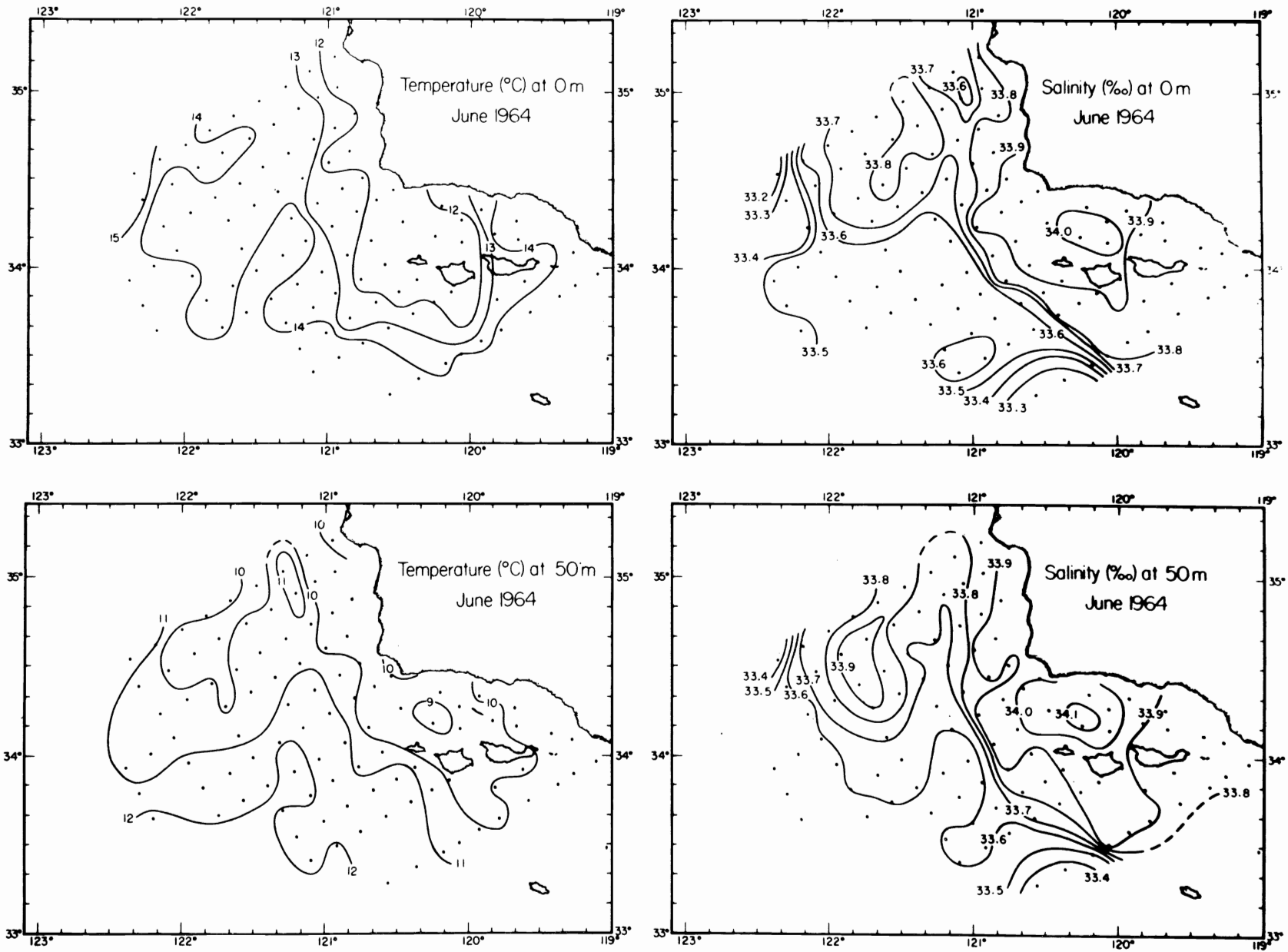
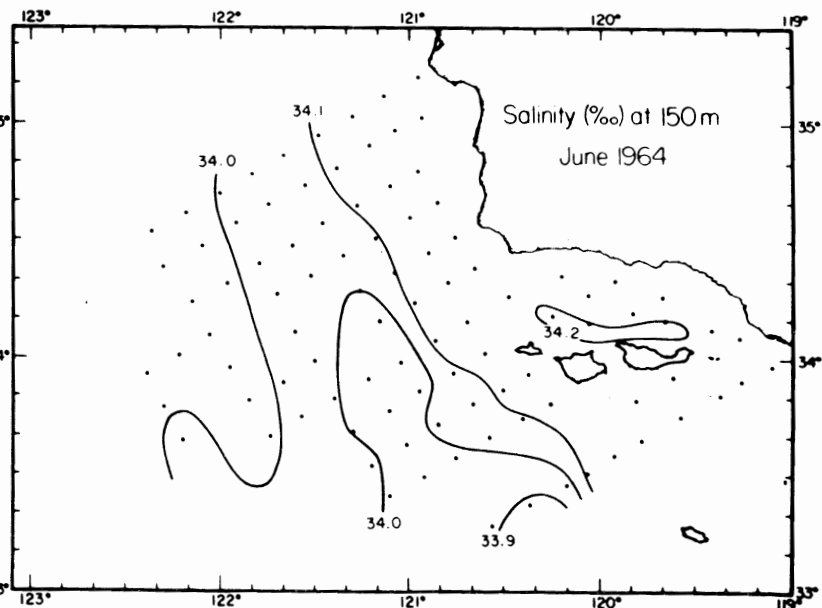
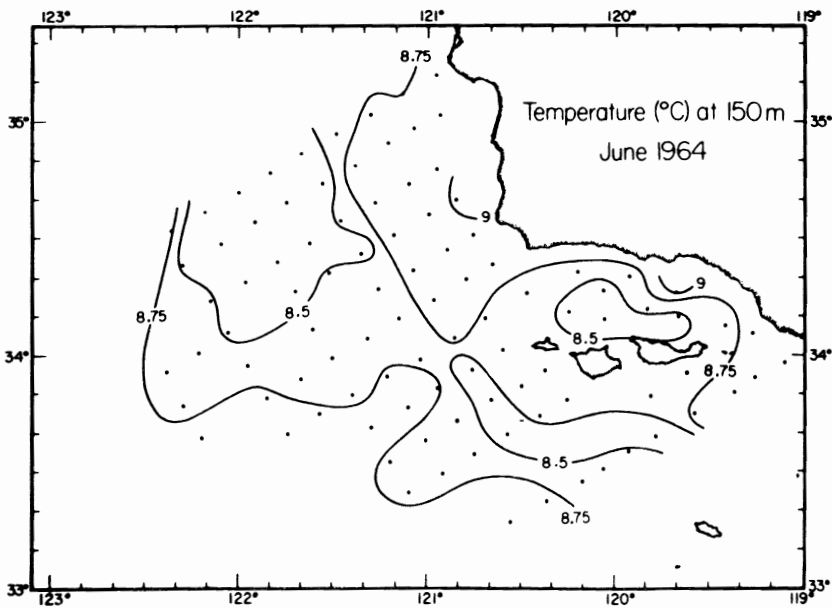
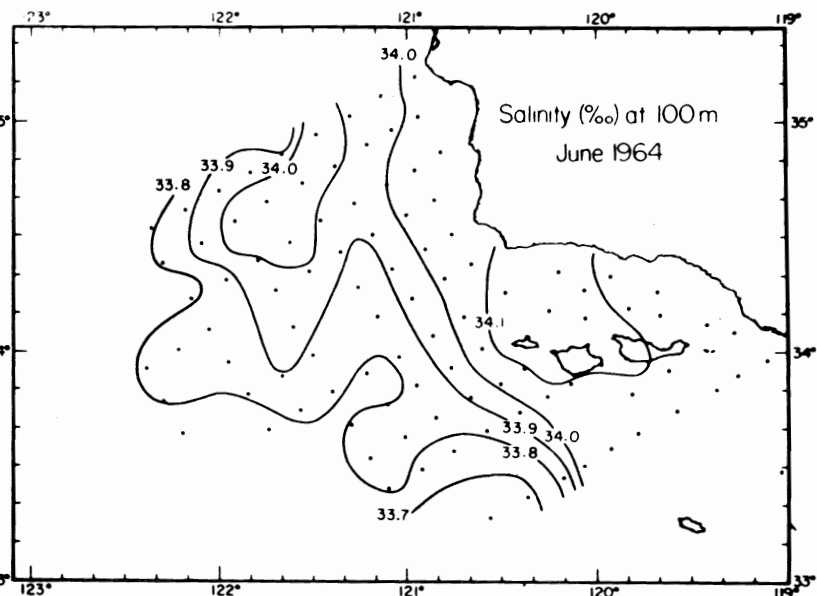
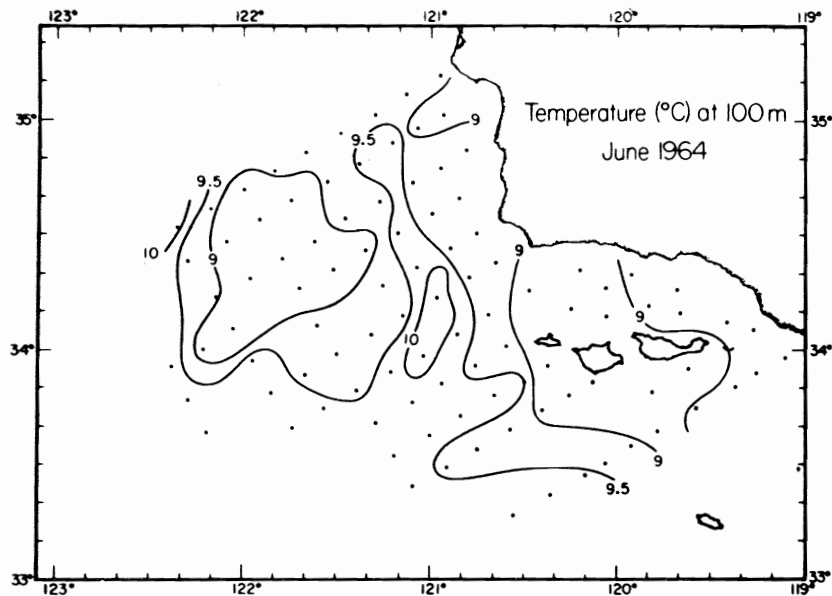


FIG. 45. Temperature ( $^{\circ}\text{C}$ ) and salinity ( $\text{‰}$ ) at 100 m and 150 m depth in June 1964.



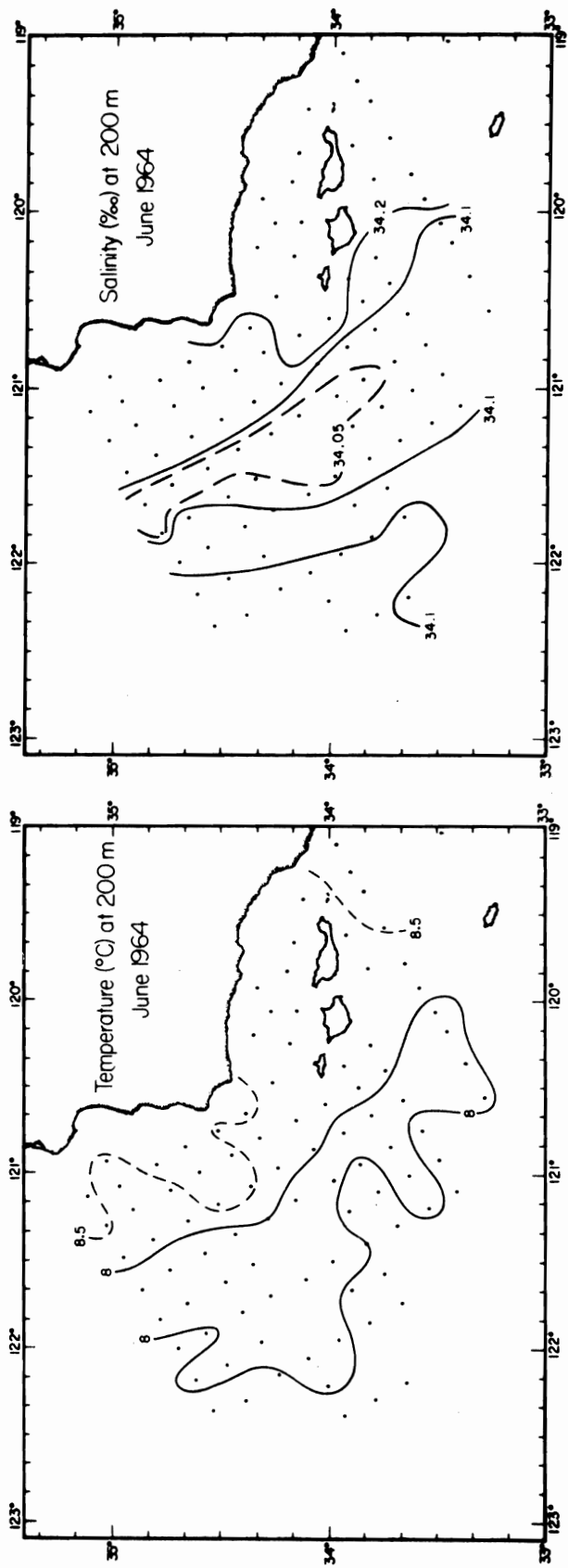


Fig. 46. Temperature (°C) and salinity (‰) at 200 m depth in June 1964.



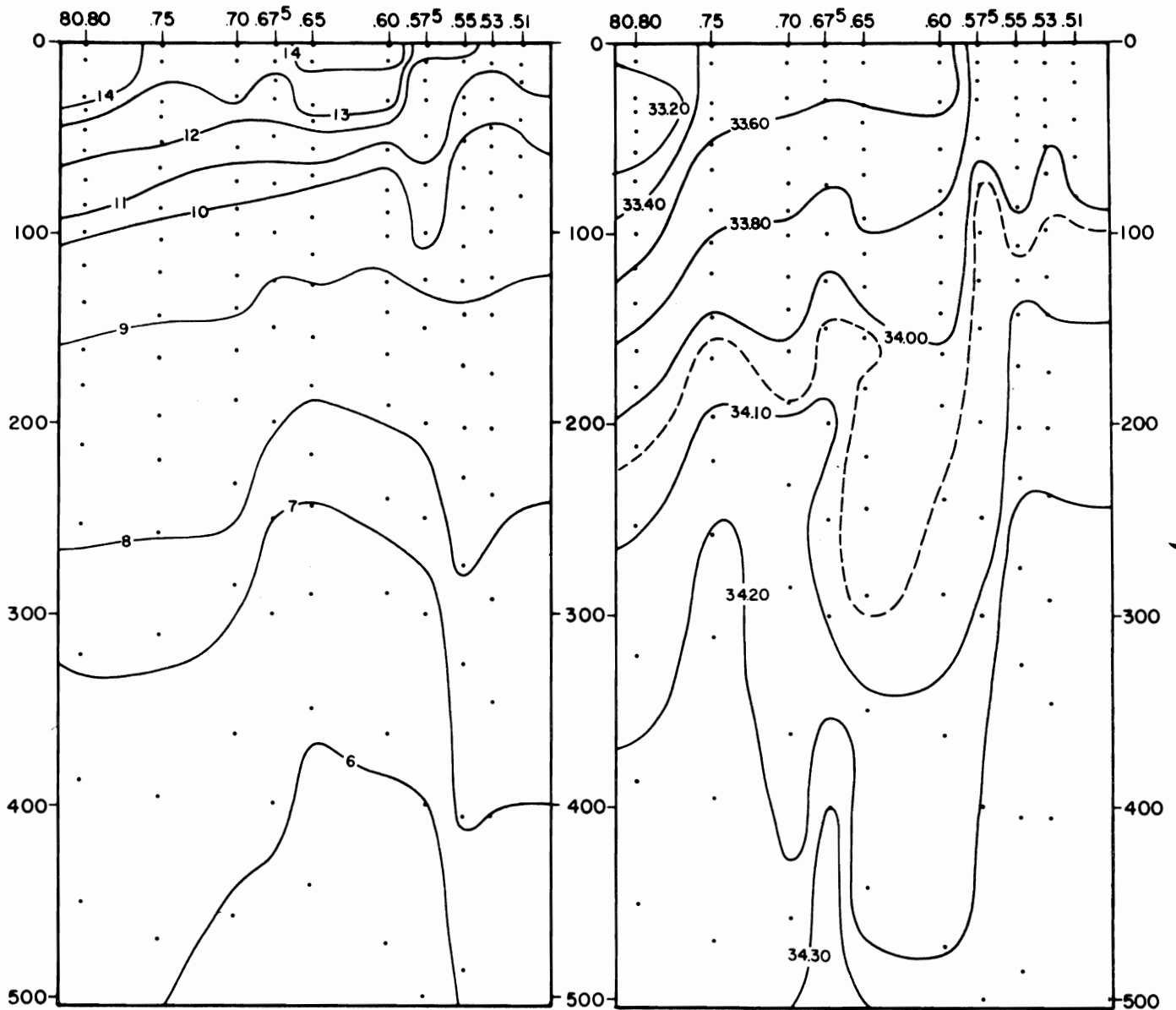


Fig. 47. Temperature ( $^{\circ}\text{C}$ ) and salinity ( $\text{‰}$ ) in June 1964 in a vertical section extending 118 miles from Point Arguello and to a depth of 500 m. Position shown in fig. 26.

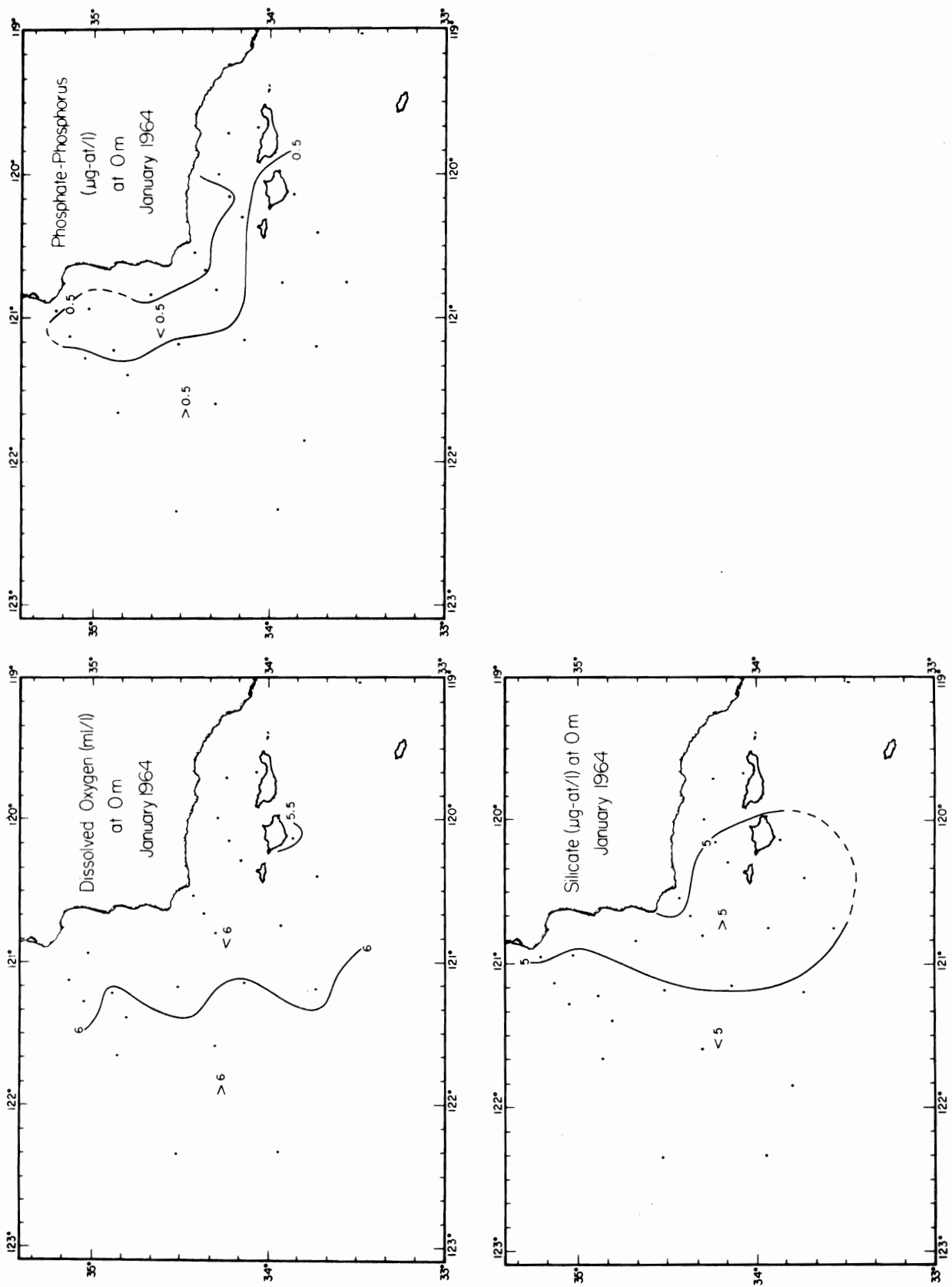


Fig. 48. Dissolved oxygen (ml/L), inorganic phosphate-phosphorus ( $\mu\text{g-at/L}$ ) and silicate ( $\mu\text{g-at/L}$ ) at the sea surface in January 1964.

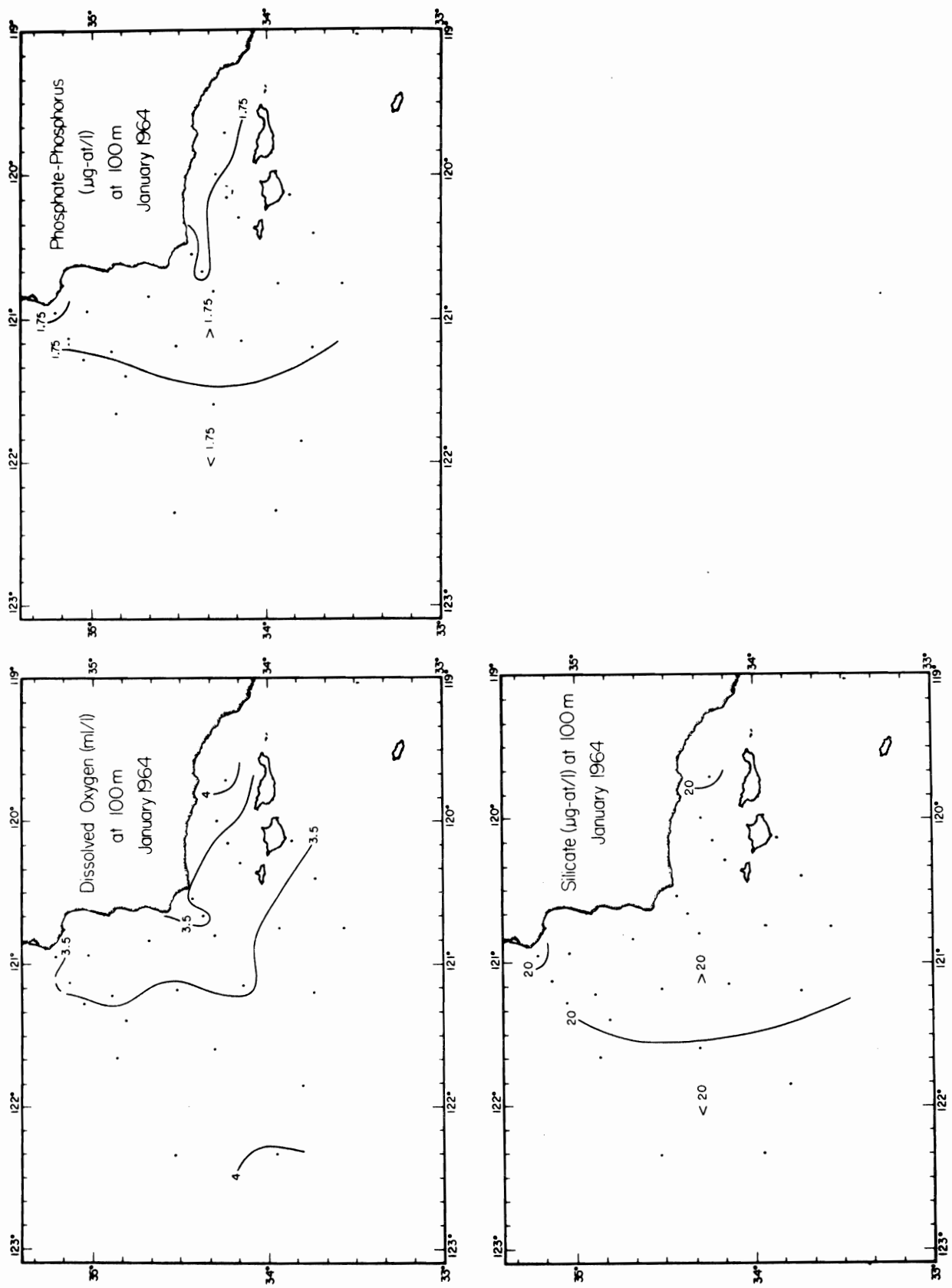


Fig. 49. Dissolved oxygen (ml/L), inorganic phosphate-phosphorus ( $\mu\text{g-at/L}$ ) and silicate ( $\mu\text{g-at/L}$ ) at 100 m depth in January 1964.

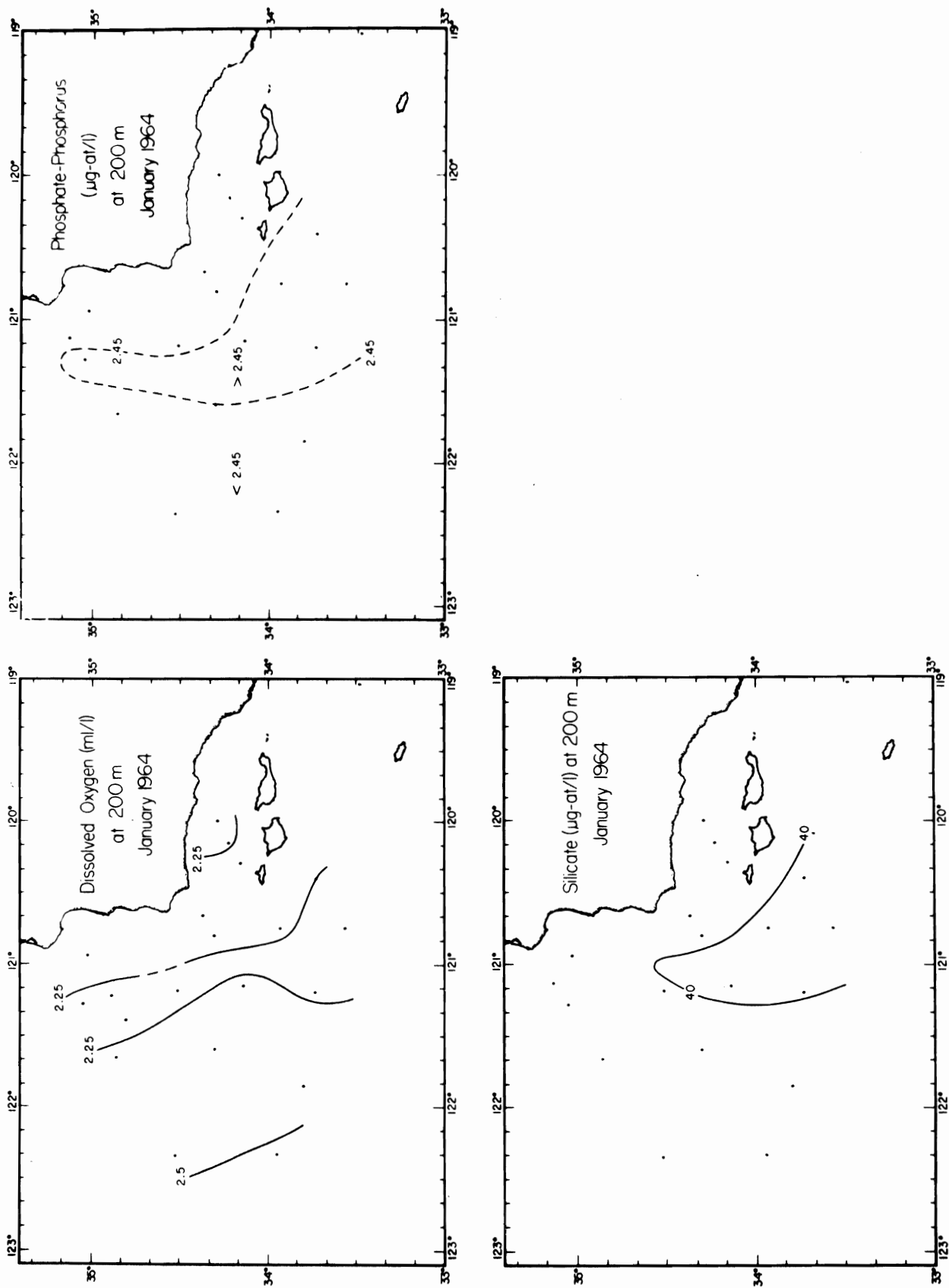


Fig. 50. Dissolved oxygen (ml/L), inorganic phosphate-phosphorus ( $\mu\text{g-at/L}$ ) and silicate ( $\mu\text{g-at/L}$ ) at 200 m depth in January 1964.

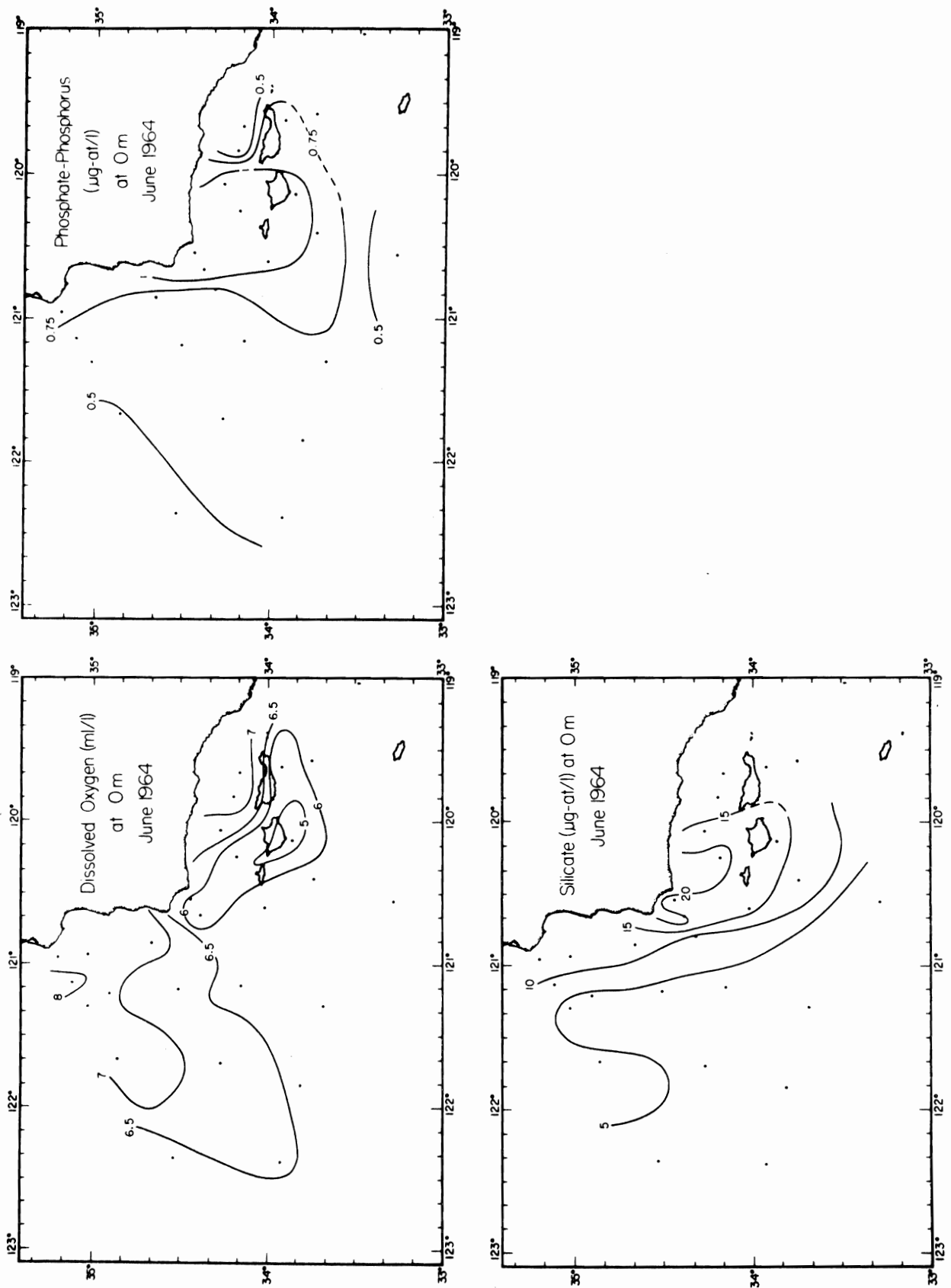


Fig. 51. Dissolved oxygen (ml/L), inorganic phosphate-phosphorus ( $\mu\text{g-at/L}$ ) and silicate ( $\mu\text{g-at/L}$ ) at the sea surface in June 1964.

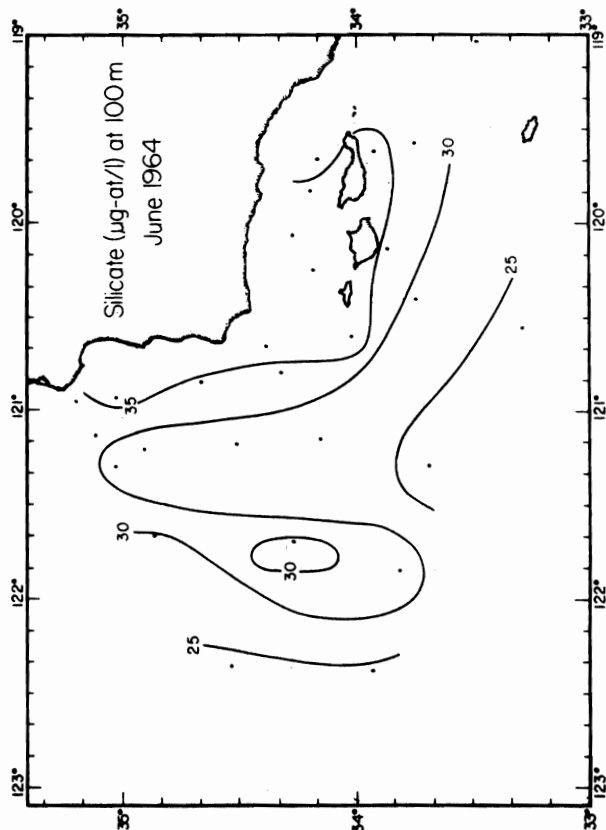
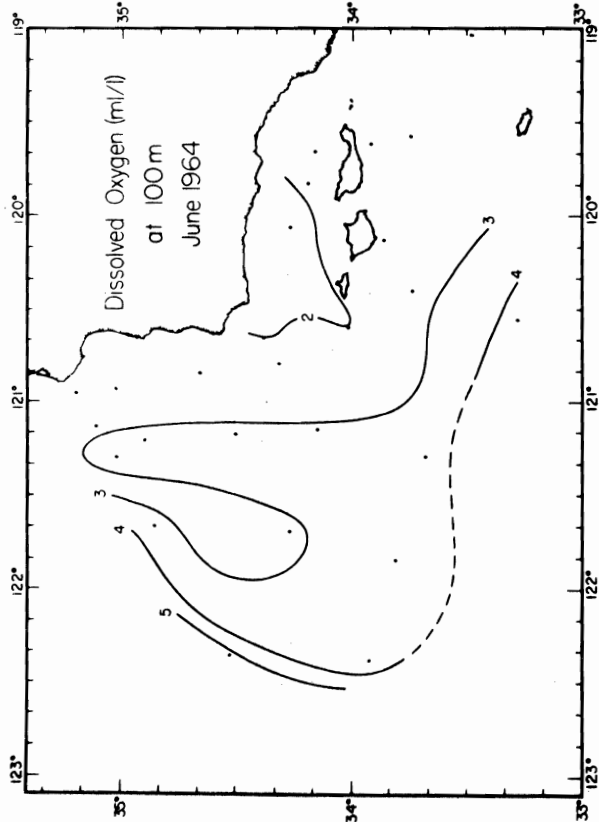
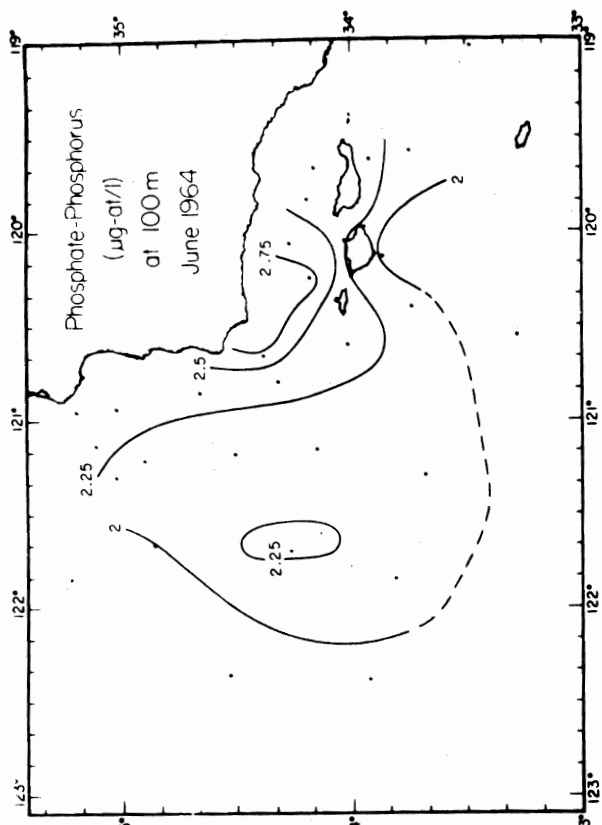


Fig. 52. Dissolved oxygen (ml/L), inorganic phosphate-phosphorus ( $\mu\text{g-at/L}$ ) and silicate ( $\mu\text{g-at/L}$ ) at 100 m depth in June 1964.

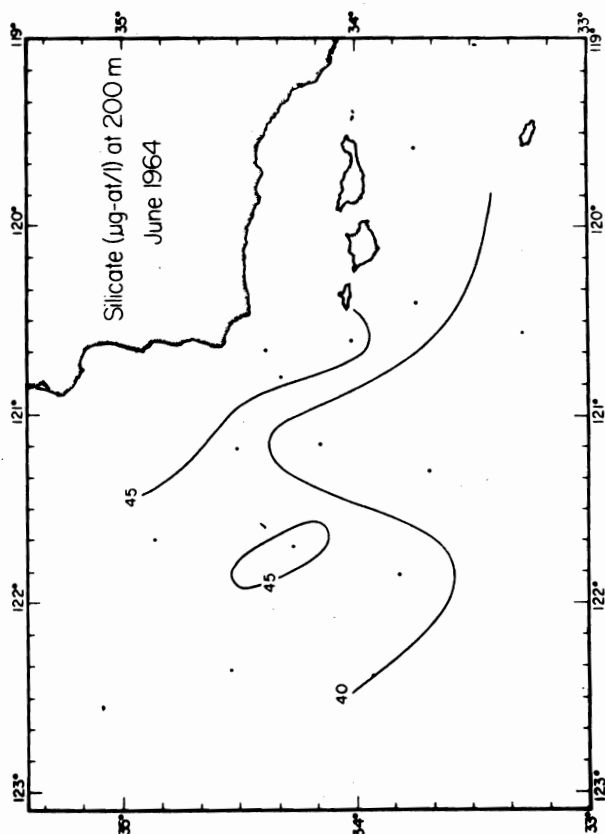
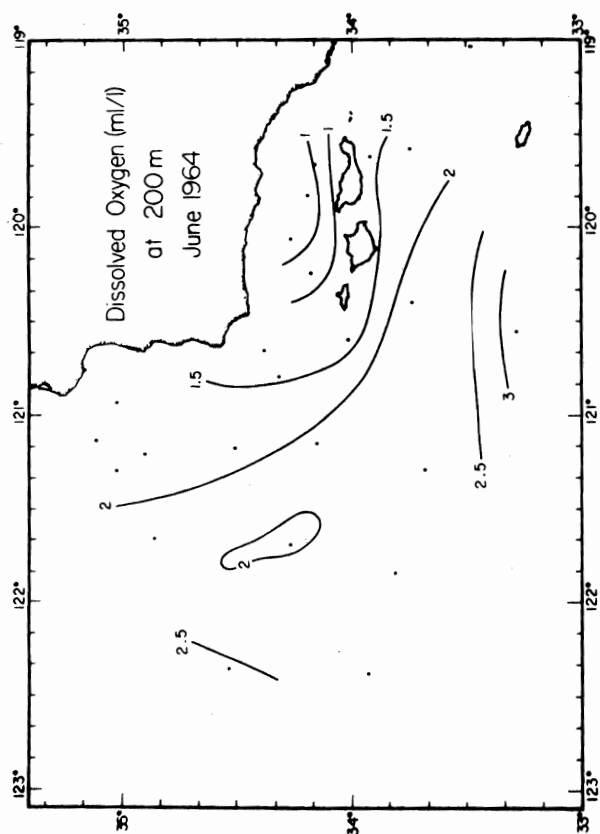
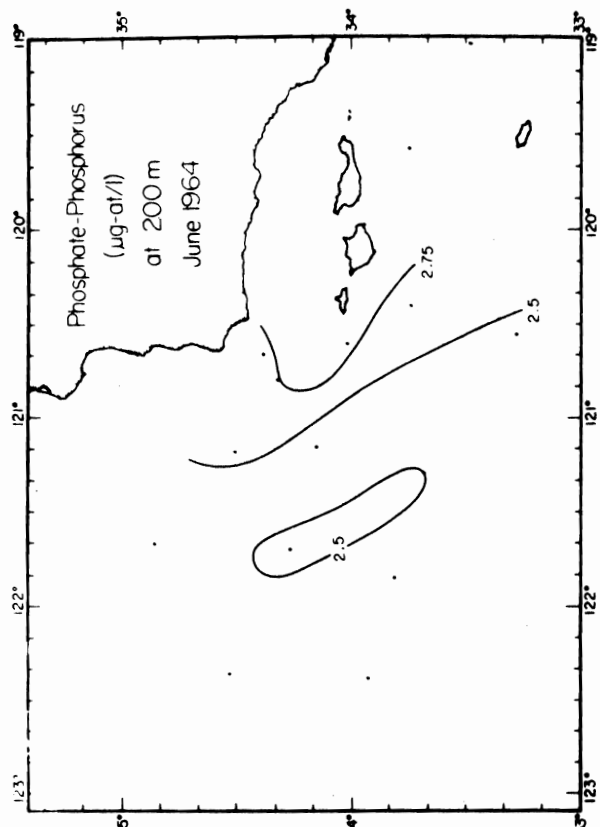


Fig. 53. Dissolved oxygen (ml/L), inorganic phosphate-phosphorus ( $\mu\text{g-at/L}$ ) and silicate ( $\mu\text{g-at/L}$ ) at 200 m depth in June 1964.